Sustainable Design of Industrial Energy Supply Systems

Development of a model-based decision support framework
Zur Erlangung des akademischen Grades Doktor-Ingenieur (Dr.-Ing.)
Genehmigte Dissertation von Lukas Höttecke aus Paderborn, Deutschland
Tag der Einreichung: 27. März 2023, Tag der Prüfung: 06. Oktober 2023

1. Gutachten: Prof. Dr.-Ing. Stefan Niessen, MBA
2. Gutachten: Prof. Dr. rer. nat. Florian Steinke
Darmstadt – D17, Technische Universität Darmstadt

TECHNISCHE UNIVERSITÄT DARMSTADT

Electrical Engineering and Information Technology Department

Technology and Economics of Multimodal Energy Systems

Sustainable Design of Industrial Energy Supply Systems
Development of a model-based decision support framework

Accepted doctoral thesis by Lukas Höttecke

Date of submission: 27. März 2023
Date of thesis defense: 06. Oktober 2023

Darmstadt – D17, Technische Universität Darmstadt

Bitte zitieren Sie dieses Dokument als:
URN: urn:nbn:de:tuda-tuprints-247857
URL: http://tuprints.ulb.tu-darmstadt.de/24785
Jahr der Veröffentlichung auf TUprints: 2023

Dieses Dokument wird bereitgestellt von tuprints,
E-Publishing-Service der TU Darmstadt
http://tuprints.ulb.tu-darmstadt.de
tuprints@ulb.tu-darmstadt.de

Acknowledgements

This Thesis is the final result of my work as a doctoral student in the Siemens Technology Center Erlangen. My PhD journey has been a marathon with both stimulating growth phases and enduring dry spells. I was accompanied by numerous creative and supportive people on this journey. I would like to take this opportunity to thank them all for their contributions to the success of this Thesis in the past four years.

First and foremost, I express my deepest gratitude to my university supervisor Professor Stefan Niessen for arranging the cooperation between Siemens and the Technical University of Darmstadt and offering me his encouraging feedback, support and enriching discussions throughout the PhD journey. In addition, I thank my co-supervisor Professor Florian Steinke for his co-supervision of this Thesis, in particular his very valuable comments to the manuscript of this Thesis.

The work was carried out in the research and pre-development department of Siemens, where I received extensive support from many technology and businuess experts. First, I thank my group leaders Jochen, Sebastian and Hans Jörg for their proactive feedback and growth culture. In particular, I wish to highlight Sebastian's contributions who has facilitated the start of my PhD journey as my supervisor and shaped the relevance of my work in countless hours. Moreover, his trust offered me the opportunity to build a growing user community for the prototype tool *mm.esd*. A big thanks to all who contributed to the *mm.esd* community, especially to Florian, Martin, Peter, Dominik, Paul, Sissi and Dieter. I highly appreciated not only the time and patience while fixing bugs and testing new features, but also the fruitful discussions in numerous consulting projects. During my PhD journey, I enjoyed working with brite and inspiring people. I wish to thank my office mates and colleagues Oliver, Sebastian, Thanh, Robin and Thomas for their openess, delightful conversations, and enlightening suggestions through the past four years. Next to my colleagues, I was delighted to supervise great students who have brought their own ideas and mastered various challenges of my research. Thank you Cyril, Ariane, Lola, Kris, Quentin, Paul, Flore and David. This Thesis would have not been possible without the help of all these people.

Finally, I wish to express my special thanks to all friends from Greven, Dortmund, and Erlangen as well as my family. My parents Maria and Martin as well as my sister Lara have supported me in particular also during the challenging parts of this PhD journey and the Covid pandemic. Last and most important, I need to express my deepest gratitude to Nina for the trust and loving support during the creation of this Thesis.

Abstract

Energy and media supply systems and related infrastructure at industrial sites have grown historically and is largely dependent on the use of fossil fuels. High fuel prices and the emission reduction targets of companies challenge existing supply concepts. Supply concepts usually remain in place for decades due to the long-lived nature of generation technologies and distribution systems. Today's investment decisions are therefore confronted with a changing environment in which the share of volatile renewables from solar and wind is continuously increasing. The long planning horizons make design decisions very complex. Optimization-based design approaches automatically derive cost- or carbon-optimal selections of generation technologies and procurement tariffs. Thus, they enable faster and more accurate planning decisions in techno-economic feasibility studies.

In this work, a novel optimization model for techno-economic feasibility studies in industrial sites is developed. The optimization model uses a generic technology formulation with base classes, which takes into account the large variety of technologies and procurement tariffs at industrial sites. The optimization model also includes two reserve concepts: an operating reserve concept for short-term disruptions and a redundancy concept for long-term plant failures. The two concepts ensure security of supply for production-related energy requirements and thereby contributes to avoidance of costly production outages.

The optimization model is integrated into an optimization framework to effectively calculate decarbonization strategies. The framework uses time series aggregation and heuristic decomposition techniques. Time series aggregation is performed by an integer program and results in a robust selection of representative days. The selection of representative days is used in a multi-year planning model to derive transformation roadmaps. Transformation roadmaps analyze the evolution of energy supply systems to long-term trends and consider adaptive investment decisions. A transformation strategy with myopic foresight (MYOP) solves the multi-year planning problem sequentially and is solved up to 98 % faster than a transformation approach with perfect foresight (PERF). The high uncertainties in early planning phases and the resulting need for detailed sensitivity analysis make this approach the preferred choice for many feasibility studies.

The newly developed optimization framework is used in numerous research and consulting projects for urban districts, microgrids and factories. In this work, the capabilities of the framework are demonstrated for three use cases (automotive, pharmaceutical, dairy) of factory sites in southern Germany. In the use cases, decarbonization strategies for electricity, steam, heating and cooling supply are analyzed. Simulation evaluations identify changing operating patterns of combined heat and power (CHP) plants along the 15-year planning horizon. In addition, electrification of heating demand leads to a significant increase of total electricity demands. The results derived with the framework provide decision makers in industrial companies a clear view of the long-term impact of their investment decisions on decarbonization strategies.

Zusammenfassung

Die Energie- und Medienversorgung sowie die dafür notwendige Infrastruktur an Industriestandorten ist häufig historisch gewachsen und hängt maßgeblich vom Einsatz fossiler Brennstoffe ab. Hohe Brennstoffpreise und die Emissionsminderungsziele der Unternehmen stellen bestehende Versorgungskonzepte in Frage. Aufgrund des langlebigen Charakters der Anlagentechnik und der Verteilsysteme bleiben Versorgungskonzepte meist über Jahrzehnte bestehen. Heutige Investitionsentscheidungen werden daher mit einem sich verändernden Umfeld konfrontiert, in der der Anteil der volatilen erneuerbaren Energien aus Sonne und Wind kontinuierlich zunimmt. Optimierungsbasierte Auslegungsansätze leiten automatisch eine kostenoptimale Auswahl der Anlagentechnik und Beschaffungstarifen ab. Dadurch ermöglichen sie schnellere und genauere Planungsentscheidungen in techno-ökonomischen Machbarkeitsstudien.

In dieser Arbeit wird ein neuartiges Planungsmodell für Machbarkeitsstudien an Industriestandorten entwickelt. Das Planungsmodell verwendet eine generische Technologieformulierung mit Basisklassen, die der großen Vielfalt an Technologien und Beschaffungstarifen an Industriestandorten Rechnung trägt. Das Planungsmodell beinhaltet darüber hinaus zwei Reservekonzepte: ein Betriebsreservekonzept für kurzfristige Störungen und ein Redundanzkonzept für langfristige Anlagenausfälle. Die beiden Konzepte gewährleisten die Versorgungssicherheit des produktionsbedingten Energiebedarfs und vermeiden so kostspielige Produktionsausfälle.

Das Planungsmodell wird in einen Optimierungsframework integriert, um effektiv Dekarbonisierungsstrategien zu berechnen. Die Aggregation von Zeitreihen wird in dem Framework als mathematisches Optimierungsproblem formuliert und führt auf eine robusten Auswahl repräsentativer Tage. Diese robuste Auswahl wird in einem Planungsmodell mit mehreren Ausbaustufen zur Ableitung von Transformationsplänen verwendet. Transformationsplänen analysieren die Anpassungsfähigkeit von Energieversorgungssystemen an langfristige Entwicklungen. Eine Transformations-Strategie mit einer kurzfristigen Vorausschau löst das Planungsmodell sequentiell und wird bis zu 98 % schneller gelöst als ein Ansatz mit perfekter Vorausschau auf zukünftige Entwicklungen. Die hohen Unsicherheiten in frühen Planungsphasen und der daraus resultierende Bedarf an umfassenden Sensitivitätsanalysen machen diesen Ansatz zur bevorzugten Wahl für viele Machbarkeitsstudien.

Die Fähigkeiten des Frameworks werden anhand von drei Anwendungsbeispiele von Industriestandorten (Automobil, Pharma, Molkerei) aufgezeigt. In den Anwendungsbeispielen werden Strategien für die Strom-, Dampf-, Wärme- und Kälteversorgung analysiert. Simulationsauswertungen identifizieren veränderte Betriebsweisen von Anlagen zur Kraft-Wärme-Kopplung (KWK) entlang des 15-jährigen Planungshorizonts. Darüber hinaus führt die Elektrifizierung des Wärmebedarfs zu einer signifikanten Erhöhung des gesamten Strombedarfs. Die mit dem Framework abgeleiteten Ergebnisse geben Entscheidungsträgern in Industrieunternehmen einen klaren Überblick über die langfristigen Auswirkungen heutiger Investitionsentscheidungen auf Dekarbonisierungsstrategien.

Contents

List of Figures

List of Tables

Nomenclature

Remarks on nomenclature

The symbols for sets and variables are denoted in this Thesis as follows: All variables of the optimization model are defined with upper case letters. Parameters are mostly defined with lower case letters. Superscripts of parameters and variables are descriptive. Subscripts define variable indices. Indices are presented in italics. For example, $c_{k,t}^{\text{Energy}}$ describes the costs associated with energy for the technology indexed with k and a time step indexed with t. Parameters describing lower and upper bounds of optimization variables are highlighted by underbars or overbars respectively. For example, $\underline{P}^{\text{R}}$ defines the lower bound of the variable P^{R} for rated power capacity. Subsets are notated with a sub- or superscripts. For example, $\mathcal{T}_y \subseteq \mathcal{T}$ denotes the subset of all time steps $\mathcal{T}$ belonging to the extension stage y. Terms of the objective function use the letter ζ.

Sets

Set	Description
$\mathcal{C}$	Set of commodities, indexed with c
$\mathcal{D}$	Set of representative periods, indexed with d
$\mathcal{K}$	Set ofn technologies, indexed with k
$\mathcal{L}$	Set of loads, indexed with l
$\mathcal{N}$	Set of nodes, indexed with n
$\mathcal{Q}$	Set of linkages between two technologies, indexed with q
$\mathcal{R}$	Set of reserve requirements, indexed with r
$\mathcal{S}$	Set of stakeholders, indexed with s
$\mathcal{T}$	Set of time steps, indexed with t
$\mathcal{Y}$	Set of extension stages, indexed with y

Parameters

Scope	Parameter	Unit	Description
General	w	-	Weight factor
	Δt	h	Duration of time step t
	i	100 %	Interest rate
	h		Helper parameter
Economic	$c^{\text{Inv,cap}}$	€/MWh	Rated capacity specific investment costs
	$c^{\text{Inv,fix}}$	€	Fixed costs for an investment decision
	$c^{\text{Inv,var}}$	€/MW	Rated power specific investment costs
	$c^{\text{OM,curtail}}$	€/MWh	Costs for load or renewable curtailment
	$c^{\text{OM,cap}}$	€/MWh/a	Rated capacity specific annual maintenance costs
	$c^{\text{OM,CO2}}$	€/tCO2	Specific costs for carbon emissions
	$c^{\text{OM,energy}}$	€/MWh	Energy specific operation costs
	$c^{\text{OM,fix}}$	€/a	Fixed annual maintenance costs
	$c^{\text{OM,peak}}$	€/MWp/a	Annual specific demand charges
	$c^{\text{OM,run,fix}}$	€/h	Runtime specific maintenance costs
	$c^{\text{OM,run,var}}$	€/MW/h	Runtime and rated power specific maintenance costs
	$c^{\text{OM,start,fix}}$	€/start	Start up specific maintenance costs
	$c^{\text{OM,start,var}}$	€/MW/start	Start up and rated power specific maintenance costs
	$c^{\text{OM,var}}$	€/MW/a	Rated power specific annual maintenance costs
	$e^{\text{CO2,energy}}$	kgCO2/MWh	Energy specific carbon emissions
Technical	l	km	Length of a line technology
	n^{Cycle}	1/a	Maximum number of annual full load cycles
	n^{Start}	1/a	Maximum number of annual starts
	r^{Ch}	%/h	Maximum charging rate
	r^{Dis}	%/h	Maximum discharging rate
	r^{Down}	1/h	Specific ramp-down limits
	r^{Up}	1/h	Specific ramp-up limits
	u	-	Part-load ratio
	y^{Tech}	a	Technical lifetime of new technology
	y^{Inst}	a	Remaining lifetime of installed technology
	η^{Ch}	100 %	Charging efficiency
	η^{Dch}	100 %	Discharging efficiency
	η^{Loss}	%/km	Loss coefficient of a lines
	η^{Self}	a	Self-discharge rate
	ϑ	K	Absolute temperature
Reserve	a^{OR}	-	Availability factor
	$p^{\text{RED,L}}$	MW	Critical load
	$T^{\text{OR,D}}$	h	Duration of a reserve call
	$T^{\text{OR,T}}$	h	Response time for a reserve call
	α^{OR}	-	Load factors for operating reserve
	γ^{RED}	-	Module size for redundancy allocation
	ρ^{OR}	1/a	Proability of reserve activation

Variables

Scope	Variable	Unit	Description
Design	P^{R}	MW	Installed rated power capacity of a technology
	P^{Inv}	MW	New installed rated power capacity of a technology
	P^{Repl}	MW	Replaced rated power capacity of a technology
	C^{R}	MWh	Installed rated storage capacity of a storage
	C^{Inv}	MWh	New installed rated storage capacity of a storage
	C^{Repl}	MWh	Replaced rated storage capacity of a storage
	B^{Inv}	-	Investment decision {0,1} in a technology
	B^{R}	-	Installation status {0,1} of a technology
Operation	P^{In}	MW	Input power flow of a technology
	P^{Out}	MW	Outlet power flow of a technology
	P^{L}	MW	Load power flow
	E	MWh	Energy content of a storage
	B^{Opr}	-	Operational status {0,1} of a technology
	H^{Start}	-	Helper variable for a converter technology with startup costs
Reserve	P^{OR}	MW	Power flows for operating reserve
	P^{RED}	MW	Power flows for redundancy allocation

Acronyms

AC absorption chiller

B&B branch and bound

BAT lithium-ion battery

BB biomass boiler

CAPEX capital expenditures

CC compression chiller

CHP combined heat-and-power

COP coefficient Of performance

CWS chilled water storage

EB electric boiler

EER energy efficiency ratio

FLA forward-looking design approach

FSP full-scale problem

GB gas boiler

GT gas turbine

HP heat pump

HWS hot water storage

ICE internal combustion engine

IP integer program

KPI key performance indicator

LP linear program

MILP mixed integer linear program

MINLP mixed integer non-linear program

MYOP roadmap approach with myopic foresight

OPEX operational expenditures

OPS optimized period selection

PERF roadmap approach with perfect foresight

PV photovoltaic

SOC state of charge

SPS seasonal period selection

TC total project costs

TOTEX total expenditures

ToU time of use

1. Introduction

1.1. Motivation

Energy supply concepts in industrial sites are fundamentally challenged by the on-going energy transition. Whereas traditional concepts have been based on fossil fuels, future energy supply systems will integrate volatile renewable energy sources. The integration of renewables adds significant complexity to planning processes. At the same time, continuous progress in digital technologies opens up new opportunities for optimization-based design approaches. Optimization-based design approaches automatically determine a technology selection, equipment sizing, and dispatch strategy by means of mathematical optimization. These approaches assist energy system planners and consultants in computing design variants and thereby enhance quality and speed of planning processes [1]–[3]. The following section outlines four major trends in energy and digital transformation which support and enable the application of optimization-based design approaches.

Decarbonization initiatives from governments and companies
Climate change is widely acknowledged as a key challenge of the 21st century. The Paris Agreement has internationally manifested the long-term goal of holding the global temperature rise below 2 °C of the pre-industrial level. The European Union has announced the target of climate neutrality till 2050, while the German government recently updated their target to 2045 [4]. Industrial sites account for one third of the global energy demand and are thus a crucial element of decarbonization strategies. The European Commission plans a 55 % reduction of greenhouse gases by 2030 and seeks to achieve net-zero by 2050 for all European industrial sites [5]. Climate neutrality requires fundamental changes in energy supply to reduce the use of fossil fuels. Latest developments in the Ukraine conflict in 2022 have led to a significant increase of fuel prices and raised concerns about security of natural gas supply. These developments can accelerate the transition process to alternative renewable sources [6]. The challenge of decarbonization has been recognized by industrial companies [7]: Siemens has announced to reach carbon neutrality for its production sites by 2030 [8]. Similar corporate targets have been announced by the electricity supplier RWE for 2040 [9], the steel manufacturer thyssenkrupp Steel for 2045 [10] and the food processing company Nestlé for 2050 [11]. Both national and corporate initiatives underline a growing recognition that on-site energy supply concepts will face a transformation process with tightened policies towards renewable sources.

Flexibility requirements from volatile renewable generation
Wind farms and photovoltaic plants are widely accepted as key technologies in the energy transition [12]–[14]. These renewable technologies have shown significant learning rates in the past decade:

The installation costs have declined by 81 % for utility-scale photovoltaic and by 31 % for onshore wind from 2010 to 2020 [15]. Decreases in costs accelerate the wide spread application of these technologies. However, solar and wind generation is not dispatchable and thus requires sources of flexibility [16]: End users can profit from cheap electricity prices, e.g., by optimized control of existing on-site power plants or the integration of storage technologies. The flexible operation adds significant complexity to planning processes. Traditional planning processes based on spreadsheet solutions estimate demands and costs on monthly or annual values [17]. These approaches cannot handle time varying attributes introduced by intermittent renewable generation. In contrast, optimization-based design approaches enable efficient simulation in (sub-)hourly resolution. Thereby, they help to integrate storage technologies and account for inherent flexibility options from industrial energy supply systems.

Availability of consistent data from energy monitoring

A key challenge for optimization-based design approaches is the availability of consistent data in adequate time resolution [18]. Environmental and energy management standards such as ISO 14001 and ISO 50001 recommend the deployment of energy monitoring systems to gain transparency of energy use. The number of sites with energy management systems has increased in last years: 6,500 sites were certified according to ISO 50001 standard in Germany in 2020 [19]. Cloud-based monitoring systems continuously document the on-site energy demands. Sub-meters for individual processes help to gain additional transparency over energy demands. The data from the monitoring systems is available for optimization-based design approaches and thereby can improve the accuracy of design decisions.

Enhancements of computer hardware and software

Optimization-based design approaches require large computational resources to solve the underlying mathematical models. The available computational resources have significantly increased in recent years due to both hardware and software enhancements. Advances in silicon lithography have enabled an extension of Moore's law: The performance of digital electronics has roughly doubled in every two years with huge improvements in computational power [20]. Simultaneously, algorithms for solving optimization models have improved, both in speed and in robustness. Commercial software providers such as Gurobi and CPLEX report speed-ups by orders of magnitudes in the last two decades [21], [22]. The number of unsolvable models has decreased by more than 90 % [21]. Enhancements in hardware and software enable more complex optimization models to be solved within practical computation times.

Optimization-based design approaches help to identify sustainable design concepts with reasonable efforts. These approaches have been demonstrated in various use cases, including the design of microgrids [23], [24], buildings [25], [26], infrastructures [27], city districts [28], [29] and industrial sites [18], [30]. This Thesis extends existing work on optimization-based design for distributed energy system. The newly developed optimization framework has been successfully applied in all described use cases during energy consultancy activities. The following work will focus on the application in industrial sites.

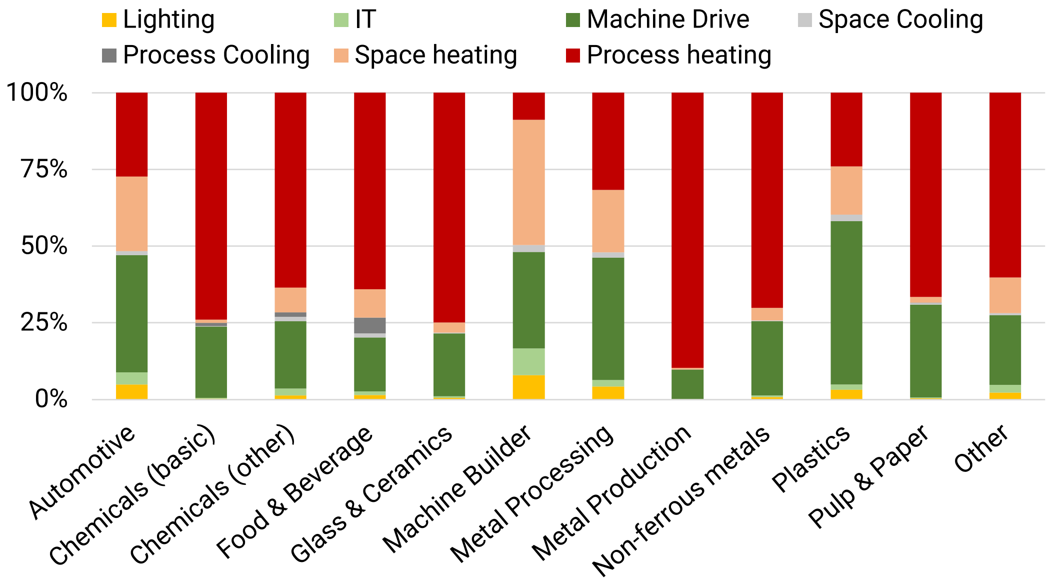

Figure 1.1.: Types of energy use in German industrial sites for 2015 [36]

1.2. Background and context

Integration of renewable sources in industrial sites has gained little attention in the past [31]. Stakeholder attention has mostly focused on energy efficiency measures instead. These measures reduce process demands, e.g., by use of efficient light sources or speed-regulated drives, through avoidance of compressed air leaks and with heat recovery strategies. The impact and costs of energy efficiency measures is thus generally well understood today [32], [33]. An impressive example is the De-risking Energy Efficiency Platform (DEEP). The platform summarizes experiences from more than 12,000 efficiency measures in industrial sites across Europe [34]. It finds a median payback period of 2.8 years. Efficiency measures allow a cost-effective reduction of energy demands and thus reduce the dependency on fossil fuels. However, efficiency measures alone are not sufficient to reach the described decarbonization targets [5]. The full replacement of fossil fuels requires changes in energy supply concepts. Optimization-based design approaches help to find the most effective options to meet decarbonization targets for industrial energy supply.

Industrial sites combine high on-site electrical and thermal demands. Statistics on types of energy end use in German industry are shown in Figure 1.2. Thermal demands are needed mostly for process heating and in smaller amounts also for space heating. Process heating requirements are highly diverse: Temperature requirements range from below 80 °C for tempering and washing in the food and beverage sector to above 1000 °C for metal melting. Low temperatures can be supplied by heat pump and solar technologies, whereas high temperature processes often require the use of burners based on fossil or renewable fuels. A detailed analysis on process heating requirements is provided by Lauterbach [35]. The share of thermal demands varies significantly across sectors: Industrial sites in the basic material sector comprise high shares of process heating, e.g., 90 % in the metal production. Sites in manufacturing sector account for higher shares of electricity. For instance, machine drives account for 38 % of energy use in automotive industry.

The simultaneous demand of electricity and thermal demands favours the integration of energy supply systems: Co-generation plants generate electricity for machine drives, lighting and IT. The

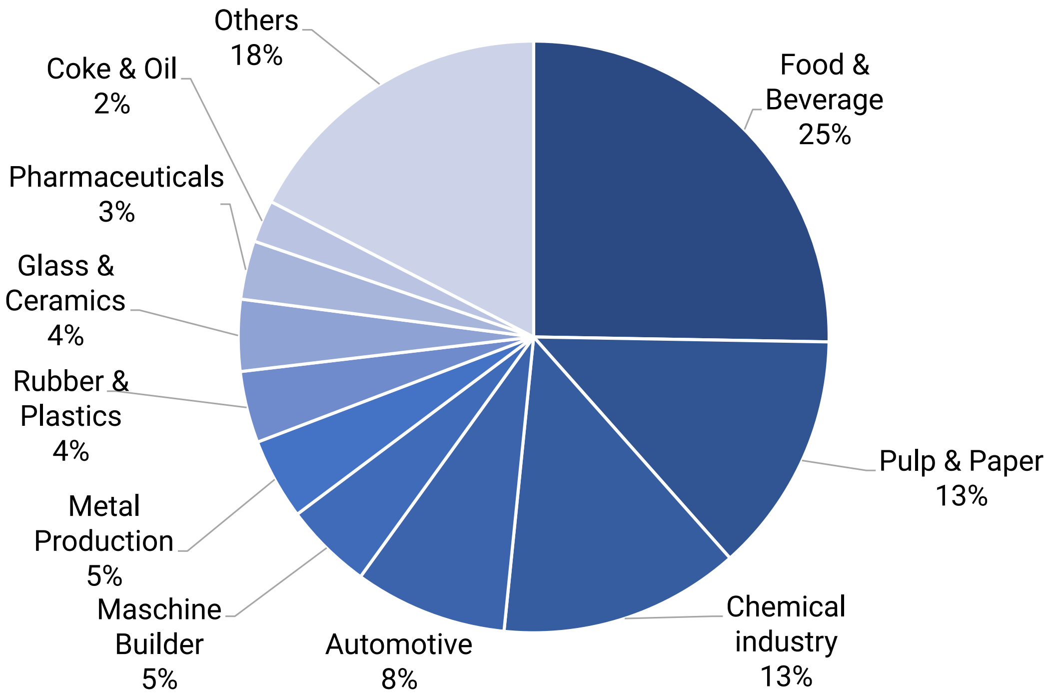

Figure 1.2.: Industrial sectors with large cogeneration plants (> 1 MW) in Germany 2019 (N = 562) based on [40]

waste heat from co-generation is effectively used for process steam demands or recovered by absorption chillers to deliver cooling [32], [33]. In Germany, the deployment of co-generation plants has been supported by favorable electricity-to-gas price ratios and governmental subsidies. Figure 1.2 shows the number of industrial sites with large scale co-generation plants in 2019. Co-generation is intensively used in sectors with high heating or steam demands such as the food and beverage, pulp and paper, automotive or chemical industry. These sectors account for 60 % of the sites with large-scale co-generation plants. Several studies have successfully demonstrated the capabilities of optimization-based design approaches for complex energy supply systems including co-generation plants [37]–[39].

Equipment in industrial energy supply systems typically has long depreciation periods: Boilers and co-generation plants are replaced after 12 to 25 years. Distribution systems for heating and cooling have even longer lifetimes of 30 to 50 years [41]. The economic and regulatory conditions are projected to change significantly during these depreciation periods, as outlined in Section 1.1. Decision makers in industrial companies are becoming increasingly aware that their long-lived equipment might be stranded with increasing shares of renewables [42]. In particular, the role of co-generation plants is expected to change with ongoing decarbonization initiatives [43], [44]. Renewable generation from wind and solar could be integrated by heat pumps to meet process and space heating demands. Fossil fuels might also be replaced by biomass or synthetic fuels [45]–[47]. In this challenging context, energy system planners and consultants need to find sustainable design concepts for complex industrial energy supply systems. Optimization-based design approaches help to gain clarity on design trade-offs and thereby identify non-regret decisions considering financial and climate targets.

1.3. Objective, contributions and structure

The trends described favor the use of optimization-based design approaches for the investment planning of industrial energy supply systems. The benefits of these approaches have been highlighted by various authors [18], [27], [29], [30], [48]. Major advantages compared to existing spreadsheet solutions are threefold. First, optimization-based design approaches require no manual pre-selection of technologies based on planners' individual experiences. They are thus more time efficient, particularly if extensive scenario analysis in multi-year concepts is required. Simulation of multiple scenarios provides a solid information basis for decision-makeres, resulting in non-regret investment decisions. Second, optimization-based design approaches automate parts of the decision process. Automation leads to more reproducible results across project development teams and production sites. Experience from similar projects is available in a standardized format and can be easily used to refine estimations for new projects. Third, optimization-based design approaches enable enhanced visualization techniques, in particular for complex energy supply concepts with high shares of volatile renewable generation. Interactive visualization techniques help to explain stakeholders with different levels of technical understanding complex design decisions.

Optimization-based design approaches thus have the potential to assist energy system planners and consultants in their daily work and thereby lead to faster and more accurate planning decisions for industrial energy supply infrastructure. The main research topic of this Thesis is defined as follows:

How can sustainable transformation concepts for the complex energy and media supply at industrial sites be efficiently determined?

This work extends existing work for practical applications. The major contributions of this Thesis are related to four focus research questions:

1. Which modeling approaches are suitable to represent the multitude of technologies and regulatory frameworks at industrial sites?
2. What methods help to guarantee security of supply during grid outages and component failures and avoid costly production interruptions?
3. Which temporal aggregation is possible to obtain highly accurate design concepts from an efficient and robust solving process of the underlying mathematical models?
4. How can long-term developments in technologies, energy prices and demands be taken into account in the decision-making process for todays investments?

This Thesis develops a novel optimization framework to answer the above mentioned focus research questions. It is divided into six main chapters. This chapter has outlined the motivation and background for optimization-based planning approaches in industrial energy supply systems. Chapter 2 derives the mathematical planning problem for interlinked and heterogeneous infrastructure requirements typically found at industrial sites. A review of academic work reveals limitations of existing modeling approaches. Chapter 3 introduces the techno-economic model which handles the described complexity accounting for both security of supply requirements [49] and long-term trends of energy prices and demands [50]. The techno-economic model is integrated in a newly developed optimization framework described in Chapter 4. The framework presents modeling techniques to reduce computational complexity of the optimization model [51]. Thereby, it ensures realistic solving times for practical applications. Chapter 5 provides numerical simulation results for three examplary production sites from automotive, food, and pharmaceutical industry in Southern Germany. Results highlight the suitability of the proposed framework to identify decarbonization measures for highly complex industrial energy supply systems. Finally, Chapter 6 summarizes the relevant findings and gives outlook on future research opportunities.

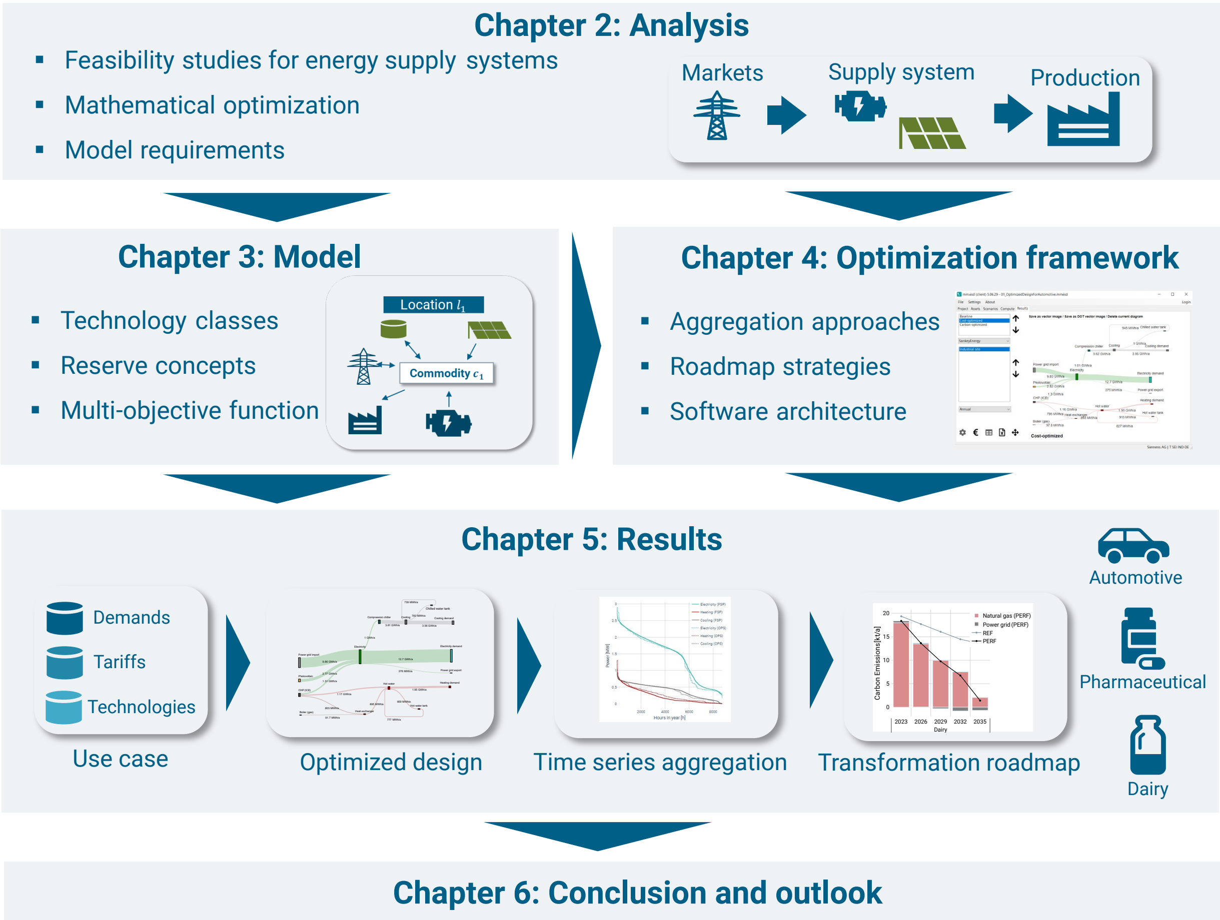

Figure 1.3.: Structure of this Thesis

2. Analysis

This chapter reviews state-of-the-art approaches to design highly complex energy supply systems in industrial sites. Section 2.1 introduces the context of on-site energy supply systems found in industrial sites. The planning process is a complex task and thus typically divided into multiple stages. Feasibility studies are conducted at the beginning of a planning process and determine a pre-liminary design concept from multiple design variants, as outlined in Section 2.2. Section 2.3 highlights how mixed-integer linear programming (MILP) can enhance this decision process during feasibility studies. Section 2.4 reviews existing research and their limitations in the field of distributed energy systems. Practical applications require high computational efficiency of optimization models. Existing techniques to improve model performance are reviewed in Section 2.5. Section 2.6 summarizes the requirements for a method to design sustainable energy supply systems for industrial sites.

2.1. Energy supply systems in industrial sites

Energy supply systems describe the on-site infrastructure which is necessary to meet various types of on-site energy demands from production processes. The demands typically exceed the on-site generation potential in industrial sites. Therefore, energy carriers need to be procured from energy markets. The system boundaries are illustrated in Figure 2.1. Energy supply systems are often highly integrated to capture benefits from multi-modal coupling. Moreover, they comprise a variety of general purpose and sector specific technologies. The interlinking and heterogeneity of these systems makes design decisions highly challenging, in particular for the integration of renewable energies in brownfield sites with historically grown infrastructure.

Interface to production processes

Energy demands in industrial sites include electricity, thermal demands at different temperature levels, compressed and fresh air as well as sector specific process gases. These demands are determined by the requirements of the production processes [32]. The consumption patterns of processes are typically described by hourly average values over one representative year [52]. Thereby, daily patterns of shift operations as well as seasonal variations in demands are adequately captured. Some energy intensive production processes generate waste heat. Waste heat can be fed as a low-grade heat source into the energy supply system.

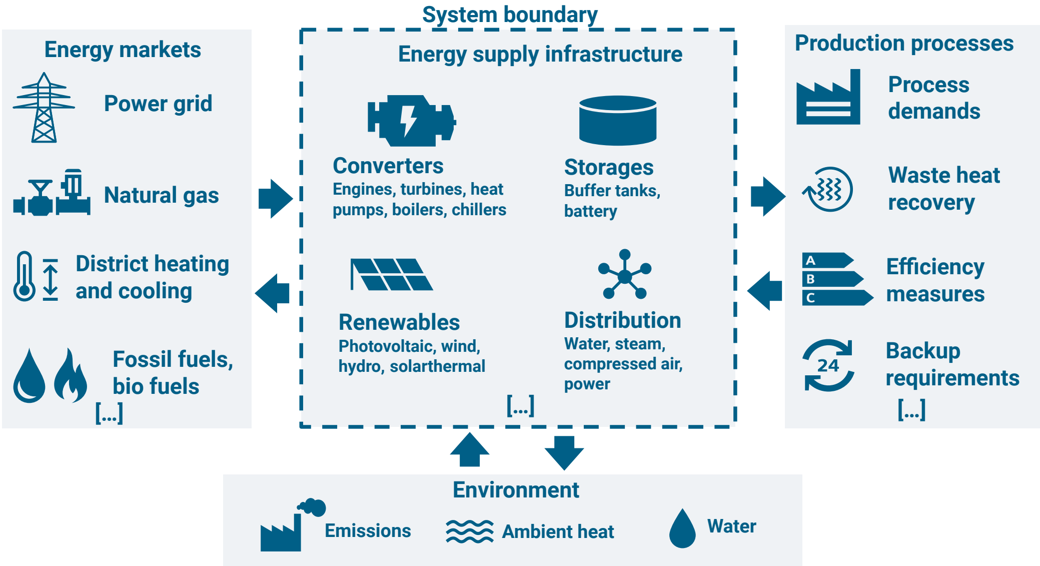

Figure 2.1.: System boundary of industrial energy supply systems (adapted from [18])

Energy supply infrastructure

The energy supply system comprises conversion technologies, storage facilities, renewable generation as well as distribution systems. Energy supply equipment is typically installed in one technical center which supplies the demands of all production facilities throughout the site. Larger sites might comprise several technical centers. Conversion technologies are placed within these technical centers. Typical conversion technologies are boilers and thermal engines which feed a local heat network. Industrial heat pumps use waste heat from processes and provide a low carbon alternative [53]. If waste heat is not available as a heat source, ambient heat from adjacent waters or geothermal sources might be used. Engines, boilers, and heat pumps are general-purpose technologies which are employed in multiple industrial sectors. General-purpose technologies are complemented by sector specific technologies. These technologies are closely linked to the production processes and their requirements, such as air separation units or electric arc furnaces in the non-ferrous metal industry [49]. Solar power systems can be installed on roofs of administrative buildings, parking places or production halls in most industrial sites. Other renewable generation such as wind turbines or ground-mounted photovoltaic panels might be installed in neighboring areas of the production plant depending on the local conditions. The increasing share of volatile renewable generation enforces more flexible operation modes of cogeneration systems with lower total utilization rates [4]. Flexible operation concepts might be complemented by storage technologies such as hot water tanks or batteries. Hot water tanks decouple peak demands and heat generation. Among others, this enables a flexible operation of cogeneration plants during times with low renewable generation. Use cases for battery energy storages are today mostly limited to reduction of peak purchase from power grid [54], [55]. However, investment costs for batteries are projected to significantly decline in the next decade [56]. Energy supply systems comprise a large variety of long-living technologies. The assets which are installed today will remain for the upcoming decades [41] and thus see the continuous integration of renewables in energy markets.

Interface to energy markets

Industrial energy supply systems are connected to energy markets, e.g., via the public power grid or the natural gas grid. Tariffs for electricity purchase typically include various components. Energy related components of tariffs comprise long-term contracts with fixed prices and volumes as well as time of use (ToU) pricing or real time pricing schemas [57], [58]. Demand charges for network usage are calculated from the peak purchase. This incentivizes active peak load management and requires high temporal granularity of planning approaches. Approaches with hourly resolutions are widely accepted for these types of simulation [59]. Some industrial sites have access to district heating and cooling networks. The energy supply system in these sites acts either as a supplier [60] or a consumer [47]. Beyond energy procurement from networks, other fossil or renewable fuels might be delivered via trucks or trains, e.g., heating oil, wood pellets, hydrogen, or propane. After delivery, these fuels are temporarily stored in on-site tanks [49].

Energy supply systems in industrial sites comprise a variety of conversion, storage, and distribution technologies as well as complex energy procurement tariffs. Integration of volatile renewable generation challenges existing energy supply concepts. The heterogeneity and interlinking of the various options make the design and operation of industrial energy supply systems a highly complex task.

2.2. Strategic planning of energy supply systems

Design of industrial energy supply systems is a highly complex task. Therefore, planning processes are divided in different stages. One of these stages are feasibility studies to determine preliminary design concepts and define a strategic vision. Requirements for feasibility studies are derived and compared to established software solutions for simulation.

Stages of planning process

Planning processes in energy consultancy projects are typically divided in several stages. Figure 2.2 illustrates a sequence based on the German standard VDI 3922. The sequence defines six stages from project definition to operation. A project starts with the definition of targets and boundary conditions. Moreover, stakeholders agree on a set of key performance indicators. Typical indicators are linked to the economic efficiency, energetic performance, and ecological impact of energy supply. The set of indicators is used in the following feasibility study to quantitatively compare multiple preliminary design variants. This comparison is based on first estimations which include the relevant techno-economic characteristics for the decision process. Different design variants are presented to and discussed with all relevant stakeholders. Feasibility studies result in a selection of one design concept from the analyzed design variants. The selected design concept is refined in the detailed engineering stage. The detailed engineering stage is followed by a specification stage which plans the implementation of the design concept. The commissioning of new plants and systems defines the transition from the implementation to the operation stage. The operational data is usually monitored to optimize planning decisions.

Feasibility studies illustrate the benefits and drawbacks of different design variants in early project phases. Providing clear understanding of business and engineering requirements, feasibility studies increase stakeholders confidence and consequently the chances of realization. Major design changes become practically infeasible with increasing level of detail being added in the course of a project. The selection of a robust design variant avoids time consuming replanning in later project stages. Therefore, feasibility studies are an established element in the planning process for sustainable

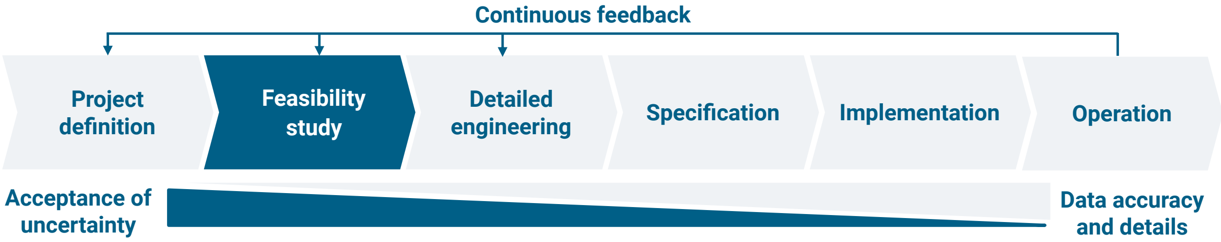

Figure 2.2.: Typical stages of energy consultancy projects based on VDI 3922 [52]. Techno-economic data is estimated during feasibility studies with high acceptance of uncertainty. Data accuracy is continuously increased in the following stages by adding technical details (adapted from [3]).

energy supply systems. This Thesis develops an optimization-based decision support framework for feasibility studies.

Challenges during feasibility studies

Feasibility studies target at preliminary design variants with a selection and sizing of technologies as well as decisions for procurement options. Decision-making requires a clear understanding of the implications which results from a comparison of multiple design variants and can be communicated across all stakeholders. Design variants are analyzed regarding their cost structure and economic robustness over the entire project horizon. The project horizon covers several decades due to the long-living character of energy supply equipment. The analysis is typically conducted based on normative standards such as VDI 2067 [41] and VDI 6025 [61]. It includes an economic assessment of annualized capital-related costs, demand-related costs for commodity procurements and operational-related costs for maintenance and servicing. Parameters for this economic assessment are generally not known exactly during feasibility studies. Thus, they need to be estimated based on available knowledge. The estimations introduce significant uncertainty to the planning process. A good summary on this topic is given by Mavromatidis in [62]. Three major sources of uncertainty are technology characteristics, energy demands and energy procurement costs.

- **Technology characteristics:** Investment costs, efficiencies, and degradation for all technology options need to be estimated. Detailed information of on-site conditions for installations is generally not available during feasibility studies. Therefore, cost estimations are limited to preliminary rule of thumb estimations. Figure 2.3 shows an example of investment cost estimations for a CHP plant.

- **Energy demand forecasts**: Energy demands are taken either from measurements of production processes or from profile generators based on corporate and normative standards. The use of production facilities and its related energy demands is likely to change during the lifetime of energy supply equipment, e.g., by process innovation or market changes.

- **Energy procurement projections:** Procurement costs for electricity and fuels are estimated for the entire multi-decade project horizons. Recent political developments in the global energy markets have highlighted the high uncertainty of medium- to long-term cost projections.

Two types of parameter uncertainty are distinguished: epistemic and aleatoric uncertainties [63], [64]. Epistemic uncertainty reduces with increasing knowledge and data during later stages of energy consultancy projects. For instance, binding offers with costs and performance guarantees are aligned with vendors in the specification phase reducing the uncertainty in technology characteristics. Additional simulation techniques help to enhance transparency on input parameters, e.g., shading simulations for roof-top PV installations. In contrast, aleatoric uncertainty results from various random or political prosses and cannot be significantly reduced with additional efforts for data acquisition. For instance, tariffs for electricity procurement are highly impacted by changes in the regulatory framework and developments on fuel markets. These uncertainties are not adequately described by stochastic processes or probability functions [63], [65]. Consequently, the risks arising from uncertainties need to be evaluated by rigorous scenario analysis or parameter variations. These approaches allow to identify tipping points where investments turn to be not economically viable [52]. Thereby, the robustness of the design concept is approved leading to no-regret investment decisions.

Requirements for industrial energy supply systems

Feasibility studies prove the technical and economic robustness of a preliminary design concept and support stakeholders in making non-regret investment decisions. Therefore, approaches to support feasibility studies need to meet certain requirements. These requirements serve as criteria to analyze existing solutions and mathematical modeling approaches. Following the recommendations in VDI 3922 [52], the requirements are defined as follows:

1. **Evaluation of economic, ecological and energetic performance:** Methods supporting feasibility studies derive key indicators to compare multiple design variants regarding their economic, ecological and energetic performance. The comparison of design variants depicts all technical solutions available in the market. The method thus needs to be vendor neutral, e.g., not limiting itself to the offerings of a single manufacturer. Assessments of economic and ecological performance shall consider the long-living character of energy supply equipment and associated impact of long-term trends.

2. **Multi-modal coupling and heterogenity of energy supply:** Sector-coupling technologies such as CHPs and HPs interlink energy supply systems for electricity, steam, heating and cooling. The method thus captures the interaction between the various on-site energy supply systems. Requirements for industrial energy supply are highly application specific. A method shall thus be adaptable to sector-specific technologies and consider value of storage technologies.

3. **Adequate technology and load models:** Characteristics of energy supply equipment and energy demands are reflected as far as they are known during a feasibility study. Characteristics of conversion technologies might include temperature and part-load dependent behavior [18]. Demand representation depends on the availability and granularity of on-site measurements. Changes in energy demands occur due to continuous implementations of efficiency measures or expected expansions of on-site production facilities. These changes need to be captured by a methodology.

4. **Complex procurement tariffs:** The method accounts for complex energy procurement tariffs. Increasing penetration of renewable energy leads to more volatility of spot market prices. Electricity generation from roof-top photovoltaic might exceed on-site demand during

noon in the summer. Both spot market prices and on-site photovoltaic installations promote a more flexible operation of energy supply equipment. Moreover, active management of peak loads can reduce network charges. Storage technologies and advanced control schemes enable cost savings and reduce carbon footprints [66].

5. **Applicability in consultancy projects:** The method leads to reproduceable and comprehensible results. Dynamic changes in customer requirements can be included during the course of a consultancy project. Therefore, results from the method are available in an adequate time frame, e.g., in minutes to hours. Moreover, results need to be comprehensible for all relevant stakeholders. Relevant stakeholders in factories have different levels of technical understanding, e.g., factory management, procurement, production planning and energy management [67].

Established solutions for feasibility studies

Established design approaches are often based on simplified calculations conducted in spreadsheet solutions [68]. These calculations typically rely on normative standards, such as DIN 18599 [17]. They enable first and quick estimations from monthly or yearly values. Spreadsheet approaches do not provide the temporal granularity to reflect complex procurement tariffs which become more viable with increasing penetration of renewables. Moreover, technology models are strongly simplified. This drawback is overcome by commercial simulation tools. Notable simulation tools are energyPRO [69], HomerPro® [70] and TOP-Energy® [71]. These tools simulate optimal dispatch strategies for pre-defined configurations. Simulations allow to derive key performance indicator (KPI) that can be studied within a graphical user interface. The dispatch strategies are determined in a rolling horizon approach, either by means of heuristics (energyPro and HomerPro®) or by mathematical optimization (energyPro and TopEnergy®). Modeling approaches applied by these tools require high manual efforts and experience to manually define configurations for multiple design variants. Efforts further increase if transformation roadmaps include long-term climate targets. Time coupling constraints such as constraints on annual full load hours cannot be adequately reflected by existing simulation approaches. Moreover, the selection of technologies is often limited to a pre-defined selection. For instance, HomerPro® does not include heat pumps or thermal storage technologies. Therefore, the applicability of these simulation tools is limited for the highly complex design of industrial energy supply system. Various researchers have identified mathematical optimization as a promising alternative to design industrial energy systems [18], [27], [30].

2.3. Mathematical optimization

Feasibility studies target at the definition of preliminary design concepts for industrial energy supply systems. Optimization-based design approaches allow to formulate the described domain specific planning problem as a mathematical optimization problem. Solving the mathematical problem provides a design variant for a defined set of input parameters. Possible solutions are restricted by constraints which represent the technical and economical boundary conditions. Optimization models are typically divided into linear program (LP), integer program (IP), mixed integer non-linear program (MINLP) and mixed integer linear program (MILP) depending on the types of variables and the formulation of the objective and constraints.

Comparison of LP, IP, MILP and MINLP

Linear programs (LP) enable modelling of continuous properties and scale well on large energy supply systems. However, typical design problems include non-linear characteristics: Technologies such as cogeneration plants have lower specific investment costs for larger units due to economies of scale. Moreover, the behavior in part-load operation is strongly non-linear which cannot be reflected by a continuous modelling approach [29]. In contrast to linear programs, integer programs include discrete variables but do not account for continuous design and operating ranges. IPs include only discrete unit sizes (e.g., modules of a single vendor) and discrete operating states (on and off states). Given these drawbacks, MINLP approaches have been proposed for energy system design problems [18], [72]. MINLP enables modelling of a large variety of functions. The major drawback of MINLP is the solving process: Global optimization strategies are not capable of finding solutions in adequate solving times [18]. Therefore, metaheuristic solving techniques are proposed such as evolutionary algorithms. These solving techniques often find local minima instead of the global optimum [73]. The solution quality cannot be obtained from the solving process. Therefore, solving processes might converge to suboptimal mathematical solutions [29], [74]. As an alternative, non-linear functions from MINLP can be approximated by piece-wise linear functions, e.g., by Glovers linearization scheme ("big-M" method) [75], [76]. The resulting optimization problem is formulated as a MILP. Therefore, the majority of existing work identifies MILP as the most suitable choice for techno-economic planning models [29], [74], [77], [78].

An example for a piece-wise linearization of investment costs is provided in Figure 2.3. Investment costs for a CHP plant have been analyzed in an extensive vendor survey with 295 modules in [79]. The consideration of all possible modules would reflect the reality on the market exactly. However, this approach requires enormous knowledge on all vendors and detailed assumptions on installation and assembly setups. This knowledge is not available in the required level of detail during feasibility studies [80]. Alternatively, the report of the survey provides piecewise defined power functions to estimated investment costs. This non-linear behavior is well approximated by a MILP approach: Smaller CHP module sizes have higher specific investment costs. A LP assumes investment costs to be independent of the module size. LPs thus cannot reflect the economy of scales making MILP the preferred choice for on-site energy systems. A detailed analysis of investment models for other conversion, renewable and storage technologies is provided in [27].

Generic formulation and solving process of MILPs

This Thesis employs a MILP approach to design energy supply systems. A MILP in its generic formulation is given in Equation 2.1. The variable vector X comprises both continuous variables $x^{\text{Cont}} \in \mathbb{R}^+$ and discrete variables $x^{\text{Disc}} \in \{0, 1\}$. These variables are subjected to boundary conditions described in the matrix A and penalized with costs c^T. The global optimum is derived by minimizing the costs associated with the solution. The solution vector for X comprises all design and operational decisions associated with the cost optimal solution. It can therefore be used to determine the relevant KPIs of the design concept.

$$\min_{x \in X} c^T x \tag{2.1}$$

$$s.t. Ax \leq b \tag{2.2}$$

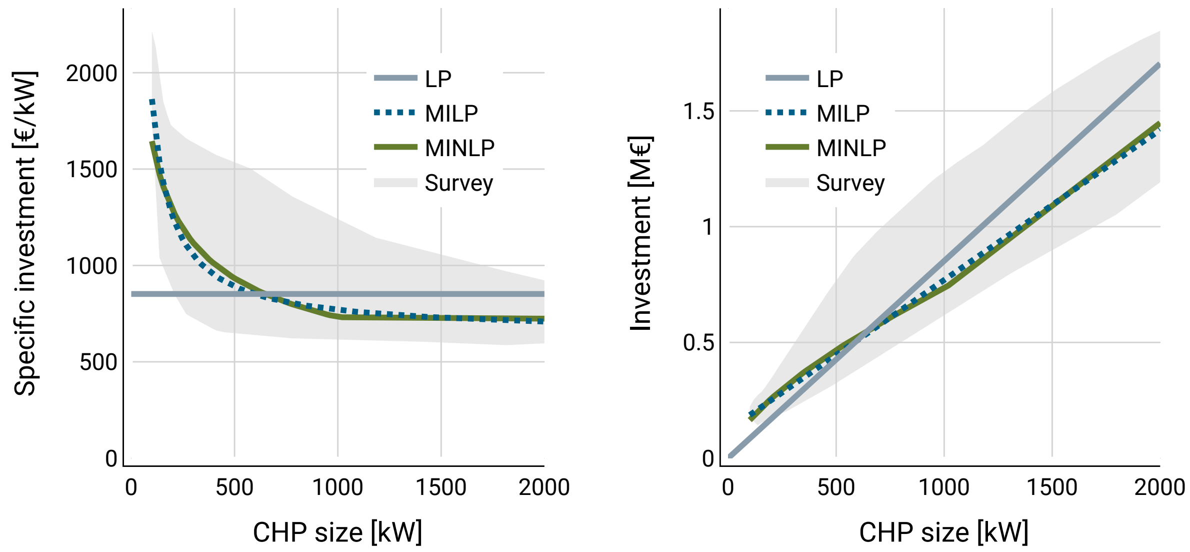

(a) Specific investment costs

(b) Absolute investment costs

Figure 2.3.: Comparison of LP, MILP and MINLP modeling approaches to estimate the investment costs for the example of a CHP plant with internal combustion engines. Non-linear cost estimations and uncertainty range is based on a survey for 295 modules from 61 vendors [79]

MILP problems are non-convex problems. However, they can be efficiently solved by branch and bound (B&B) algorithms [29], [48]. In the first step of a B&B algorithm, all discrete variables are relaxed to continuous variables. The resulting linear program is solved by simplex or interior point methods. This step is called root relaxation. The root relaxation defines a first lower bound for the objective function. The relaxed variables are iteratively fixed to discrete variables. If all relaxed variables take discrete values, a feasible solution of the optimization problem is found which defines an upper bound for the objective function. Based on systematic search strategies, the gap between upper and lower bound is iteratively decreased. For practical applications, this process is often aborted if a user specified termination criterion ("MIP gap") is met. If a feasible solution exists, the B&B algorithm converges to the global optimum solution [81]. Commercial and open-source solvers offer high performance implementations of the Branch-And-Bound algorithm [21], [22]. This work employs a commercial solving software and focuses on the formulation and application of optimization models for the sustainable design of industrial energy supply systems.

2.4. Multi-modal energy system design

Techno-economic planning models have intensively applied MILP optimization to determine sustainable design conceptsfor multi-modal energy supply systems. A selection of related academic work is provided in Table 2.1. The use of optimization techniques for energy system design has a long history: Papoulias and Grossmann are considered as the pioneers in the field of optimization-based energy system design. They have proposed an optimization model of a utility system for electricity and steam in 1983 [82]. Their model includes a single time step assuming constant demands over the entire planning horizon. With developments in hardware and software, models have become more complex: Yokoyama et al. have proposed a MILP model to design an energy supply system for electricity, steam, heating and cooling in 2002 [83]. The proposed model includes three representative days in different time resolutions. In this study, CPLEX has been employed as a commercial solving software. The authors find only suboptimal solutions if hourly time steps are considered. Similar issues have apparently been solved in the later work of the authors published in 2015 [84]. The authors find for engineering practice acceptable solving times between one second and 2.5 h depending on the model type and solving strategy. Enhancements in commercial solvers have enabled the solving of complex MILP for energy system design. MILP is thus frequently employed by multiple researchers. The following paragraphs summarize research on optimized design approaches for distributed energy systems and identify gaps in existing work for industrial energy supply systems.

Application for buildings, urban districts and microgrids

Mancarella have reviewed techno-economic planning approaches for urban energy planning in 2014 [77]. He finds MILP planning approaches being underestimated compared to classical techniques and sees the role of these models needs to be re-defined in future energy systems with high shares of volatile renewable generation. This trend in urban energy system planning is highlighted by a high number of research activities in this field [28], [29], [105], [106]. Various authors have added additional technology and tariff details to the techno-economic models, e.g., to consider retrofit measures for building envelopes [29]. Beyond city districts, planning approaches have been adapted for building energy systems in airports by Thiem [66]. Besides applications in the area of buildings and city districts, techno-economic planning approaches are applied to design microgrid solutions for off-grid communities or military sites. Stadler et al. in [88] apply their approach to 13 microgrid projects. They find their planning model being viable for the design of energy supply systems with photovoltaic and batteries with Diesel backups. Microgrid planning approaches strongly focus on the electricity sector and typically omit thermal energy demands. In contrast, energy supply systems in industrial sites combine on-site electricity and thermal demands.

Application for industrial energy supply systems

Planning models based on MILPs have also been demonstrated for the design of energy supply infrastructure of industrial sites. Andiappan et al. analyze the impact of reliability on the design of biomass-fired trigeneration systems [39], [86]. The authors formulate a redundancy allocation problem for failure of the largest unit. They find redundant equipment to have a great impact on the unit capacity for each technology. Hollermann et al. [102] integrate redundant equipment in the energy supply system of a pharmaceutical site. Authors find an increase of 4 % of total annualized costs for redundant equipment whereas the solving times almost triple by considering redundancy constraints. Both the work of Andiappan and Hollermann limit themselves to trigeneration systems without considering heat pumps as a viable alternative. Latest research overcomes this limitation. Wallerand in 2018 [53] for a dairy site and Urbanucci in 2019 [96] for a pharmaceutical site discuss the integration of heat pumps in industrial energy supply systems. Wallerand proposes a methodology to integrate solar energy via heat pumps [30]. Different production processes in the dairy are analyzed via Pinch analysis. Results of the Pinch analysis are integrated as steam demands at various temperature levels in the planning model. With the planning model, Wallerand determines a Pareto trade-off between cost efficiency and environmental impact by carbon emissions from ten typical days. The work does not consider cogeneration plants. In

Table 2.1.: Selection of work on MILP design approaches in distributed energy systems

Author	Year	Description
Papoulias [82]	1983	Structural optimization of a utility system for electricity and steam at various pressure levels
Yokoyama [83], [84]	2002	Structural design of cogeneration systems considering decomposition approaches
Voll [18], [85]	2012	Automated optimization of an energy supply system in pharmaceutical industry
Mancarella [77]	2014	Local emission impact of distributed cogeneration systems in part-load ratio operation
Andiappan [39], [86]	2016	Redundancy allocation for tri-generation systems including seasonality of biomass availability and energy demand
Stadler [87], [88]	2016	Optimal design in microgrid projects with XENDEE platform
Thiem [27], [66]	2017	Optimal design of energy supply in airports considering detailed technology models
Gabrielli [89], [90]	2018	Optimal system design with thermal and hydrogen storage technologies
Bahl [91]–[93]	2018	Optimization-based design of manufacturing energy systems by time-series aggregation
Schütz [29], [80], [94]	2018	Optimal design of city districts with decomposition and clustering approaches
Wallerand [30], [95]	2018	Integration of solar energy in dairy industry with coupling of pinch analysis and techno-economic optimization
Urbanucci [96], [97]	2019	Optimal design and operation of cogeneration-based distributed energy systems with focus on integration of heat pumps
Teichgräber [98]	2019	Time series aggregation for optimization of generic energy systems
Bohlayer [99], [100]	2020	Multi-period transformation roadmaps for distributed energy systems
Hollermann [101], [102]	2020	Robust optimal design of distributed energy supply systems
Mavromatidis [63], [103]	2021	Long-term investment planning of building multi-energy system and envelope retrofits
Richarz [104]	2022	Optimal scheduling of retrofit measures for equipment and envelope in commercial buildings

contrast, Urbanucci model formulation focus on the integration of heat pumps in trigeneration systems with CHP plant and absorption chillers for an entire year with 8760 h. Both authors find cost and carbon saving potentials from the integration of heat pumps.

Technology pathways in generation expansion planning

The previously described work has determined optimal design concepts for microgrids, urban districts or industrial sites based on an entire base year or a selection of representative periods from a base year. Energy supply concepts are expected to evolve over time, as outlined in Section 1.1. Long-term trends can be integrated into techno-economic planning models by roadmap optimization considering multiple extension stages. Techno-economic optimization models help to derive technology pathways. These pathways account for future replacement in aged infrastructure as well as the ability to delay investment decisions ("wait-and-see"). Moreover, roadmaps ensure non-regret investment decision as lock-in effects are considered [50]. Technology pathways are widely employed in generation expansion planning of regions and countries [2], [107], [108]. These models strongly aggregate demands and simplify technology models. For instance, replacement decisions before end of technical lifetime are not adequately reflected in the model formulations. The model formulations from generation expansion planning are thus not directly applicable for distributed energy systems.

Transformation roadmaps for distributed energy systems

Transformation roadmaps with multiple extension stages describe the evolution of an distributed energy system. Roadmaps have not been frequently considered in the past. Latest reasearch work in the last three years have shown significant progress in this field: Pecenak for microgrids in 2019 [109], Bohlayer for an industrial complex in 2021 [99], Mavromatidis for a city district in 2021 [63], [103] and Richarz for non-residential buildings in 2022 [104] have demonstrated the capabilities of multi-year planning. Pecenak et al. [109] analyze the impact of investment decline in photovoltaic and batteries as well as the introduction of a carbon tax in a multi-decade planning horizon. The authors compare a sequential roadmap approach ("adaptive planning model") with myopic foresight to a strategic roadmap approach ("forward-looking model") with perfect foresight over the entire planning horizon. The two approaches result in similar design concepts with 1.6 MW photovoltaic installations and 4 MWh battery storage. The authors find the sequential approach to be more than nine times faster compared to the strategic approach. Bohlayer et al. [99] apply a multi-year planning approach to various industrial sites. The authors formulate both stochastic and deterministic multi-year investment models. For the analyzed industrial energy system, the deterministic formulation is found to be superior in terms of accuracy and solving time. Mavromatidis et al. introduce the MANGO [63] for multi-stage energy optimization of campus solutions. Results indicate that the long-term perspective of a growing city district is well captured by a multi-year planning approach. The authors consider extension of floor area, varying investment costs for supply technologies and rising energy carrier prices with five years long extension stages for a 30 year planning horizon. An extension of the MANGO framework [103] allows to integrate capital intensive retrofit measures in the decision process. Richarz et al. [104] propose a model formulation for buildings with retrofit measures. The authors consider every third year as an extension stage with a planning horizon of 30 years. The results indicate significant potential for carbon and cost savings by an improved schedule of optimization measures. The four approaches from Pecenak, Bohlayer, Mavromatidis and Richarz have proposed planning models with multiple extension stages. However, the effect of foresight on investment decisions have been

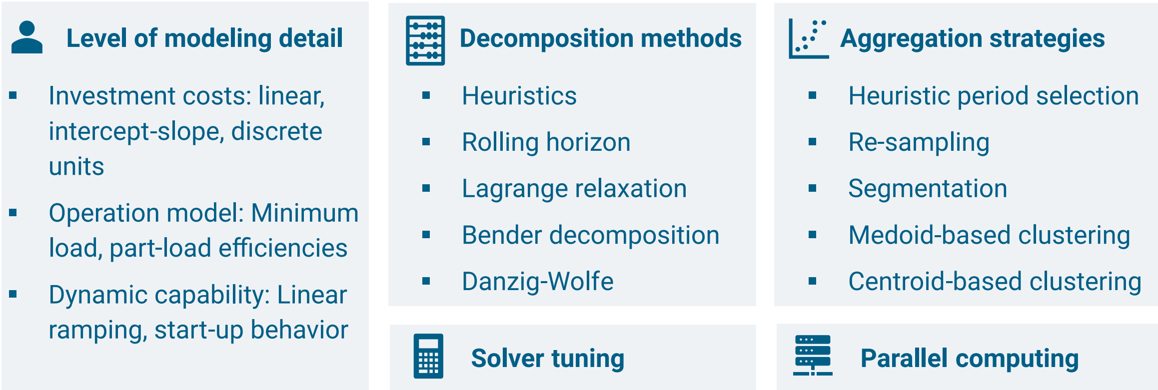

Figure 2.4.: Overview on concepts for improving performance of energy system design models

only discussed by Pecenak. Their model approach targets at microgrid designs of photovoltaic and battery systems with Diesel backup. The effect of multi-modal coupling has thus not been analyzed in their work. This Thesis will propose a novel framework which captures the impact of long-term trends for multi-modal energy supply systems.

Summary

MILP-based planning models are well established for design of distributed energy systems. Transformation roadmaps for sustainable evolution of energy supply systems are not widely applied yet, but promise a clear strategic view for industrial stakeholders. Integration of multiple extension stages leads to increased model sizes and computational complexities [109]. However, the computation of full scale model for a base year with 8760 h can take up to several days [88]. Therefore, full scale models with multiple extension stages are not applicable for feasibility studies, in particular if extensive scenarios analysis and dynamic consideration of customer feedback is conducted. Consequently, techniques for compact model formulations and reduced computation times are required. The following section will discuss approaches to improve model performance.

2.5. Improvement of model performance

Techno-economic planning models based on MILP are computational complex, in particular if non-convex characteristics such as economies of scale or part-load capabilities are considered. Parameters of these models comprise significant uncertainty as outlined in Section 2.2. Near-optimal solutions are sufficient for practical applications [110], e.g., resulting from minor reduction of modeling accuracy. An overview of possible strategies to improve model performance is shown in Figure 2.5. Excellent reviews on this topic are provided by Kotzur et al. for distributed energy systems [78] and by Cao et al. for regional energy systems [111]. Solver tuning targets at optimized settings of commercial solvers. Authors of [111] recommend to adapt tolerance settings of the barrier algorithm and enable multi-threading. Additional performance improvements are achieved by computing multiple scenarios in parallel. The two strategies are not directly linked to the formulation of the optimization model. The following analysis will thus focus on the level of modeling detail, decomposition methods and aggregation strategies.

Level of modeling detail

Multi-modal energy supply systems in industrial sites comprise a variety of technologies. Discrete characteristics such as non-linear investment costs or part-load capabilities add high computationally complexity to the model. The level of detail for investment costs and operational models thus has a significant impact on model performance.[1] Limiting the level of detail is a common approach to improve model performance [78].

Models of investment costs reflect the sizing characteristics of a technology. Linear approaches consider constant specific investment costs for all unit sizes. In contrast, intercept slope approaches consider economies of scale effects as shown in Figure 2.3a. Additional details can be considered by piece-wise definition of technology models depending on the unit size. Some researchers have proposed to consider discrete module sizes in their formulations [113], [114]. These approaches add multiple binaries per technology. Moreover, they require detailed knowledge on module costs. This level of detail is typically not available for a broad range of technologies during feasibility studies. Therefore, this work follows the majority of existing research [78] and applies an intercept slope approach.

Operational characteristics of conversion technologies are typically defined by their ramping, part-load, and start-up capabilities. Ramping capabilities introduce liner ramp rates constraints to the model. Part-load capabilities are described by the minimum operating levels as well as part-load dependent efficiencies. The modeling of part-load capabilities requires binary variables per time step. Thiem [27] finds an intercept slope formulation of part-load capabilities to be sufficient to approximate real-world performance curves of multiple technologies. This formulation of part-load capabilities can be extended to penalize start-up and shut down process in the objective function. The formulation leads to a coupling of adjacent time steps adding computational complexity [115]. Therefore, part-load capabilities are often replaced by a simplified linear formulations with constant efficiencies [78]. Additional operational details such as maximum runtimes, minimum downtimes, maintenance intervals or cold start capabilities couple multiple adjacent binary variables. The additional computational complexity from these formulations is typically avoided in models for energy system design [66].

The level of modelling detail has been intensively discussed by various authors [26], [66], [112]. Results indicate that the required level strongly depends on the use case. The newly developed optimization framework in this work comprises highly detailed model formulations for both investment and operational details based on work from Thiem [66]. These formulations can be easily replaced by simplified model formulations within the developed framework.

Decomposition methods

Decomposition approaches divide a complex planning model into several smaller problems which can be solved more efficiently than the original problem. Decomposition approaches are divided in exact decomposition approaches and heuristic approaches [111]. Exact approaches divide the original model into a master problem and several smaller sub-problems. Interlinking variables (Benders) or constraints (Lagrangian, Danzig-Wolfe) couple master and sub-problems. Identification of interlinking variables and constraints is tailored to the model formulation and manually conducted by researchers [78]. Industrial energy systems have various technologies and tariffs with diverse

[1]The interaction of sizing and operational models is not discussed here, e.g., the dependence of efficiencies on the unit size. The interested reader is guided to [112] for a detailed discussion.

regulatory and economic boundary conditions as outlined in Section 2.1. Interlinking variables and constraints thus strongly differ between projects. The use of exact decomposition approaches is thus limited for practical application. In contrast to exact decomposition, heuristics target at near-optimal solutions by simplifying interlinking constraints in the problem formulation. They sequentially solve part of a complex optimization problem. Heuristic decomposition can be applied on spatial or temporal coupling constraints. Spatial aggregation is not in focus for industrial sites as energy supply equipment is typically installed in a single technical center. Therefore, temporal coupling constraints are highly relevant for design of energy supply equipment in industrial sites. For dispatch simulations, rolling horizon approaches have been suggested by various authors [116], [117]. These approaches determine an optimal dispatch sequentially for each day or week of the year. However, investment planning models typically comprise multiple interlinking constraints from the equipment and tariff selection on the operational model. These constraints cannot be omitted. This makes rolling horizon approaches not directly applicable in design models. Required model extensions have been described by Thiem [66]. The approach separates time scales in hourly, daily, monthly, and annual time steps. These time scales are solved sequentially with increasing time step resolution considering model decisions from previous time scales. Each time scale comprises several subproblems which are solved sequentially and treat installed capacities of preceding periods as lower bounds. The described decomposition strategies focus on optimizations of a single year. They are thus not applicable for transformation roadmaps with multiple extension stages. Heuristic decomposition approaches have also been proposed for planning models with multiple extension stages. Investment decisions of consecutive extension stages are computed sequentially. The technology options of the previous periods are fixed for the computation of the following extension stages. In contrast to the original model, investment decisions in a certain extension stage are not influenced by long-term projections of energy demands and prices, but purely based on the input data of this extension stage. The approach is referred to as "myopic" [2], "adaptive" [109] or "sequential" [50] planning approach. This type of heuristic decomposition has been analyzed for microgrid systems in [109] and by various authors for expansion planning models [2], [78]. This work applies the approach to the complex design of multi-modal energy supply systems in industrial sites. To the best of author's knowledge, this analysis has not been conducted by other researchers.

Aggregation strategies

Aggregation strategies reduce the spatial or temporal scope of energy system models and thereby the number of variables of the optimization model. If the relevant characteristics are captured by an aggregation approach, the model results in equal or near-optimal solutions with notable lower solving times. The spatial scope of a design model is pre-defined by the technical centers of the industrial sites. Spatial aggregation approaches are thus not further discussed here. The temporal scope describes how the operation of energy supply equipment is reflected. It depends on the selected temporal resolution. An intuitive way to reduce model size is a decrease of temporal resolution, either in a regular manner ("down sampling") or with smart approaches ("segmentation"). However, procurement tariffs require high time resolutions with hourly time steps as outlined in Section 3.1. The design of industrial sites thus requires enhanced approaches.

The most common approach for time series aggregation is the selection of representative periods [59], [118], [119]. The idea of representative periods relies on repeating patterns in energy related time series. For instance, energy demand and renewable generation profiles show strong daily repetitions. Exemplary daily patterns are shown in Figure 2.5. Techno-economic planning

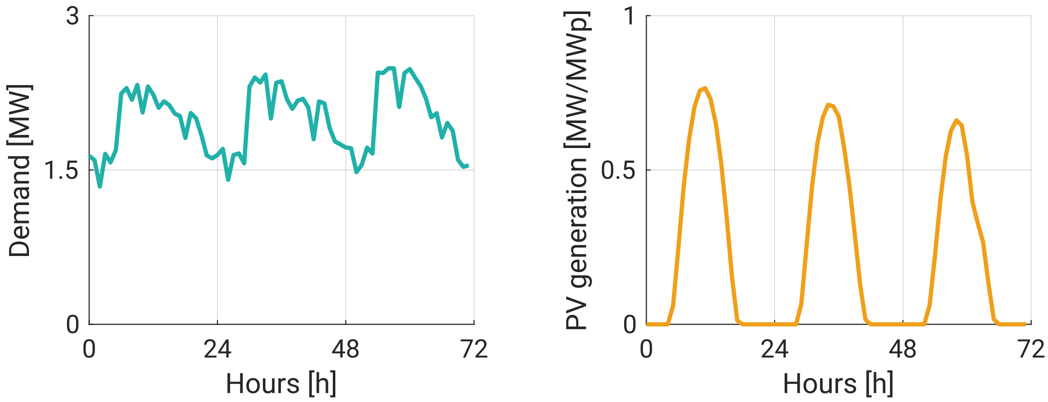

(a) Electricity demand

(b) Photovoltaic generation

Figure 2.5.: Examples of daily patterns of electricity demands and solar generation potential [124] for three days in April

models often consider not all days of an entire base year, but a well selected set of representative days in the optimization model [119], [120]. Seasonal storages can be considered by advanced coupling constraints for representative periods [121], [122]. These formulations add additional computational complexity. Kotzur et al. recommend to use these formulations only for systems that anticipate seasonal storage technologies to be part of an optimized design concept [122]. The key issue arising from this aggregation approach is how to derive a reasonable selection of representative periods from the energy-related time series. Heuristic approaches select representative periods from simple decision rules based on seasonality, peak demands, or weather conditions. VDI 4655 [120] proposes a methodology for residential buildings with twelve seasonally distributed days. Other approaches select days with lowest and highest demands as well as days with the largest demand spread [123]. Heuristic approaches do not account for the statistical characteristics in the time series. For instance, they do not reflect periods of plant shutdowns due to maintenance and holidays. Therefore, advanced approaches are required for design of complex industrial energy supply systems.

Existing literature proposes a variety of algorithms to automatically select representative periods. A good review of existing work is provided by Hoffmann [119]. Representative periods can be either newly calculated averaged periods ("centroid") or part of the original time series ("medoid") or. Algorithms for centroid and medoid based clustering have been intensively evaluated in the field of building energy systems [80], [118] and city districts [125], [126]. Majority of work applies either k-means ("centroid") or k-medoids ("medoid") algorithms. Results of [80], [118] show a better performance of medoid based clustering approaches in comparison to centroid based approaches. Representative periods from centroid clustering average intradaily variations. This smoothing effect results in a systematic underestimation of system costs. Therefore, medoid-based algorithms are clearly the preferred option for design of industrial energy supply systems. Implementations of k-medoid algorithms are available as pre-implemented packages in Python environment such as scikit-learn. However, these implementations do not allow to directly include peak periods in the selection of representative periods. These periods determine the system's ability to serve peak demands and thereby the sizing of peak-load technologies. Therefore, complicated post-processing routines are required to adapt the results of a pre-implemented clustering algorithm

[118]. Moreover, these implementations are often implemented as greedy algorithms which rapidly converge to local optima depending on randomly selected starting points [118]. Optimization results for design concepts can thus become non-deterministic.

This limitation of existing work is overcome by an alternative implementation of the k-medoids clustering approach. The clustering approach is formulated as an integer program which is efficiently solved by commercial solving software till global optimality. Approaches have been demonstrated for a transmission grid expansion model in [123], a university campus in [127] and a city district with two hotels and four office buildings in [113]. The suitability of aggregation approaches strongly depends on the number of relevant time-series and their patterns. Results are thus not directly transferable to industrial energy supply systems [80]. To the best of author's knowledge, time series aggregation based on this clustering approach has not yet been validated for multi-modal energy demands in industrial sites.

2.6. Summary

This chapter has outlined requirements for sustainable design of industrial energy supply systems. Techno-economic feasibility studies derive preliminary design concepts under various uncertainties. Optimization-based design approaches can assist energy system planners and consultants to compare multiple design . Approaches based on MILP automatically derive KPIs, e.g., to study the trade-off between costs and carbon emissions. Model formulations for distributed energy system account for detailed technology models and complex procurement tariffs. Existing work for distributed energy systems typically omits long-term trends, such as projected evolution of energy carrier prices or expected changes in on-site energy demands [50]. This work considers these trends in the formulation of the techno-economic planning model. The planning model is integrated in an optimization framework. The framework efficiently determines sustainable design variants based on optimized selection of representative periods [51]. The entire functionality of the optimization framework can be accessed via a desktop application. This approach ensures the reproducibility of the presented results across multiple energy consultancy projects.

3. Energy supply system modeling

Existing industrial sites often have historically grown energy supply infrastructure. Energy supply systems include a large variety of technologies and complex energy procurement tariffs. This chapter introduces the mathematical optimization model which handles the complexity and diversity of industrial energy supply systems. First, the overall approach developed in this Thesis is outlined in Section 3.1. In the following Sections 3.2 to 3.4, the detailed formulation for different technology base classes including linkage and reserve constraints are derived. An optimal technology sizing and dispatch strategy is determined by minimizing the objective function defined in Section 3.5. Finally, Section 3.6 summarizes general assumptions and underlying limitations of the proposed model formulation.

3.1. Integrated investment planning

Integrated investment planning [128], also referred to as sector-coupled [76], multi-energy [28], [77] or multi-modal [27] energy system design, derives holistic concepts for all energy related demands within the system boundaries of an industrial sites. In contrast to traditional separated approaches, the synergies between the various energy supply systems for electricity, heating and steam demands, cooling systems, transport, ventilation, compressed air, and process gases are fully captured by such approaches. The rising complexity is effectively handled by mathematical optimization. The input data and results of the optimization model are illustrated in Figure 3.1. The optimization model captures the relevant attributes associated with the design and operational decisions in the energy supply infrastructure along the entire planning horizon. Consequently, the input data summarizes technical, economic, and environmental parameters. The input includes projected cost and footprint developments for electricity and fuel purchase as well as investment cost and efficiency estimations for all relevant technology options. Demands are represented by (sub-)hourly load profiles. A design concept including an optimal technology selection and equipment sizing as well as an optimal dispatch strategy is computed for the specified input data. The model formulation employed in this work is based on the generic superstructure approach from Thiem [27] and extended for multi-node, multi-stakeholder and multi-year system analysis as well as the ability to account for reserve requirements.

The superstructure defines the relevant technologies and spatial granularity of the techno-economic planning model. It is described by a set $\mathcal{K}$ of existing technologies and possible technology extensions. Technologies are connected via a set of nodes ($\mathcal{N}$). A node ($n \in \mathcal{N}$) is defined as a unique tuple of a location and a commodity. The introduction of the location concept, sometimes also referred to as "energy hubs" [62], [129], enables the analysis of distribution systems, e.g., for large industrial facilities with multiple technical centers. A location comprises nodes for multiple energy commodities ($c \in \mathcal{C}$) such as electricity, heating, or cooling. The energy demands for a

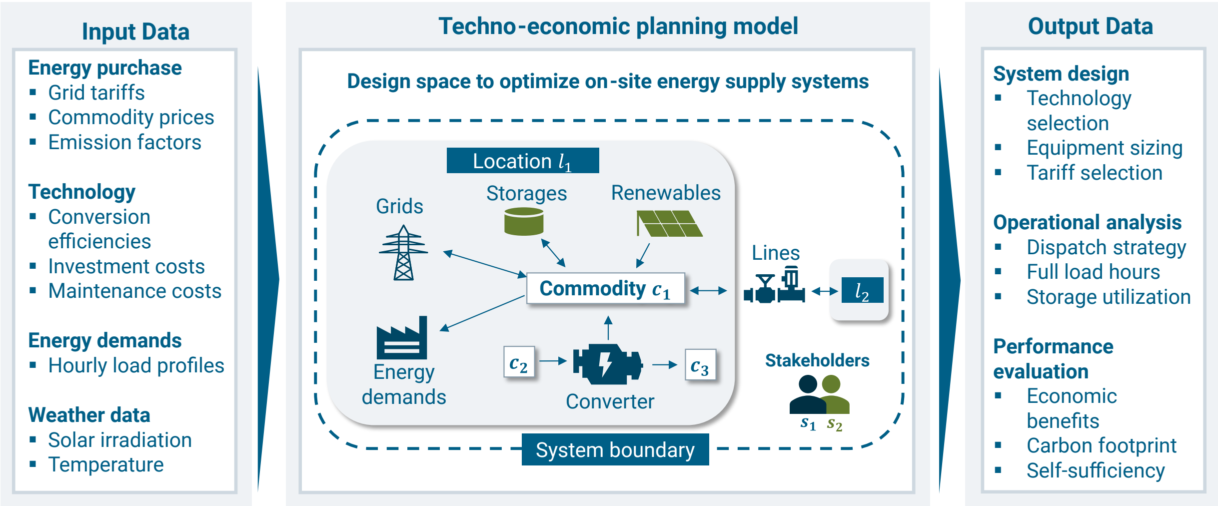

Figure 3.1.: Overview of input and output parameters of the newly developed techno-economic planning model for energy system design

specified commodity and location are summarized in a set $\mathcal{L}_n \subseteq \mathcal{L}$. These demands need to be served by the technologies of the superstructure. Technologies are divided into five generic base classes: Grid, renewable, conversion, storage and line technologies. Grid technologies ($\mathcal{K}_G \subset \mathcal{K}$) describe dispatchable commodity sources and sinks at a node whereas renewable technologies ($\mathcal{K}_R \subset \mathcal{K}$) provide a non-dispatchable alternative. Conversion technologies ($\mathcal{K}_C \subset \mathcal{K}$) represent conversion processes from multiple input commodities to multiple output commodities. Storage technologies ($\mathcal{K}_S \subset \mathcal{K}$) temporarily store energy commodities. An exchange of commodities between two locations is modelled via line technologies ($\mathcal{K}_L \subset \mathcal{K}$).

The temporal granularity of the model is described by sets for extension stages ($\mathcal{Y}$), representative periods ($\mathcal{D}$) and time steps ($\mathcal{T}$). Their relation is visualized in Figure 3.2. The proposed concepts allows to consider adaptations in technology selection and equipment sizing due to demand or price changes as well as required replacements for aged equipment. The equipment capacities are thus optimized for a set $\mathcal{Y}$ of extension stages. The initial extension stage is referred to by y_0. Each extension stage $y \in \mathcal{Y}$ comprises a set of representative periods $\mathcal{D}_y \subseteq \mathcal{D}$ and time steps $\mathcal{T}_y \subseteq \mathcal{T}$. The system operation in y is modelled by a set $\mathcal{D}_y$ of representative periods. Representative periods are selected to approximate the annual operation of the energy supply equipment in a typical year and ensure an efficient solving process. A typical year might be sufficiently represented by 20 representative days [51]. Weight factors (w_d) describe how many periods of a typical year are represented by a representative period ($d \subseteq \mathcal{D}$). Cycling conditions are assumed within each representative period. This means that all system states, such as energy content in a storage, at the end of d equal the states at the beginning of d.[2] The schedule within a representative period d is described by a set $\mathcal{T}_d \subseteq \mathcal{T}$ of time steps. Each time step t has a defined time step resolution (Δt).

The optimization variables describe the sizing and power set points of the technologies along the entire planning horizon. The installation status and rated power capacities are described by binary variables ($B^{\mathrm{R}}_{k,y} \in \{0,1\}$) and continuous variables ($P^{\mathrm{R}}_{k,y} \in \mathbb{R}^+$) for each technology $k \in \mathcal{K}$ at the extension stage $y \in \mathcal{Y}$. Investment decisions for additonal equipment are allowed

[2] Cycling conditions prohibit energy exchange between adjacent representative periods. The assumption prevents seasonal storage operation. Details are discussed in Section 4.2.

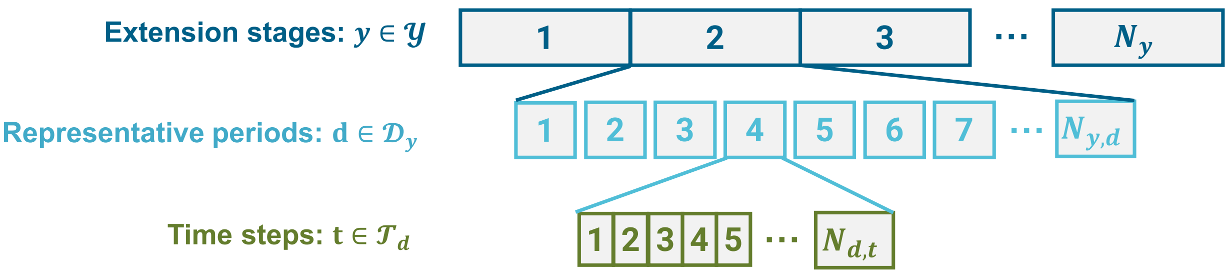

Figure 3.2.: Relation of sets for extension stages, representative periods and time steps

in each extension stage. They are represented by additional binary variables ($B_{k,y}^{\text{Inv}} \in \{0,1\}$) and continuous variables ($P_{k,y}^{\text{Inv}} \in \mathbb{R}^+$). Latest at the end of technical lifetime, technologiees are replaced which is represented by continuous variables ($P_{k,y}^{\text{Repl}} \in \mathbb{R}^+$). Storage technologies are characterized by their rated power and storage capacity, e.g. for inverter and cell packages of a battery energy storage. The rated storage capacities are reflected by additional continuous variables $C_{k,y}^{\text{R}} \in \mathbb{R}^+$, $C_{k,y}^{\text{Inv}} \in \mathbb{R}^+$ and $C_{k,y}^{\text{Repl}} \in \mathbb{R}^+$ for $k \in \mathcal{K}_S$. The generic base classes have a defined number of inputs and outputs indicated by an additional index i. The operation of each technology is thus described by continuous variables $P_{k,i,t}^{\text{In}} \in \mathbb{R}^+$ and $P_{k,i,t}^{\text{Out}} \in \mathbb{R}^+$ for each input and output power flow of a technology k at a time step t. The operational status (on, off) is modelled by additional binary variables ($B_{k,t}^{\text{Opr}} \in \{0,1\}$).

A set $\mathcal{K}_n^{\text{In}}$ summarizes tuples for technologies k which are connected with the input flow i to node n. Another set $\mathcal{K}_n^{\text{Out}}$ summarizes tuples for technologies which are connected with the output power flow to n. The technologies serve time-dependent energy demands. Energy demands are defined as additional variables ($P_{n,i,t}^{L} \in \mathbb{R}^+$) with i being the index of a load connected to node n. The model aims at identifying a cost-optimal technology selection to meet the time dependent energy demands along the entire planning horizon. Therefore, power balances at each node (n) and for each time step (t) need to be fulfilled:

$$\sum_{(k,i)\in\mathcal{K}_n^{\text{Out}}} P_{k,i,t}^{\text{Out}} = \sum_{(k,i)\in\mathcal{K}_n^{In}} P_{k,i,t}^{\text{In}} + \sum_{i\,\in\,\mathcal{L}_n} P_{n,i,t}^{\text{L}} \quad \forall n \in \mathcal{N}, t \in \mathcal{T} \tag{3.1}$$

3.2. Technology models

Technologies are modelled in a modular approach based on five generic base classes illustrated in Figure 3.3. The generic base class approach depicts various general purpose technologies, sector-specific efficiency measures and complex procurement tariffs. Differences between these technologies are defined by model parameterization. The rated sizing ($P_{k,y}^{\text{R}}$) of a technology is constraint by a lower bound ($\underline{P}_{k,y}^{\text{R}}$) and an upper bound ($\overline{P}_{k,y}^{\text{R}}$).

$$\underline{P}_{k,y}^{\text{R}} B_{k,y}^{\text{R}} \leq P_{k,y}^{\text{R}} \leq \overline{P}_{k,y}^{\text{R}} B_{k,y}^{\text{R}} \quad \forall k \in \mathcal{K}, y \in \mathcal{Y} \tag{3.2}$$

$$\underline{P}^{\mathrm{R}}_{k,y} B^{\mathrm{Inv}}_{k,y} \leq P^{\mathrm{Inv}}_{k,y} \leq \overline{P}^{\mathrm{R}}_{k,y} B^{\mathrm{Inv}}_{k,y} \quad \forall k \in \mathcal{K}, y \in \mathcal{Y} \tag{3.3}$$

$P^{\mathrm{R}}_{k,y}$ at the extension stage y depends on previous installations and the investment and replacement decisions of the current extension stage. Equipment needs to be removed latest at the end of its technical lifetime (y^{Tech}_k) which is enforced by Equation 3.6. Existing infrastructure in brownfield sites is explicitly accounted for by the model formulation: The parameter p^{Inst}_k denotes the installed rated power capacity. p^{Inst}_k requires expenditures for maintenance and operation only. The Heaviside function $H(y \geq y^{\mathrm{Inst}}_k)$ indicates if p^{Inst}_k needs to have been replaced in the extension stage y depending on the remaining lifetime y^{Inst}_k. The remaining lifetime is smaller than or equal to the technical lifetime y^{Tech}_k.

$$P^{R}_{k,y_0} = p^{\mathrm{Inst}}_k + P^{\mathrm{Inv}}_{k,y_0} - P^{\mathrm{Repl}}_{k,y_0} \quad \forall k \in \mathcal{K} \tag{3.4}$$

$$P^{\mathrm{R}}_{k,y} = P^{\mathrm{R}}_{k,y-1} + P^{\mathrm{Inv}}_{k,y} - P^{\mathrm{Repl}}_{k,y} \quad \forall k \in \mathcal{K}, y > y_0 \tag{3.5}$$

$$\sum_{y_1=y_0}^{y} P^{\mathrm{Repl}}_{k,y_1} \geq p^{\mathrm{Inst}}_k H(y \geq y^{\mathrm{Inst}}_k) + \sum_{y_1=y_0}^{y-y^{\mathrm{Tech}}_k} P^{\mathrm{New}}_{k,y_1} \quad \forall k \in \mathcal{K}, y > y_0 \tag{3.6}$$

The power set points $P_{k,t}$ of grid, renewable and conversion technologies is defined as the first output power flow as visualized in Figure 3.3. An exceptation are grid sink technologies which will be outlined in detail within the next paragraph. The operating range is limited by time-dependent minimum part load ratios ($\underline{u}_{k,t}$) and maximum part load ratios ($\overline{u}_{k,t}$). $\underline{u}_{k,t}$ and $\overline{u}_{k,t}$ are considered as time-dependent exogenous model variables. Thereby, the model accounts for various (e.g., climate-dependent) technology characteristics such as temperature dependence of gas turbines. Dynamic capabilities are accounted by ramp up rates (r^{Up}_k) and ramp down rates (r^{Down}_k).

$$\underline{u}_{k,t} P^{\mathrm{R}}_{k,y} B^{\mathrm{Opr}}_{k,t} \leq P_{k,t} \leq \overline{u}_{k,t} P^{\mathrm{R}}_{k,y} B^{\mathrm{Opr}}_{k,t} \quad \forall k \in \{\mathcal{K}_G, \mathcal{K}_R, \mathcal{K}_C\}, y \in \mathcal{Y}, t \in \mathcal{T}_y \tag{3.7}$$

$$r^{\mathrm{Down}}_k P^{\mathrm{R}}_{k,y} \leq \frac{P_{k,t+1} - P_{k,t}}{\Delta t} \leq r^{\mathrm{Up}}_k P^{\mathrm{R}}_{k,y} \quad \forall k \in \{\mathcal{K}_G, \mathcal{K}_R, \mathcal{K}_C\}, y \in \mathcal{Y}, t \in \mathcal{T}_y \tag{3.8}$$

The operational behavior of lines and storage technologies is denoted by two or three continuous variables per time step respectively. This allows to consider distribution losses of bidirectional lines and charging behavior of storage technologies. Variables and constraints for lines and storages are outlined in the corresponding sections.

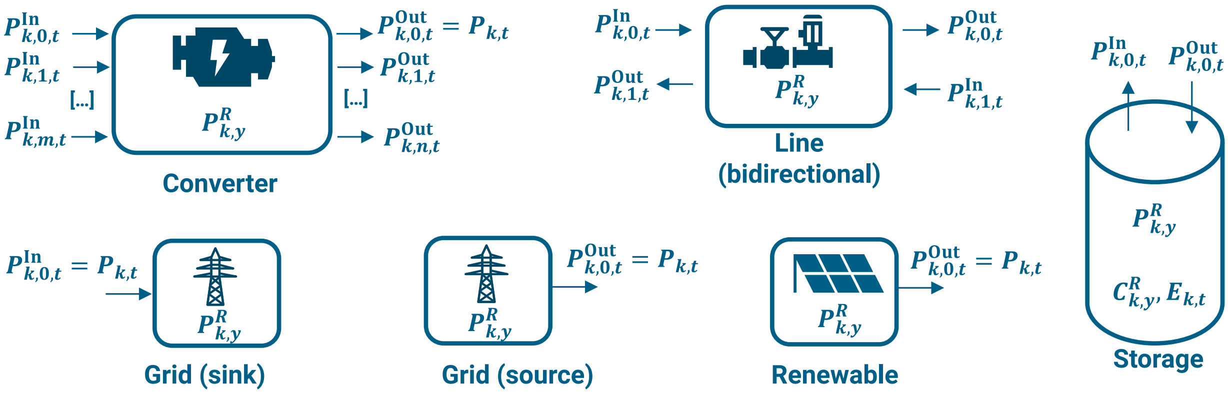

Figure 3.3.: Overview of input and output flows of the five generic technology base classes

3.2.1. Grids

Grid technologies describe connections to energy markets and the surrounding environment. Grids are divided into sinks and sources depending on the flow direction of the connection. Sinks represent technologies which take energy from the energy supply system such as feed-in tariffs or cooling vents. In contrast, sources describe options for energy procurement, e.g., for fuels or use of ambient heat.

Operational costs $\zeta^{\text{OM}}_{k,y}$ for grid technologies comprise fixed annual costs $\zeta^{\text{OM,fix}}_{k,y}$, energy related costs $\zeta^{\text{OM,energy}}_{k,y}$, demand charges $\zeta^{\text{OM,peak}}_{k,y}$ and carbon prices $\zeta^{\text{OM,Env}}_{k,y}$. Demand charges are approximated from the maximum annual peak power with the annual demand price $c^{\text{OM,peak}}_{k,y} > 0$.[3] Within this work, costs for fuel and electricity purchase is denoted with positive values for $\zeta^{\text{OM,energy}}_{k,y}$. Negative values for $\zeta^{\text{OM,energy}}_{k,y}$ describe revenues from feed-in tariffs.

$$\zeta^{\text{OM}}_{k,y} = \zeta^{\text{OM,fix}}_{k,y} + \zeta^{\text{OM,energy}}_{k,y} + \zeta^{\text{OM,peak}}_{k,y} + \zeta^{\text{OM,CO2}}_{k,y} \quad \forall k \in \mathcal{K}_G, y \in \mathcal{Y} \tag{3.9}$$

$$\zeta^{\text{OM,fix}}_{k,y} = c^{\text{OM,fix}}_{k,y} B^{\text{R}}_{k,y} \tag{3.10}$$

$$\zeta^{\text{OM,energy}}_{k,y} = \sum_{d \in \mathcal{D}_y} w_d \sum_{t \in \mathcal{T}_d} c^{\text{OM,energy}}_{k,t} \Delta t P_{k,t} \tag{3.11}$$

$$\zeta^{\text{OM,peak}}_{k,y} = c^{\text{OM,peak}}_{k,y} \sup_{t \in \mathcal{T}_y} P_{k,t} \tag{3.12}$$

The environmental impact of energy supply is measured by various key indicators associated with emissions, primary energy use, noise ratios or freshwater consumption. Emission ratios

[3] The annual peak power is the supremum of the time-dependent power flow variables and derived with a continous helper variable. The helper variable is constraint by all power flow variables as lower bounds. The helper variable is minimized in the solving process as it contributes to the objective function.

are related to sulfur dioxide, nitrogen dioxide, particulate matter or greenhouse gases [37], [52]. The developed model formulation accounts for these factors. Due to its prominent role in decarbonization concepts, this Thesis limits itself to the analysis of carbon dioxide emissions. The impact of carbon emissions is classified in three scopes according to international standards such as ISO 14064. Scope 3 emissions from upstream supply chains are not considered within this work. Scope 1 and Scope 2 describe direct on-site emissions and indirect emissions from energy procurement. They are included by considering time-dependent emission factors $c_{k,e,t}^{\text{CO2,energy}}$ for grid technologies.

$$\zeta_{k,y}^{\text{CO2}} = \sum_{d \in \mathcal{D}_y} w_d \sum_{t \in \mathcal{T}_d} e_{k,t}^{\text{CO2,energy}} \Delta t P_{k,t} \tag{3.13}$$

Environmental laws and regulations target at minimizing the environmental impact of energy supply. One incentive for low carbon solutions are carbon pricing systems, e.g., the European Emission Trading System for large-scale industry (> 20 MW). Therefore, the environmental impact is included as part of the cost function.

$$\zeta_{k,y}^{\text{OM,CO2}} = c_{k,y}^{\text{CO2}} \zeta_{k,y}^{\text{CO2}} \tag{3.14}$$

3.2.2. Renewables

Renewable technologies represent non-dispatchable energy sources, in particular solar and wind plants. The power set point $P_{k,t} = P_{k,0,t}^{\text{Out}}$ of a renewable technology is determined by its weather dependent generation potential $u_{k,t}^{\text{fix}}$. $u_{k,t}^{\text{fix}}$ is an exogenous model parameter. For instance, hourly generation profiles for photovoltaic and wind generation can be estimated from local climate data and technical parameters based on the models from Pfenninger [124] and Staffel [130]. The difference between $P_{k,t}$ and the available power $u_{k,t}^{\text{fix}} P_{k,y}^{\text{R}}$ describes the curtailed power of a renewable technology at time step t.

$$P_{k,t} \leq u_{k,t}^{\text{fix}} P_{k,y}^{\text{R}} \quad \forall k \in \mathcal{K}_R, y \in \mathcal{Y}, t \in \mathcal{T}_y \tag{3.15}$$

Operational costs $\zeta_{k,y}^{\text{OM}}$ of renewable technologies include fixed and variable expenses for plant maintenance as well as a cost term $\zeta_{k,y}^{\text{OM,curtail}}$ for renewable curtailment. $\zeta_{k,y}^{\text{OM,curtail}}$ is part of the objective function. As the objective function is minimized, renewable energy is preferably used in the energy supply system.

$$\zeta_{k,y}^{\text{OM}} = \zeta_{k,y}^{\text{OM,fix}} + \zeta_{k,y}^{\text{OM,var}} + \zeta_{k,y}^{\text{OM,curtail}} \quad \forall k \in \mathcal{K}_R, y \in \mathcal{Y} \tag{3.16}$$

$$\zeta_{k,y}^{\text{OM,var}} = c_{k,y}^{\text{OM,var}} P_{k,y}^{\text{R}} \tag{3.17}$$

$$\zeta_{k,y}^{\text{OM,curtail}} = c_{k,y}^{\text{OM,curtail}} \sum_{d \in \mathcal{D}_y} w_d \sum_{t \in \mathcal{T}_d} (u_{k,t}^{\text{fix}} P_{k,y}^{\text{R}} - P_{k,t}) \Delta t \tag{3.18}$$

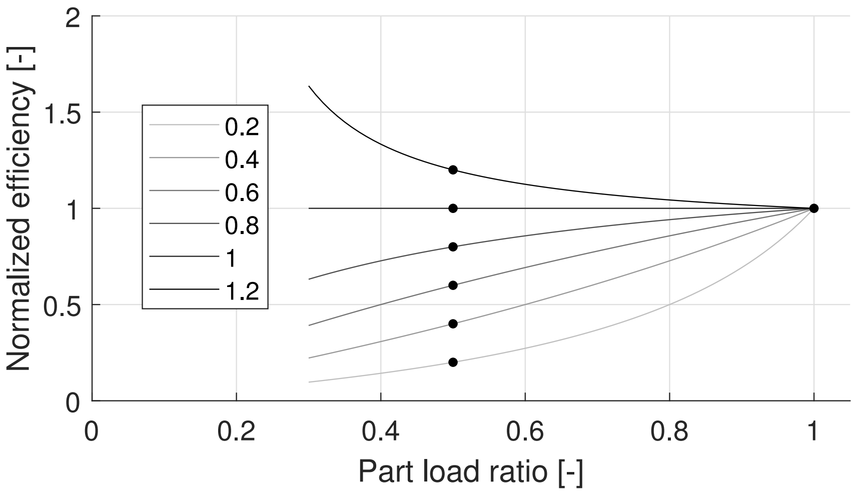

Figure 3.4.: Performance curves for conversion technologies based on two sampling points approach from [66]. The curves show the modelled curves for a minimum part-load ratio $\underline{u} = 0.3$ and various ratios of η^{50} and η^{100}.

3.2.3. Energy converters

Conversion technologies describe conversion processes between one or multiple input commodities and one or multiple output commodities. Examples of on-site conversion technologies are gas turbines and heat pumps. This work proposes a generic modelling approach for energy converters to account for the variety of general purpose and sector-specific technologies typically found in industrial energy supply systems. Following the analysis in Section 2.4, feasibility studies need to account for complex operational characteristics of energy converters such as part-load capabilities and start-up costs.

Power set points $P_{k,t} = P^{\text{Out}}_{k,0,t}$ of conversion technologies are determined by the first output flows, as illustrated in Figure 3.3. This definition is in accordance with engineering practice for heat pump and combined heat-and-power plants. The input and remaining output flows are denoted by the sets $\mathcal{N}^{\text{In}}_k$ and $\mathcal{N}^{\text{Out}}_k$. These flows are defined as functions of $P^{\text{Out}}_{k,0,t}$.

Detailed efficiency models of conversion technologies include performance maps which consider the impact of both ambient climate conditions (temperature, humidity, pressure) and part-load behavior. For instance, the electric performance of gas turbines without inlet air cooling increases with lower ambient air temperatures and substantially reduces in part-load operation. Therefore, the converter efficiency model is based on the two sampling point approach introduced by Thiem in [66]. The two sampling points describe the performance characteristics at 50 % and 100 % of full load at the respective time step. The shape of the performance curve can be adjusted from the ratio of the two sampling points. Figure 3.4 illustrates six exemplary shapes. The efficiency values have been normalized to the efficiency η^{100} at full load. The time dependence of the sampling points allows to account for highly complex climate influences on technology performance. The proposed approach matches a variety of technology performance characteristics, such as large-scale gas turbines [66].

Following the two sampling point approach of Thiem [66], the relation of each input power flow i

to $P^{\text{Out}}_{k,0,t}$ is described by two time-dependent parameter vectors $\eta^{\text{In},50}_{k,i,t}$ and $\eta^{\text{In},100}_{k,i,t}$ for efficiencies at 50 % and 100 % of nominal load respectively. The two parameter vectors are reformulated as a fixed proportion ($h^{\text{In,fix}}$) independent of the part-load ratio and a variable proportion ($h^{\text{In,var}}$) depending on the part-load ratio.[4]

$$P^{\text{In}}_{k,i,t} = (h^{\text{In,fix}}_{k,i,t} P^{\text{R}}_{k,y} + h^{\text{In,var}}_{k,i,t} P^{\text{Out}}_{k,0,t}) B^{\text{Opr}}_{k,t} \quad \forall k \in \mathcal{K}_C, i \in \mathcal{N}^{\text{In}}_k, y \in \mathcal{Y}, t \in \mathcal{T}_y \tag{3.19}$$

$$h^{\text{In,fix}}_{k,i,t} = \frac{1}{\eta^{\text{In},50}_{k,i,t}} - \frac{1}{\eta^{\text{In},100}_{k,i,t}} \tag{3.20}$$

$$h^{\text{In,var}}_{k,i,t} = \frac{2}{\eta^{\text{In},100}_{k,i,t}} - \frac{1}{\eta^{\text{In},50}_{k,i,t}} \tag{3.21}$$

The additional output power flows are related to $P^{\text{Out}}_{k,0,t}$ by two output efficiency vectors $\eta^{\text{Out},50}_{k,i,t}$ and $\eta^{\text{Out},100}_{k,i,t}$. The efficiencies describe the ratio of the output flow i and the first input flow. For a CHP plant, $\eta^{\text{Out},50}_{k,i,t}$ and $\eta^{\text{Out},100}_{k,i,t}$ equal the heat recovery efficiency at 50 % and 100 % of nominal load. In accordance with the mathematical description in Thiem [27], the parameters are determined as follows: [4]

$$P^{\text{Out}}_{k,i,t} = (h^{\text{Out,fix}}_{k,i,t} P^{\text{R}}_{k,y} + h^{\text{Out,var}}_{k,i,t} P^{\text{Out}}_{k,0,t}) B^{\text{Opr}}_{k,t} \quad \forall k \in \mathcal{K}_C, i \in \mathcal{N}^{\text{Out}}_k, y \in \mathcal{Y}, t \in \mathcal{T}_y \tag{3.22}$$

$$h^{\text{Out,fix}}_{k,i,t} = \frac{2\eta^{\text{In},50}_{k,0,t}}{\eta^{\text{Out},50}_{k,i,t}} - \frac{\eta^{\text{In},100}_{k,0,t}}{\eta^{\text{Out},100}_{k,i,t}} \tag{3.23}$$

$$h^{\text{Out,var}}_{k,i,t} = \frac{\eta^{\text{In},100}_{k,0,t}}{\eta^{\text{Out},100}_{k,i,t}} - \frac{\eta^{\text{In},50}_{k,0,t}}{\eta^{\text{Out},50}_{k,i,t}} \tag{3.24}$$

Startup and shutdown processes of energy converters are associated with accelerated aging and associated higher maintenance costs. The operational schedule should thus preferably operate on-site equipment continuously. One approach to facilitate a more continuous operation schedule is the introduction of minimum runtime and downtime constraints. These approaches couple multiple time steps and thereby add significant computational complexity to the optimization problem. The proposed formulation in this work applies an alternative approach based on the number of startups. The maximum number of annual startups is limited to n^{Start}_k. The tracing of startup occurrence requires one continuous helper variable $H^{\text{start}}_{k,t} \in [0,1]$ per time step. $H^{\text{start}}_{k,t}$ is enforced to be equal to one if a startup happens. In all other cases, the value will become zero as startup costs are part of the objective function and the solver targets at minimizing the costs associated with startups.

[4]The model equations comprise non-linear terms. These terms are linearized in the implemented model formulation. Section A.1 in the annex of this Thesis outlines the applied linearization approaches.

$$\sum_{d\in\mathcal{D}_y} w_d \sum_{t\in\mathcal{T}_d} H^{\text{start}}_{k,t} \leq n^{\text{Start}}_{k} \quad \forall k \in \mathcal{K}_C, y \in \mathcal{Y} \tag{3.25}$$

$$H^{\text{start}}_{k,t} \leq B^{\text{Opr}}_{k,t} - B^{\text{Opr}}_{k,t-1} \quad \forall k \in \mathcal{K}_C, t \in \mathcal{T} \tag{3.26}$$

$\zeta^{\text{OM}}_{k,y}$ summarizes operational and maintenance efforts in five generic cost terms. Fixed costs $\zeta^{\text{OM,fix}}_{k,y}$ and variable costs $\zeta^{\text{OM,fix}}_{k,y}$ depend on the installation status and sizing of a technology. Wear and tear of a technology depend highly on the utilization. Therefore, maintenance cost may include energy related costs $\zeta^{\text{OM,energy}}_{k,y}$, start up costs $\zeta^{\text{OM,start}}_{k,y}$ and runtime costs $\zeta^{\text{OM,run}}_{k,y}$. Larger sizes of technologies typically cause higher maintenance efforts. For instance, a larger CHP plant might comprise additional motors which require regular inspections. $\zeta^{\text{OM,start}}_{k,y}$ is thus divided into a technology specific fixed proportion $c^{\text{OM,start,fix}}_{k,t}$ and a size dependent proportion $c^{\text{OM,start,var}}_{k,t}$. A similar formulation is chosen for $\zeta^{\text{OM,run}}_{k,y}$.[4]

$$\zeta^{\text{OM}}_{k,y} = \zeta^{\text{OM,fix}}_{k,y} + \zeta^{\text{OM,var}}_{k,y} + \zeta^{\text{OM,energy}}_{k,y} + \zeta^{\text{OM,start}}_{k,y} + \zeta^{\text{OM,run}}_{k,y} \quad \forall k \in \mathcal{K}_C, y \in \mathcal{Y} \tag{3.27}$$

$$\zeta^{\text{OM,start}}_{k,y} = \sum_{d\in\mathcal{D}_y} w_d \sum_{t\in\mathcal{T}_d} (c^{\text{OM,start,fix}}_{k,y} + c^{\text{OM,start,var}}_{k,y} P^{\text{R}}_{k,y}) H^{\text{start}}_{k,t} \tag{3.28}$$

$$\zeta^{\text{OM,run}}_{k,y} = \sum_{d\in\mathcal{D}_y} w_d \sum_{t\in\mathcal{T}_d} (c^{\text{OM,run,fix}}_{k,y} + c^{\text{OM,run,var}}_{k,y} P^{\text{R}}_{k,y}) \Delta t B^{\text{Opr}}_{k,t} \tag{3.29}$$

3.2.4. Lines

Line technologies establish connections between two distinct locations l_1 and l_2 with a distance $l_{1,2}$. Lines describe the pipes of water and steam distribution systems as well as cables of the on-site microgrid. Pipes and cables enable bidirectional energy flows: For instance, a manufacturing hall may consume electricity from the microgrid during production shifts in the night and feed back electricity from rooftop photovoltaic during noon in the summer with strong solar irradiation. Therefore, the operational behavior of line technologies is described by two continuous variables $P^{\text{In}}_{k,0,t} \in \mathbb{R}^+$ and $P^{\text{In}}_{k,1,t} \in \mathbb{R}^+$. Each variable denotes the possible input power flow for the two interconnected locations. The concept is illustrated in Figure 3.3. The input power flows are limited by the rated power capacity $P^{\text{R}}_{k,y}$ of the line technology. The transmission of energy over a line is associated with length dependent losses η^{Loss}_{k}.

$$P^{\text{In}}_{k,i,t} \leq P^{\text{R}}_{k,y} B^{\text{Opr}}_{k,t} \quad \forall k \in \mathcal{K}_L, i \in \{0,1\}, y \in \mathcal{Y}, t \in \mathcal{T}_y \tag{3.30}$$

$$P^{\text{Out}}_{k,i,t} = (1 - \eta^{\text{Loss}}_{k})^{l_{1,2}} P^{\text{In}}_{k,i,t} \quad \forall k \in \mathcal{K}_L, i \in \{0,1\}, y \in \mathcal{Y}, t \in \mathcal{T}_y \tag{3.31}$$

Economic and regulatory conditions can make waste of energy economically beneficial under certain conditions. For instance, the low-temperature heat from a cogeneration plant might not be used for space heating demands during the entire year. The introduced formulation would enable physically infeasible solutions to waste energy by simultaneous power flows in both directions of line technologies. These model artifacts can be avoided by adding a bilinear equation. The constraint enforces to be at least one of the two power flow variables to be zero at each time step. Thereby, it effectively prevents cyclical power flows.[4]

$$P^{\mathrm{In}}_{k,0,t} P^{\mathrm{In}}_{k,1,t} \leq 0 \quad \forall k \in \mathcal{K}_L, t \in \mathcal{T} \tag{3.32}$$

The operational costs $\zeta^{\mathrm{OM}}_{k,y}$ of line technologies comprise a fixed and a variable cost term. The definition of the cost terms is provided in Equations 3.10 and 3.17.

$$\zeta^{\mathrm{OM}}_{k,y} = \zeta^{\mathrm{OM,fix}}_{k,y} + \zeta^{\mathrm{OM,var}}_{k,y} \quad \forall k \in \mathcal{K}_L, y \in \mathcal{Y} \tag{3.33}$$

3.2.5. Energy storages

Storage technologies decouple generation and demand. They help to integrate time varying waste heat sources and volatile renewable generation in on-site energy supply systems. Industrial sites can comprise a variety of storage technologies including batteries, thermal storages and cryogenic tanks for process gases. In addition to its rated power capacity $(P^{\mathrm{R}}_{k,y})$, the sizing of storage technology is defined by its rated storage capacity $(C^{\mathrm{R}}_{k,y})$. Boundary and extension constraints for installed capacity $(C^{\mathrm{R}}_{k,y})$, new installed capacity $(C^{\mathrm{R}}_{k,y})$ and replaced capacity $(C^{\mathrm{Repl}}_{k,y})$ are defined analogous to Equations 3.2 to 3.6.

The storage operation is described by three continuous variables per time step: the charging power $(P^{\mathrm{In}}_{k,0,t})$, the discharging power $(P^{\mathrm{Out}}_{k,t})$ and the energy content $(E_{k,t})$. These variables are limited by the power and capacity sizing of the storage, e.g., the inverter size and the number of racks of a battery storage. The state of charge (SOC) describes the energy content of the storage related to its capacity $C^{\mathrm{R}}_{k,y}$. Thereby, the maximum discharge depth is given with $\underline{SOC}_{k,t}$.

$$P^{\mathrm{In}}_{k,0,t} \leq P^{\mathrm{R}}_{k,y} \quad \forall k \in \mathcal{K}_S, y \in \mathcal{Y}, t \in \mathcal{T}_y \tag{3.34}$$

$$P^{\mathrm{Out}}_{k,0,t} \leq P^{\mathrm{R}}_{k,y} \quad \forall k \in \mathcal{K}_S, y \in \mathcal{Y}, t \in \mathcal{T}_y \tag{3.35}$$

$$\underline{SOC}_{k,t} C^{\mathrm{R}}_{k,y} \leq E_{k,t} \leq \overline{SOC}_{k,t} C^{\mathrm{R}}_{k,y} \quad \forall k \in \mathcal{K}_S, y \in \mathcal{Y}, t \in \mathcal{T}_y \tag{3.36}$$

The operational variables are coupled by the internal energy balance of the storage. Storage losses are described by the charging efficiency $(\eta^{\mathrm{Ch}}_{k,t})$, the discharge efficiency $(\eta^{\mathrm{Dch}}_{k,t})$ and specific self-discharge rate ($\eta^{\text{Self}}_{k,t}$). The energy balance of storage technologies couples adjacent time steps and thereby adds significant computational complexity to the optimization model.

$$E_{k,t+1} = \left(1 - \eta^{Self}_{k,t}\right) E_{k,t} + \Delta t \left(\eta^{\text{Ch}}_{k,t} P^{\text{In}}_{k,0,t} + \frac{1}{\eta^{\text{Dch}}_{k,t}} P^{\text{Out}}_{k,0,t}\right) \quad \forall k \in \mathcal{K}_S, t \in \mathcal{T} \tag{3.37}$$

The dynamic capabilities of storage technologies are described by maximum charging (r^{Ch}_k) and discharging rates (r^{Dch}_k).

$$r^{\text{Dch}}_k C^{\text{R}}_{k,y} \leq \frac{E_{k,t+1} - E_{k,t}}{\Delta t} \leq r^{\text{Ch}}_k C^{\text{R}}_{k,y} \quad \forall k \in \mathcal{K}_S, y \in \mathcal{Y}, t \in \mathcal{T}_y \tag{3.38}$$

The challenge of simultaneous power flows in both directions of line technologies has been highlighted in Section 3.2.4. Similar modelling artifacts can occur for storage technologies. A bilinear equation is introduced to prohibit simultaneous charging and discharging.[4]

$$P^{\text{In}}_{k,0,t} P^{\text{Out}}_{k,0,t} \leq 0 \quad \forall k \in \mathcal{K}_S, t \in \mathcal{T} \tag{3.39}$$

Batteries are a major type of storage technology for industrial load balancing and peak shaving. Aging processes of battery technologies are typically divided into calendar and cycling aging. Calendar aging is described by the technical lifetime y^{Tech}_k. In contrast, battery manufactures describe cycling aging impacts by a maximum number of cycles over the entire lifetime. This specification is considered in the optimization problem: the annual equivalent full cycles are limited to a maximum number $n^{\text{Cycle,max}}_k$.

$$\sum_{d \in \mathcal{D}_y} w_d \sum_{t \in \mathcal{T}_d} \Delta t P^{\text{Out}}_{k,0,t} \leq n^{\text{Cycle,max}}_k C^{\text{R}}_{k,y} \quad \forall k \in \mathcal{K}_S, y \in \mathcal{Y} \tag{3.40}$$

The operation and maintenance costs of storage technologies are divided into a fixed proportion $\zeta^{\text{OM,fix}}_{k,y}$, a variable part $\zeta^{\text{OM,var}}_{k,y}$ proportional to the rated power, a capacity dependent proportion $\zeta^{\text{OM,cap}}_{k,y}$ as well as cycle costs $\zeta^{\text{OM,cycle}}_{k,y}$ for each equivalent full cycle.

$$\zeta^{\text{OM}}_{k,y} = \zeta^{\text{OM,fix}}_{k,y} + \zeta^{\text{OM,var}}_{k,y} + \zeta^{\text{OM,cap}}_{k,y} + \zeta^{\text{OM,cycle}}_{k,y} \quad \forall k \in \mathcal{K}_S, y \in \mathcal{Y} \tag{3.41}$$

$$\zeta^{\text{OM,cap}}_{k,y} = c^{\text{OM,cap}}_{k,y} C^{\text{R}}_{k,y} \tag{3.42}$$

$$\zeta^{\text{OM,cycle}}_{k,y} = c^{\text{OM,cycle}}_{k,y} \sum_{d \in \mathcal{D}_y} w_d \sum_{t \in \mathcal{T}_d} \Delta t P^{\text{Out}}_{k,0,t} \tag{3.43}$$

3.2.6. Energy demands

Energy demands are represented by (sub-)hourly load profiles. The profiles are ideally directly extracted from monitoring systems in brownfield sites. If measurement data is not available, demands can be estimated based on synthetic load profile generators [66] or normative references [17]. Energy demands are defined for each location and each commodity. Thereby, the variety of electrical, thermal, and material demands found in industrial sites are represented in the techno-economic model. In contrast to other technology base classes, energy demands are not associated with sizing parameters. Loads are described by power consumptions $P^{L}_{n,i,t} \in \mathbb{R}^{+}$ at each time step t. This work distinguishes two types of demands: fixed loads ($\mathcal{L}^{\text{fixed}} \subseteq \mathcal{L}$) and interruptible loads ($\mathcal{L}^{\text{curtail}} \subseteq \mathcal{L}$).

Fixed loads ($\mathcal{L}^{\text{fixed}}$) comprise no flexibility potential. The power demand is exactly met at each time step. $\mathcal{L}^{\text{fixed}}$ are not associated with any costs in the objective function ($\zeta^{\text{L}}_{n,i,y} = 0$).

$$P^{\text{L}}_{n,i,t} = \overline{P}^{\text{L}}_{n,i,t} \quad \forall n \in \mathcal{N}, i \in \mathcal{L}^{\text{fixed}}_{n}, t \in \mathcal{T} \tag{3.44}$$

Some energy demands can be reduced for short times, e.g., due to the thermal inertia of an industrial process. These types of demands are referred to as interruptible loads ($\mathcal{L}^{\text{curtail}}$). Interruption is associated with penalty costs $c^{\text{L,curtail}}_{n,i,t}$ for load curtailment. The value of $c^{\text{L,curtail}}_{n,i,t}$ might be interpreted as the Value of Lost Load (VoLL).

$$P^{\text{L}}_{n,i,t} \leq \overline{P}^{\text{L}}_{n,i,t} \quad \forall n \in \mathcal{N}, i \in \mathcal{L}^{\text{curtail}}_{n}, t \in \mathcal{T} \tag{3.45}$$

$$\zeta^{\text{L}}_{n,i,y} = \sum_{d \in \mathcal{D}_y} w_d \sum_{t \in \mathcal{T}_d} c^{\text{L,curtail}}_{n,i,t} (\overline{P}^{\text{L}}_{n,i,t} - P^{\text{L}}_{n,i,t}) \quad \forall n \in \mathcal{N}, i \in \mathcal{L}^{\text{curtail}}_{n}, y \in \mathcal{Y} \tag{3.46}$$

Energy demands might have additional characteristics which are not covered by the described features. Charging of electric vehicles might be shifted from peak demand hours. Thermal inertia of buildings provides another source of flexibility. These types of energy demands are beyond the scope of this work. However, they can be represented by combination of multiple base technology classes, e.g., a virtual energy storage and an energy demand. The combination of base technology classes requires linkages which are introduced in the following.

3.3. Technology linkage

The optimization model comprises a set of technology options derived from five generic base technology classes. Some technologies and physical processes are not represented adequately by a single base technology, but require a combination of several technologies. Example of complex processes are flexible demands which can be represented by a combination of virtual storage and energy demand. Regulatory constraints add additional interconnections between base technologies, e.g., high efficiency criterions or self-consumption shares of cogeneration plants. These requirements enforce fixed relationships between one or several base technologies. Therefore, this work proposes a linkage concept for grid, renewable and conversion technologies. A linkage $q \in \mathcal{Q}$ couples one or multiple attributes of two technologies $k_{q,1} \in \{\mathcal{K}_G, \mathcal{K}_R, \mathcal{K}_C\}$ and $k_{q,2} \in \{\mathcal{K}_G, \mathcal{K}_R, \mathcal{K}_C\}$. Linkages enable to constrain the minimum ratio ($h^{\text{Min}} \in \mathbb{R}^+$) or maximum ratio ($h^{\text{Max}} \in \mathbb{R}^+$) of rated design ($\mathcal{Q}^{P^{\text{R}}} \subseteq \mathcal{Q}$), the operational behavior ($\mathcal{Q}^{\text{P}} \subseteq \mathcal{Q}$) as well as the annual energy output ($\mathcal{Q}^{\text{Energy}} \subseteq \mathcal{Q}$). Linkages of discrete investment decisions ($\mathcal{Q}^{\text{Inv}} \subseteq \mathcal{Q}$) and operational decisions ($\mathcal{Q}^{\text{Opr}} \subseteq \mathcal{Q}$) can be mutually inclusive ($h = 1$) or exclusive ($h = -1$).

$$h_q^{P^{\text{R}},\text{Min}} P^{\text{R}}_{k_{q,2},y} \leq P^{\text{R}}_{k_{q,1},y} \leq h_q^{P^{\text{R}},\text{Max}} P^{\text{R}}_{k_{q,2},y} \quad \forall q \in \mathcal{Q}^{P^{\text{R}}}, y \in \mathcal{Y} \tag{3.47}$$

$$h_q^{\text{P,Min}} P_{k_{q,2},t} \leq P_{k_{q,1},t} \leq h_q^{\text{P,Max}} P_{k_{q,2},t} \quad \forall q \in \mathcal{Q}^{\text{P}}, t \in \mathcal{T} \tag{3.48}$$

$$h_q^{\text{Energy,Min}} \sum_{d \in \mathcal{D}_y} w_d \sum_{t \in \mathcal{T}_d} P_{k_{q,2},t} \leq \sum_{d \in \mathcal{D}_y} w_d \sum_{t \in \mathcal{T}_d} P_{k_{q,1},t} \leq h_q^{\text{Energy,Max}} \sum_{d \in \mathcal{D}_y} w_d \sum_{t \in \mathcal{T}_d} P_{k_{q,2},t} \quad \forall q \in \mathcal{Q}^{\text{Energy}}, t \in \mathcal{T} \tag{3.49}$$

$$B^{\text{Inv}}_{k_{q,1},y} = h_q^{\text{Inv}} B^{\text{Inv}}_{k_{q,2},y} \quad \forall q \in \mathcal{Q}^{\text{Inv}}, y \in \mathcal{Y} \tag{3.50}$$

$$B^{\text{Opr}}_{k_{q,1},t} = h_q^{\text{Opr}} B^{\text{Opr}}_{k_{q,2},t} \quad \forall q \in \mathcal{Q}^{\text{Opr}}, t \in \mathcal{T} \tag{3.51}$$

3.4. Reserve concepts

The proposed optimization model targets at minimizing the project costs and the environmental impact of on-site energy supply for the entire planning horizon. Resulting design concepts might not be feasible in practical applications due to uncertainty in energy demands and technology availability. Probabilistic approaches based on Markov chains have been proposed by multiple researchers [131]–[133] to adress reliability considerations in energy system modeling. However, the practical application of these models dependent on the availability of sufficient amount of reliability data in high quality. This data is typically not available in early project phases as outlined in Section 2.1. Deterministic reserve concepts ensure feasibility of design concepts requiring less data input. They guarantee a required level of security of supply during grid outages and equipment failures. In this work, two deterministic reserve concepts are proposed: an operating reserve concept for short-term events and a redundancy concept for long-term events. Both reserve concepts are implemented as additional constraints of the optimization model. These constraints enforce sufficient generation capacities to meet the energy demands in all possible situations and thus avoid costly production interruptions. Additional equipment capacities lead to additional investment expenses which are directly included in the model formulation of this work. Therefore, the proposed reserve concepts enable the computation of more realistic design concepts and improve the estimation accuracies of total project costs.

3.4.1. Operating reserve

Operating reserves introduce short-term reserve margins at each time step to balance temporary power disturbances. Thereby, the supply system can reliably handle short-term imbalances due to temporary outages of public power grids, intermittent renewable generation or sudden peak demands. Reserve concepts have been extensively used in security-constraint economic dispatch models. Research developments in this field have been reviewed in [134] or [135]. In contrast to the presented work, these types of models account only for a single existing design and target at an optimal operation. This work integrates the reliability considerations for a dispatch into a planning model accounting for possible design upgrades.

In the proposed concept, converter, grid, renewable, line, and storage technologies can adapt their dispatch and thereby contribute to the operating reserve. Contributions are limited by the rated power and storage capacities and the dynamic capabilities of each technology. Thereby, sufficient generation and storage capacities are included to meet energy demands during temporary events. The model is extended by a set of operating reserve provisions ($\mathcal{R}^{\text{OR}}$). Following the reserve concept introduced by Mashayekh [136], each reserve provision (r) is described by five key parameters: a response time ($T_r^{\text{OR,R}}$), a duration time ($T_r^{\text{OR,D}}$), a likelihood of occurrence ($\rho_{r,t}^{\text{OR}}$), time-dependent reserve requirements ($a_{r,k,t}^{\text{OR}}$) for conversion, grid or renewable technologies and reserve requirements ($\alpha^{\text{OR,L}}$) for energy demands. $T_r^{\text{OR,R}}$ describes the response time to ramp up conversion or adapt dispatch of storage units. $T_r^{\text{OR,D}}$ defines the maximum duration of the reserve. The timing assumptions are visualized in Figure 3.5. An operating reserve is activated if a technology is enforced to change its operating set point, e.g., during an outage. All other technologies of the energy supply system can change their set points in response to this event within $T_r^{\text{OR,R}}$. After the response time, all energy demands are supplied for a maximum duration $T_r^{\text{OR,D}}$. The energy supply system needs to be able to provide operating reserves at each time step of the entire planning horizon.

Operating reserves are formulated as additional dispatch equations described by continuous variables $P_{k,r,i,t}^{\text{OR}} \in \mathbb{R}^+$ for each reserve provision r and each time step t. Therefore, each operating reserve provision introduces an additional set of power flow constraints to the optimization model. These constraints ensure that the system comprises sufficient operating reserve capacities to meet energy demands during short-term imbalances.

$$\sum_{(k,i)\in\mathcal{K}_n^{\text{Out}}} P_{k,i,r,t}^{\text{OR,Out}} \geq \sum_{(k,i)\in\mathcal{K}_n^{In}} P_{k,i,r,t}^{\text{OR,In}} + \sum_{i\in\mathcal{L}_n} P_{n,i,r,t}^{\text{OR,L}} \quad \forall n \in \mathcal{N}, r \in \mathcal{R}^{\text{OR}}, t \in \mathcal{T} \tag{3.52}$$

Technical constraints for each technology class are formulated analogously to the model equations in Section 3.2. The contribution of a conversion or grid technology is limited by its dynamic capabilities and its availability.[5] These technical boundary conditions are considered by two additional constraints: Dynamic capabilities of conversion technologies are modelled by maximum

[5]Operating reserves are included in planning models to ensure sufficient equipment capacities for short-term imbalances. In this context, relevant imbalances particularly refer to negative changes in power dispatch, either from sudden generation drops or from demand peaks. Positive power imbalances result from generation peaks and demand drops. They may have a minor impact on dispatch strategies, e.g., due to minimum part-load ratios of conversion technologies. However, positive imbalances have a negligible impact on strategic design decisions.[102] Consequently, ramping down and minimum part-load ratios are omitted by the proposed operating reserve concept.

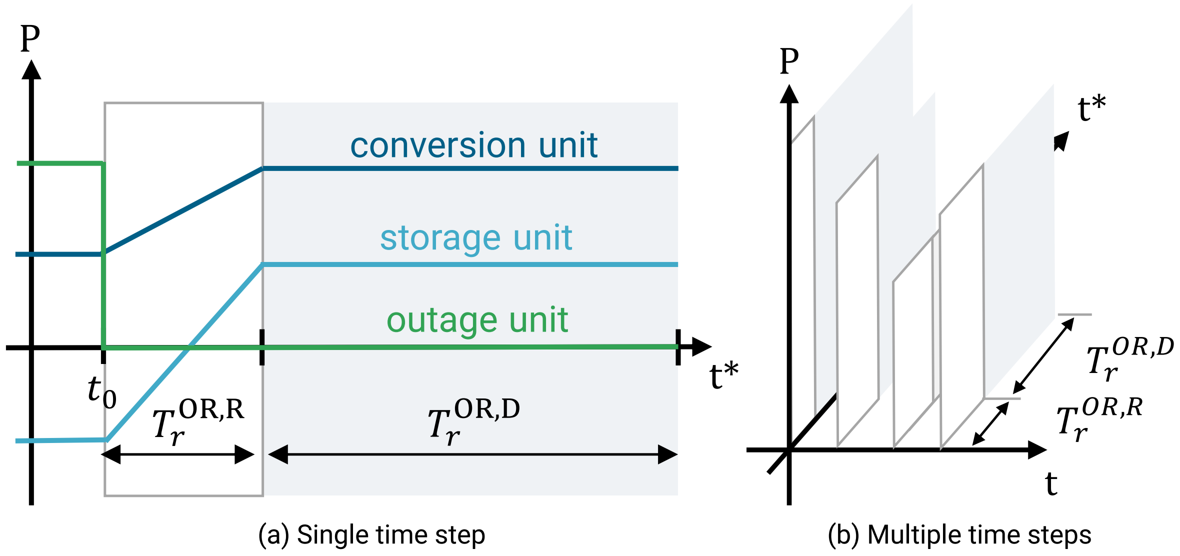

Figure 3.5.: Timing assumptions for operating reserve concept. The system adapts its dispatch for an unexpected change at time t_0 within a response time $T_r^{\mathrm{OR,R}}$ and for a duration $T_r^{\mathrm{OR,D}}$ (a). The reserve constraints are introduced for each time step of the entire planning horizon (b).

ramping rates (r_k^{Up}) which describe the maximum change of the operating set point within $T_r^{\mathrm{OR,R}}$. Operating reserve provisions describe contingency events in which only a subset of technologies is available whereas other technologies cannot contribute, e.g., due to unexpected technical failures or grid outages. The unavailability is described by discrete factors $a_{k,r,t}^{\mathrm{OR}} \in \{0,1\}$ which define if a grid or conversion technology k at time step t is available (0) or not available (1). Operating reserve calls are considered as short-term and rarely occurring events. Demand-related costs associated with the provision of reserve, e.g., for fuel purchase, are thus not included in the formulation of the optimization model. Integrating temporary unavailability of grid and conversion technologies enforces the system to provide sufficient backup capacities during these times.

$$\frac{P_{k,r,t}^{\mathrm{OR}} - P_{k,r,t}}{T_r^{\mathrm{OR,R}}} \leq r_k^{\mathrm{Up}} P_{k,y}^{\mathrm{R}} \quad \forall k \in \{\mathcal{K}_G, \mathcal{K}_C\}, r \in \mathcal{R}^{\mathrm{OR}}, t \in \mathcal{T} \tag{3.53}$$

$$P_{k,r,t}^{\mathrm{OR}} \leq (1 - a_{k,r,t}^{\mathrm{OR}}) \overline{u}_{k,t} P_{k,y}^{\mathrm{R}} B_{k,t}^{\mathrm{Opr}} \quad \forall k \in \{\mathcal{K}_G, \mathcal{K}_C\}, r \in \mathcal{R}^{\mathrm{OR}}, y \in \mathcal{Y}, t \in \mathcal{T}_y \tag{3.54}$$

Storage technologies contribute as a backup option to operating reserve requirements. Contributions of storage technologies are limited by their energy content and required duration $T_r^{\mathrm{OR,D}}$ of the reserve provision r. An empty storage cannot contribute to the reserve whereas a fully charged storage technology can contribute with its rated power ($P_{k,y}^{\mathrm{R}}$). Operating reserve requirements are considered as short-term events. Therefore, self-discharge losses during the operating reserve and the recharging process after the operating reserve are not included in the reserve concept.

$$\left(\eta_k^{\text{Ch}} P_{k,0,r,t}^{\text{OR,In}} + \frac{1}{\eta_k^{\text{Dch}}} P_{k,0,r,t}^{\text{OR,Out}}\right) T_r^{\text{OR,D}} \leq E_{k,t} - \underline{SOC}_{k,t} C_{k,y}^{\text{R}} \quad \forall k \in \mathcal{K}_S, r \in \mathcal{R}^{\text{OR}}, y \in \mathcal{Y}, t \in \mathcal{T}_y \tag{3.55}$$

Wind turbines and photovoltaic introduce short-time volatility, in particular during cloudy periods and low wind periods. The energy supply system needs to balance sudden production decreases from renewable generation. The required reserve margins are thus described by time-dependent and continuous factors $a_{r,k,t}^{\text{OR,Ren}} \in [0,1]$. Higher values for $a_{r,k,t}^{\text{OR,Ren}}$ lead to higher reserve requirements and higher backup capacities.

$$P_{k,r,t}^{\text{OR}} \leq (1 - a_{k,r,t}^{\text{OR,Ren}}) u_{k,t}^{\text{fix}} P_{k,y}^{\text{R}} \quad \forall k \in \mathcal{K}_R, r \in \mathcal{R}^{\text{OR}}, y \in \mathcal{Y}, t \in \mathcal{T}_y \tag{3.56}$$

Energy demands are typically represented by load profiles which are derived from on-site monitoring systems. The representation by measured load profiles typically provides average (hourly) values which do not account for temporary peak demands, e.g., during process starts. However, energy supply systems need to reliably serve these intermittent demands. The required reserveis defined by a time-dependent relative factor $\alpha_{r,n,t}^{\text{OR,L,rel}} \in [-1,1]$ and an absolute power factor $\alpha_{r,n}^{\text{OR,L,abs}}$. Higher values for $\alpha^{\text{OR,L,rel}}$ and $\alpha^{\text{OR,L,abs}}$ lead to higher reserve requirements and higher backup capacities.

$$P_{n,i,r,t}^{\text{OR,L}} \geq (1 + \alpha_{r,k,t}^{\text{OR,L,rel}}) P_{n,i,t}^{L} + \alpha_{r,n}^{\text{OR,L,abs}} \quad \forall n \in \mathcal{N}, i \in \mathcal{L}_n, r \in \mathcal{R}^{\text{OR}}, t \in \mathcal{T} \tag{3.57}$$

$$P_{n,i,r,t}^{\text{OR,L}} = \overline{P}_{n,i,t}^{\text{L}} \quad \forall n \in \mathcal{N}, i \in \mathcal{L}_n^{\text{fixed}}, r \in \mathcal{R}^{\text{OR}}, t \in \mathcal{T} \tag{3.58}$$

Interruptible loads ($\mathcal{L}^{\text{curtail}}$) can be reduced for short times, as described in Section 3.2.6. The reduction of energy demands for reserve provision is associated with penalty costs $c_{n,i,r,t}^{\text{L,curtail}}$ depending on the time-dependent likelihood $\rho_{r,t}^{\text{OR}}$ of an activation of the operating reserve.

$$P_{n,i,r,t}^{\text{OR,L}} \leq \overline{P}_{n,i,t}^{\text{L}} \quad \forall n \in \mathcal{N}, i \in \mathcal{L}_n^{\text{curtail}}, r \in \mathcal{R}^{\text{OR}}, t \in \mathcal{T} \tag{3.59}$$

$$\zeta_{n,i,y}^{\text{L}} = \sum_{r \in \mathcal{R}^{\text{OR}}} \sum_{d \in \mathcal{D}_y} w_d \sum_{t \in \mathcal{T}_d} \rho_{r,t}^{\text{OR}} c_{n,i,t}^{\text{L,curtail}} (\overline{P}_{n,i,t}^{\text{L}} - P_{n,i,r,t}^{\text{OR,L}}) \quad \forall n \in \mathcal{N}, i \in \mathcal{L}_n^{\text{curtail}}, y \in \mathcal{Y} \tag{3.60}$$

3.4.2. Redundancy allocation

Optimal energy supply concepts comprise sufficient capacities to meet critical energy demands during long-term equipment unavailabilities. These unavailabilities occur during maintenance periods and technical malfunctions of equipment and last for several days. They occur only rarely. Therefore, engineering practice ensures security of supply for the unavailability of one technology at the same time (N-1 criterion) [102], [136], [137]. Volatile renewable generation and storage technologies are excluded from this concept due to their intermittent behavior.[6] Reserve capacities thus need to be provided by the remaining conversion, grid, and line technologies. The introduction of redundancy requirements enforces either technologies with rated sizing larger than their nominal operating levels or additional backup technologies. Backup technologies can provide additional benefits during normal operation. For instance, a backup Diesel generator might be effectively used for peak load management. The integration of redundancy requirements in the optimization model allows to consider these benefits for the technology selection and sizing.

Introduction of redundancy requirements ensures (N-1) security of energy supply. This work applies an integrated approach for various energy commodities extending the approach of Hollermann in [102]. The proposed redundancy concept accounts for unavailabilities for all parts of energy supply system including electricity, steam, heating, and cooling. The impact of sector-coupling technologies such as cogeneration plants and heat pumps is directly considered in the techno-economic optimization model. A redundancy requirement $r \in \mathcal{R}^{\text{RED}}$ is formulated as additional power flow constraints for each set $\mathcal{K}_{n,r}^{\text{RED,Out}} \subseteq \mathcal{K}_{n}^{\text{Out}}$ of conversion, grid and line technologies with redundancy requirements and identical output commodities. In contrast to the operating reserve concept, the additional constraints are time independent and formulated for each extension stage y. The concept introduces a variable for the worst possible loss ($P_{r,y}^{\text{RED,Worst}} \in \mathbb{R}^{+}$). $P_{r,y}^{\text{RED,Worst}}$ describes the power capacity loss from a failure of the largest unit of a technology. If the optimized system is able to meet all critical loads under the worst possible loss, it can handle all other possible failures.

$$\sum_{(k,i)\in\mathcal{K}_{n,r}^{\text{Out}}} P_{k,r,i,y}^{\text{RED,Out}} - P_{n,r,y}^{\text{RED,Worst}} \geq \sum_{(k,i)\in\mathcal{K}_{n,r}^{\text{In}}} P_{k,i,r,y}^{\text{RED,In}} + p_{n,y}^{\text{RED,L}} \quad \forall n \in \mathcal{N}, r \in \mathcal{R}^{\text{RED}}, y \in \mathcal{Y} \tag{3.61}$$

$$P_{n,r,y}^{\text{RED,Worst}} \geq P_{k,i,r,y}^{\text{RED,Out}} \quad \forall n \in \mathcal{N}, r \in \mathcal{R}^{\text{RED}}, (k,i) \in \mathcal{K}_{n,r}^{\text{RED,Out}}, y \in \mathcal{Y} \tag{3.62}$$

Constraints for the technology base class are formulated analogously to equations in Section 3.2. In this context, time-dependent efficiencies are approximated with the minimum value which corresponds to the worst possible constellation. The proposed concept for redundancy allocation thus results in conservative design concepts for energy supply systems. Redundancies are allocated by implementing several smaller and standardized units of conversion technologies rather than one large unit. Modeling this effect requires the introduction of discrete unit capacities for selected energy converters $\mathcal{K}_{C}^{\text{Disc}} \subseteq \mathcal{K}_{C}$. The continuous capacity variable $P_{k,y}^{\text{R}}$ is thus enforced to be a multiple of a defined unit size u_{k}^{Disc} by adding an integer variable $N_{k,y}^{\text{R}} \in \mathbb{N}$ to the optimization problem.

[6] Storage technologies with long cycles of multiple weeks might be able to provide the required reserve. These types of storages have not been in the scope of this work as outlined in Section 3.2.

$$P^{\mathrm{R}}_{k,y} = u^{\mathrm{Disc}}_{k} N^{\mathrm{R}}_{k,y} \quad \forall k \in \mathcal{K}^{\mathrm{Disc}}_{c}, y \in \mathcal{Y} \tag{3.63}$$

$$P^{\mathrm{RED}}_{k,r,y} \leq \frac{N^{\mathrm{R}}_{k,y} - 1}{N^{\mathrm{R}}_{k,y}} P^{\mathrm{R}}_{k,y} \quad \forall k \in \mathcal{K}^{\mathrm{Disc}}_{C}, y \in \mathcal{Y} \tag{3.64}$$

Energy demands are represented as critical demands ($p^{\mathrm{RED,L}}_{n,y}$) at each node n in the proposed redundancy allocation concept. Within this work, $p^{\mathrm{RED,L}}_{n,y}$ are estimated from peak demands of load profiles in each extension stage y.

The combination of redundancy allocation and operating reserve ensures security of supply under uncertainty in energy demands, renewable generation, and technology availability. Thereby, the developed optimization model can derive highly robust design concepts which reliably serve production processes in industrial sites.

3.5. Objective function

Techno-economic optimization models target at optimal energy supply concepts comprising both equipment design decisions and an operational schedule. The optimal concept is computed by minimizing the objective function. The objective function represents the total project costs (TC) over the entire planning horizon: It summarizes capital expenditures ($\zeta^{\mathrm{CAPEX}}_{s,y}$) and operational expenditures ($\zeta^{\mathrm{OPEX}}_{s,y}$) as well as costs for load curtailment ($\zeta^{L}_{s,y}$) for each stakeholder s. The introduction of stakeholders enables the modeling of complex ownership models, in particular if the site owner is more interested in procuring energy services than investing in energy supply infrastructure. Beyond the site owner, stakeholders related to industrial energy supply infrastructure are energy service companies or adjacent facility owners. Stakeholders differ in interest rates i_s reflecting costs of capital and margin expectations. The modelling of ownership structures and service contracts is highly project dependent. A good review is provided in [138]. Therefore, this work limits itself to single party models where the site owner purchases and operates all technologies.

$$\min_{P^{\mathrm{R}},C^{\mathrm{R}}} TC = \min_{P^{\mathrm{R}},C^{\mathrm{R}}} \sum_{s \in \mathcal{S}, y \in \mathcal{Y}} \left(\zeta^{\mathrm{CAPEX}}_{s,y} + \zeta^{\mathrm{OPEX}}_{s,y} + \zeta^{\mathrm{L}}_{s,y} \right) \tag{3.65}$$

$\zeta^{\mathrm{CAPEX}}_{s,y}$ are calculated from the annualized investment costs of all assets $\mathcal{K}(s) \subseteq \mathcal{K}$ belonging to a stakeholder s. Investment costs are divided into a fixed part ($c^{\mathrm{Inv,fix}}_{k,y}$) and a variable part ($c^{\mathrm{Inv,var}}_{k,y}$). Storage technologies comprise additional terms $c^{\mathrm{Inv,cap}}_{k,y}$ for capacity related investment costs. The cost terms are assumed to include all relevant grants and subsidies. Investment costs are annualized along the entire technical lifetime (y^{Tech}_{k}). The annuity factor (af_k) depends on the interest rate (i_s) of the stakeholder.

$$\zeta^{\text{CAPEX}}_{s,y} = \sum_{k \in \mathcal{K}(s)} \zeta^{\text{CAPEX}}_{k,y} \tag{3.66}$$

$$\zeta^{\text{CAPEX}}_{k,y} = \sum_{y_1=\min\{y_0, y-y^{\text{Tech}}_k\}}^{y} af_{k,y_1} \zeta^{\text{Inv}}_{k,y_1} \tag{3.67}$$

$$\zeta^{\text{Inv}}_{k,y} = \left(c^{\text{Inv,fix}}_{k,y} + c^{\text{Inv,var}}_{k,y} P^{\text{Inv}}_{k,y} \right) B^{\text{Inv}}_{k,y} \quad \forall k \in \{\mathcal{K}_C, \mathcal{K}_G, \mathcal{K}_L, \mathcal{K}_R\}, y \in \mathcal{Y} \tag{3.68}$$

$$\zeta^{\text{Inv}}_{k,y} = \left(c^{\text{Inv,fix}}_{k,y} + c^{\text{Inv,var}}_{k,y} P^{\text{Inv}}_{k,y} + c^{\text{Inv,cap}}_{k,y} C^{\text{Inv}}_{k,y} \right) B^{\text{Inv}}_{k,y} \quad \forall k \in \mathcal{K}_S, y \in \mathcal{Y} \tag{3.69}$$

$$af_{k,y_1} = \frac{(1+i_s)^{y^{\text{Tech}}_k} i_s}{(1+i_s)^{y^{\text{Tech}}_k} - 1} \tag{3.70}$$

$\zeta^{\text{OPEX}}_{s,y}$ summarizes the operational expenses of all technologies $\mathcal{K}(s) \subseteq \mathcal{K}$ belonging to the stakeholder s. The operational costs have been defined for each technology base class in Section 3.2. Costs for load curtailment are handled analogously.

$$\zeta^{\text{OPEX}}_{s,y} = \sum_{k \in \mathcal{K}(s)} \zeta^{\text{OM}}_{k,y} \tag{3.71}$$

$$\zeta^{\text{L}}_{s,y} = \sum_{n \in \mathcal{N}} \sum_{i \in \mathcal{L}_n(s)} \zeta^{\text{L}}_{n,i,y} \tag{3.72}$$

Investment planning for energy supply infrastructure is based on long-term projections of energy demands, fuel prices and the regulatory framework. These projections introduce significant uncertainty to the planning process. The presence of uncertainty in decision-making processes cannot be adequately represented by stochastic attributes, as outlined in Section 2.2. Therefore, rigorous sensitivity analysis is a widely accepted approach to handle uncertainty. Sensitivities improve the understanding of uncertainty impact and thus ensure the robustness of the design concept. A common approach for sensitivity analysis is the computation of trade-offs between one or several conflicting key performance indicators (KPIs). Typical KPIs in design of energy supply infrastructure are investment costs, primary energy consumption and carbon footprint. Trade-off analysis is frequently also referred to as multi-objective optimization [139], [140]. The computation results of a trade-off analysis can be visualized in Pareto curves.

This work applies a lexicographic optimization approach to compute trade-offs, as suggested by [29]. The system design is computed from the defined objective function, which represent the total financial expenses along the planning horizon. The trade-off is determined by adding an ϵ constraint for the conflicting KPI to the optimization model. This constraint defines an upper bound for the KPI. Parametric variations of the upper bound lead to intermediate points. Each point defines a Pareto optimal trade-off between total project costs and the analyzed KPI. The most common trade-off in energy system design [29], [141] is the relation of project costs and carbon emissions. Therefore, the corresponding ϵ constraint is shown in Equation 3.73. Analogous constraints are added for investment costs and other ecological parameters. $\epsilon_y^{\mathrm{CO2}}$ can be interpreted as the maximum carbon budget within one extension stage. Stepwise adaptation of $\epsilon_y^{\mathrm{CO2}}$ in multiple scenarios enables the computation of transformation concepts to reach various decarbonization targets.

$$\sum_{k \in \mathcal{K}} \zeta_{k,y}^{\mathrm{CO2}} \leq \epsilon_y^{\mathrm{CO2}} \quad \forall y \in \mathcal{Y} \tag{3.73}$$

3.6. General assumptions

The developed techno-economic optimization model enables analyses of multi-year, multi-stakeholder, multi-location, multi-energy, and multi-objective transformation concepts. KPIs derived from the model can provide the basis to generate and compare multiple design variants. The proposed methodology is based on several key assumptions. Feasibility studies are made under significant uncertainties, as outlined in Section 3.1. Therefore, authors in [27], [48], [78], [142] take the presented model accuracy as sufficient for techno-economic feasibility studies in distributed energy systems.

- **Linearized power flow:** The power flows within the locations of an energy supply system are based on economic optimization. Properties of the physical power flow such as temperatures, pressures and voltages cannot be directly accessed within the proposed model formulation. Technical constraints and optimization potentials, e.g., avoidance of voltage range violations or savings from lower flow temperatures, cannot be directly determined from the proposed optimization model. However, the model considers multiple discrete voltage or temperature levels as commodities to capture the relevant techno-economic implications for strategic planning. If discretizations are not sufficient, detailed analysis might be conducted with additional simulation techniques to study voltage bounds and temperature drops. Results from the detailed analysis can be fed back as operational constraints in the proposed techno-economic model formulation.

- **Perfect foresight:** The model formulation assumes perfect foresight for demands, solar irradiation and wind velocities along the entire planning horizon. However, real-world controllers have limited foresight on demand peaks and the short-term variability of photovoltaic. Therefore, realistic control strategies are suboptimal. The impact of suboptimal strategies can be considered as operating reserve requirements based on an additional analysis of forecasting errors and dynamic capabilities of supply equipment in the proposed methodology.

- **Deterministic price and demand projections:** Prices and demands are assumed to be known along the entire planning horizon. Macroeconomic coupling effects, e.g., learning curves for novel technologies, are considered as exogenous variables inside the planning model. The stakeholder model represents a basic ownership structure. This approach does not fully reflect complex financing and stakeholder models. However, these details might be defined in later stages of an energy consultancy project.

- **Minimized lifecycle costs:** Investment and operational decisions are made by minimizing the lifecycle costs along the entire planning horizon. Other intangible aspects in planning processes such as ease of permitting or technology experience of the staff are not directly addressed within the proposed methodology. Moreover, all technologies are assumed to be available at the beginning of an extension stage. Delays in project development, e.g., due to shortage of skilled workers or approval processes by regulatory authorities, can be addressed via sizing constraints. These constraints are highly stakeholder specific and thus not further discussed here.

4. Optimization framework

The proposed model formulation from Chapter 3 is integrated in an optimization framework. The framework ensures an effective solving process to determine multiple design variants in practical times. An overview of the framework components is provided in Figure 4.1. The components include strategies for time series aggregation outlined in Section 4.2 and a heuristic decomposition approach for transformation roadmaps described in Section 4.3. The optimization functionality is implemented as a sizing service in .NET Standard 2.0. Thereby, the optimization functionality of the framework can be accessed both via a newly developed desktop application for expert users and in customized cloud applications for enlarged user groups.

4.1. Concept overview

Techno-economic planning models support energy system planners and consultants to compare multiple design variants and finally select a sustainable design concept, as outlined in Chapter 2. Therefore, the optimization model introduced in Chapter 3 is integrated into an optimization framework. The framework implements a sizing service which allows to solve optimization models computationally effective. The sizing service comprises three aggregation strategies for time series and four investment strategies for multi-year transformation roadmaps. These strategies allow reducing computational complexity with limited impact on the solution accuracy. Details on these strategies are provided in the following sections. The optimization framework supports computation of multiple design variants via scenario and sensitivity analysis. Scenario analyses enable a variety of adaptations such as changes of weather years, available technologies or solving strategies. In contrast, sensitivity analyses focus on design trade-offs and apply changes to a single parameter such as the carbon budget, gas prices or photovoltaic investment costs. The underlying optimization models for both scenarios and sensitivities are sequentially computed. The optimization model is formulated in the mathematical programing language AMPL [143]. and translated into auto-generated C# code with AutoLP [144]. The model is solved either by the open-source solver SCIP 7.0.1 [145] or the commercial solver Gurobi 9.1.0 [21]. Results presented in this work are based on computations with Gurobi. The deterministic nature of the optimization framework ensures comprehensibility and reproducibility of results. All computations presented in this Thesis have been computed on a 2.2 GHz and 256 GB RAM machine with 24 physical processor cores employing up to 7 threads.

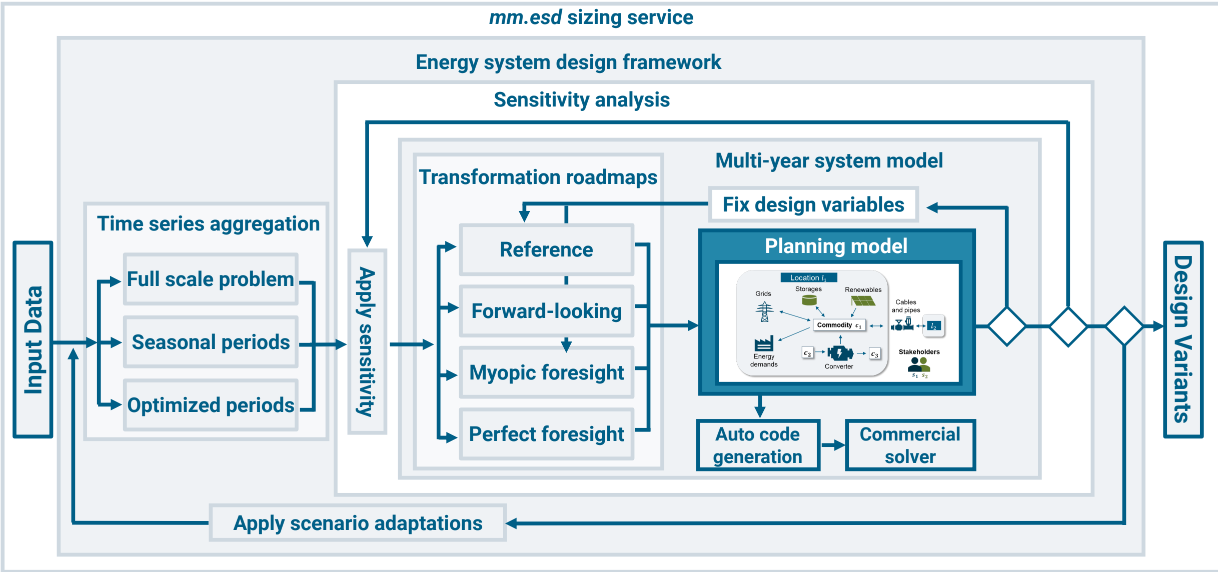

Figure 4.1.: Overview on components of the *mm.esd* sizing service

4.2. Aggregation approaches

Optimization models for industrial energy supply systems are computationally demanding, particularly if multiple technology and tariff options with discrete characteristics are included. Commercial solvers have improved in recent years, as outlined in Section 1.1. However, solving of complex models for an entire year (8760 h) for each extension stage y takes up to several days computation time [88]. This is impractical for daily applications of energy system planners and consultants. Therefore, the complexity needs to be effectively reduced. A widely accepted technique for complexity reduction is time series aggregation [80], [118], [119]. Time series aggregation targets at reducing the number of time steps in the optimization model. Instead of modeling the dispatch in each hour of a year, the operational statistics are approximated from a set of representative days or weeks, as outlined in Section 2.5. If these representative periods capture all relevant statistical information of the entire year, the model is solved faster without significant loss of modeling accuracy [51]. Time series aggregation requires approaches to derive these representative periods from the relevant time dependent attributes of the optimization model. This work proposes a newly developed medoid-based clustering algorithm.

This Thesis compares three strategies for time series aggregation: a full-scale problem (FSP), a seasonal period selection (SPS) and an optimized period selection (OPS). The strategies are sequentially applied to each extension stage of the optimization model. The FSP approach describes the baseline with operational variables and constraints for an entire year with 8760 h. For the SPS, all time series for the entire year are divided into a set $\mathcal{D}$ of candidate representative periods depending on a pre-defined length. Typical industrial energy supply systems include daily patterns for operation. Within this work, the length of representative periods is defined as 24 h.[7] The

[7]The proposed approach can be applied to energy systems with short-term storages with daily or weekly storage cycles. Energy supply systems with strong seasonal dependence might anticipate solutions with mid- to long-term storage technologies as part of an optimal solution. These technologies require advanced modeling techniques which are described in [122].

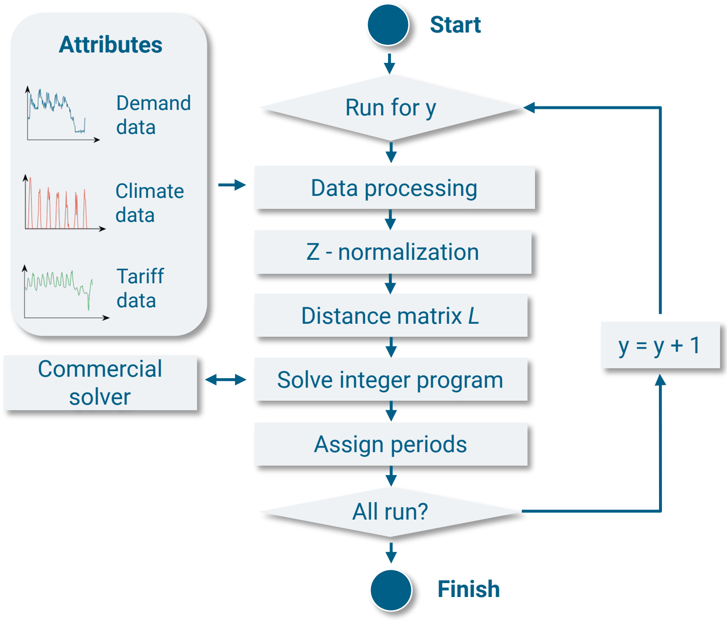

Figure 4.2.: Schematic overview of optimized period selection (OPS) approach to determine representative periods from a set of attributes for each extension stage y

SPS approach selects a pre-defined number of seasonally distributed periods $\mathcal{D}^{\mathrm{Repr}}$. Correlations between the attributes are preserved as the representative periods are directly extracted from $\mathcal{D}^{\mathrm{Repr}} \subset \mathcal{D}$. However, the SPS approach omits statistical information of the time series attributes. The weight factor w_d is thus equal for all representative periods derived by SPS.

Statistical information of the relevant time series is used in the optimized period selection (OPS). The relevant time series are referred as a set of attributes $\mathcal{A}$ in the following. Attributes are related to time varying energy demands, renewable generation profiles and market price signals within this work. The proposed algorithm derives an optimal selection $\mathcal{D}^{\mathrm{Repr}}$ of n^{Repr} representative periods from n candidate periods based on information in $\mathcal{A}$. The selection of time periods is purely driven from the input data of the planning model which is available in early planning stages. Additional information is not considered, e.g., the share of renewables to weight the impact of renewable time series. OPS is based on a five-step procedure illustrated in Figure 4.2. In a first step, all relevant time dependent attributes are divided into candidate periods $\mathcal{D}$. Periods with peak demands are assigned to a set of extreme periods. These are enforced to be included in $\mathcal{D}^{\mathrm{Repr}}$. Afterwards, all attributes are normalized. A distance matrix L is computed describing the similarity of candidate periods. The integer program (IP) model is formulated based on L and solved by the commercial solver Gurobi. The last step assigns the representative periods based on the solution of IP. The IP derives weight factors for each representative period. These factors are directly included in the optimization model. The methodology is repeated for the time depending attributes of each extension stage sequentially.

Time-varying attributes have different numerical ranges. A generation profile for photovoltaic is typically normalized to values between 0 and 1 whereas load profiles might comprise five-digit peak demands. Clustering these attributes would result in a bias with a preference to attributes with larger numerical values. The impact can be limited by normalization techniques. Therefore, all attributes $x_{a,d,t}$ are scaled to mean zero and standard deviation one ("z-normalization").

$$\tilde{x}_{a,d,t} = \frac{x_{a,d,t} - \mu_a}{\sigma_a} \tag{4.1}$$

The normalized attributes $\tilde{x}_{a,d,t}$ allow the computation of the distance matrix L. L describes the dissimilarity of a period and its representative period. This work employs the Euclidean distance to compare values of attributes a and time steps t between two candidate periods i and j. The matrix is symmetric ($l_{i,j} = l_{j,i}$). This characteristic is used to simplify the calculation of L.

$$l_{i,j} = \sqrt{\sum_{a \in A} \sum_{t \in T_i} (\tilde{x}_{a,i,t} - \tilde{x}_{a,j,t})^2} \tag{4.2}$$

$$L = \begin{bmatrix} 0 & l_{1,2} & \dots & l_{1,n} \\ l_{1,2} & \ddots & l_{2,n-1} & \vdots \\ \vdots & l_{2,n-1} & \ddots & l_{n,n-1} \\ l_{1,n} & \dots & l_{n,n-1} & 0 \end{bmatrix} \tag{4.3}$$

L summarizes the parameters for the formulation of the IP. The formulation of the IP is given in Equations 4.4. Binary variables $B_{i,j} \in \{0,1\}$ indicate whether the period i of the original attribute is represented by a period j in the aggregated set. The objective function targets at minimizing the sum of dissimilarities indicated by the elements in L. Each period needs to be assigned to exactly one representative period ($B_{j,j} = 1$). The operation during peak periods typically defines the capacity for peak technologies. Therefore, candidate periods $\mathcal{D}^{\text{Peak}}$ with peak demands are enforced to be included in the set $\mathcal{D}^{\text{Repr}}$ of representative periods.

$$\min_B \sum_{i \in \mathcal{D}} \sum_{j \in \mathcal{D}} l_{i,j} B_{i,j} \tag{4.4}$$

$$\sum_{j \in \mathcal{D}} B_{j,j} \leq n^{\text{Repr}} \tag{4.5}$$

$$\sum_{j \in \mathcal{D}} B_{i,j} = 1 \quad \forall i \in \mathcal{D} \tag{4.6}$$

$$B_{i,j} \leq B_{j,j} \quad \forall i, j \in \mathcal{D} \tag{4.7}$$

$$B_{j,j} = 1 \quad \forall j \in \mathcal{D}^{\text{Peak}} \tag{4.8}$$

The integer program is solved till optimality by one of the solvers denoted in the previous section. This approach guarantees deterministic and robust results. Solving times are below 10 seconds [51] and thus not further discussed in this work. The set $\mathcal{D}^{\text{Repr}}$ comprises those periods j with $B_{j,j} = 1$. Both regular and extreme periods are included in $\mathcal{D}^{\text{Repr}}$. In contrast to regular periods, extreme periods occur only rarely. The operation during extreme periods thus has a smaller influence on annual operational expenses such as fuel costs. The optimization model accounts for this fact by weight factors $w_j = \sum_{i \in \mathcal{D}} (B_{i,j})$ introduced in Chapter 3. This approach helps to preserve annual statistics of energy demands, market prices and renewable generation. The proposed algorithm is applied to each extension stage before solving the multi-year system model.

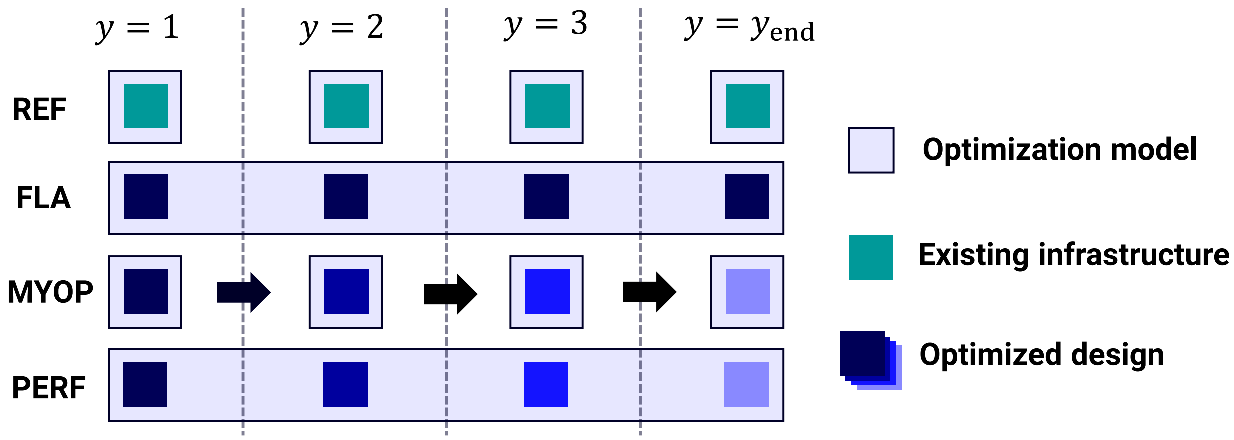

Figure 4.3.: Strategies for roadmap optimization: Reference (REF), forward-looking design approach (FLA), roadmap approach with myopic foresight (MYOP) and roadmap approach with perfect foresight (PERF)

4.3. Roadmap strategies

The multi-year model determines transformation roadmaps including multiple extension stages. Transformation roadmaps comprise recommendations for the evolution of an energy supply system: Capital intensive investment decisions might be delayed in a "wait-and-see" strategy. Recourse actions can be taken in case of unfavorable developments. Existing equipment is replaced after the end of its lifetime [50]. This gives decision makers additional transparency but adds additional computational complexity to the system model. This work proposes four strategies for roadmap computation. The strategies are illustrated in Figure 4.3.

Integration of long-term trends in planning models requires projections of all future on-site demands, energy procurement prices and technology developments as well as corporate policies such as decarbonization targets. These projections can be directly applied to optimize investment decisions using the model from Chapter 3. All extension stages are integrated in a single optimization model ($\mathcal{Y} = \mathcal{Y}'$) assuming perfect knowledge on future developments. The described approach is referred to as the roadmap approach with perfect foresight (PERF) in the following. PERF determines a cost-optimal transformation strategy over the entire planning horizon. Consequently, the approach comprises adaptive investment decisions and thus enhances robustness of energy supply concepts to projected long-term trends. However, the recommended decisions are highly dependent on the accuracy of input data. For example, an investment for a cogeneration plant might be based on the assumption of future rising electricity market prices. Input data is based on long-term projections of economic, political, and technological developments. These projections are known to comprise significant uncertainty. Therefore, three alternative strategies are introduced in this work. The reference (REF) strategy describes a strategy with minimal investments. Existing equipment is replaced by identical equipment at the end of its technical lifetime. The strategy is implemented by adding two constraints to the optimization model: The design remains constant over the entire project lifetime (4.9). No new equipment is added in first extension stage y_0 (4.10). The models for each extension stage are thus decoupled and are solved independently.

$$P^{\mathrm{R}}_{k,y} = P^{\mathrm{R}}_{k,y_0} \quad \forall k \in \mathcal{K}, y > y_0 \tag{4.9}$$

$$P^{\mathrm{R}}_{k,y_0} = P^{\mathrm{Inst}}_{k} \quad \forall k \in \mathcal{K} \tag{4.10}$$

In contrast, the forward-looking design approach (FLA) optimizes a design concept over the entire planning horizon. Therefore, the installed capacities of all technologies remain constant over the extension stages (4.9). However, investment decisions can be made in the first extension stages impacting the design and operation in all future extension stages. The planning philosophy in FLA assumes perfect knowledge on all future developments and thus results in a cost-optimal solution. However, the value of adaptive decisions, e.g., the delayed installation of battery storages, is not included in the FLA. This limitation is overcome by the roadmap approach with myopic foresight (MYOP). MYOP optimizes equipment and dispatch strategy in each extension stage starting with the first extension stage y_0. The optimizations for the following extension stages allows for new investment and replacement decisions considering previously installed equipment with respect to its end of lifetime and adapt the energy supply system to changing boundary conditions. MYOP is based on myopic foresight. Long-term trends evolve in a rolling horizon schema: Therefore, all decisions are not based on projected long-term trends, but rely on on-site demands, energy procurement prices and regulatory framework of the respective extension stage.

4.4. Software architecture

The described optimization model is the core of the newly developed prototype expert tool *mm.esd* for multi-modal energy system design. The functionality of the framework has been successfully benchmarked to a model of Thiem [27] for case studies of an office building, a city district and an airport. Reliability of novel features is ensured by automatic software unit tests. The described framework depicts the sizing service in the server application which enables users to compute multiple projects on a well-equipped remote machine with 24 physical processor cores in parallel. The remote service makes computation of complex projects practically feasible for energy planners and consultants.

The sizing service on the remote machine can be accessed via a newly developed desktop application. Users can analyze both input and result data in this desktop application. The user interface of the desktop application is shown in Figure 4.4. The application allows to define all relevant project information. The characteristics of input time series is displayed in a statistics table and in various plotting formats. In a second step, the user selects assets and determines the relevant techno-economic parameters. The user interface supports the import of models from an extensive internal database and the formulation of custom models for sector-specific technologies. In a third step, scenarios are defined. Each scenario can comprise a sensitivity analysis. The available technology set in each scenario is visualized in automatically generated topology graphs. A selection of scenarios is sent to the server for computation. After completion of the solving process, the optimization results can be directly analyzed in 18 result categories with up to six different subgraph types. The interactive visualization capabilities include pie charts, heatmaps and Sankey diagrams which are created with the JavaScript libraries D3.js and Plotly.js and rendered in an embedded Chromium browser. All numerical data can be easily imported and exported to Excel

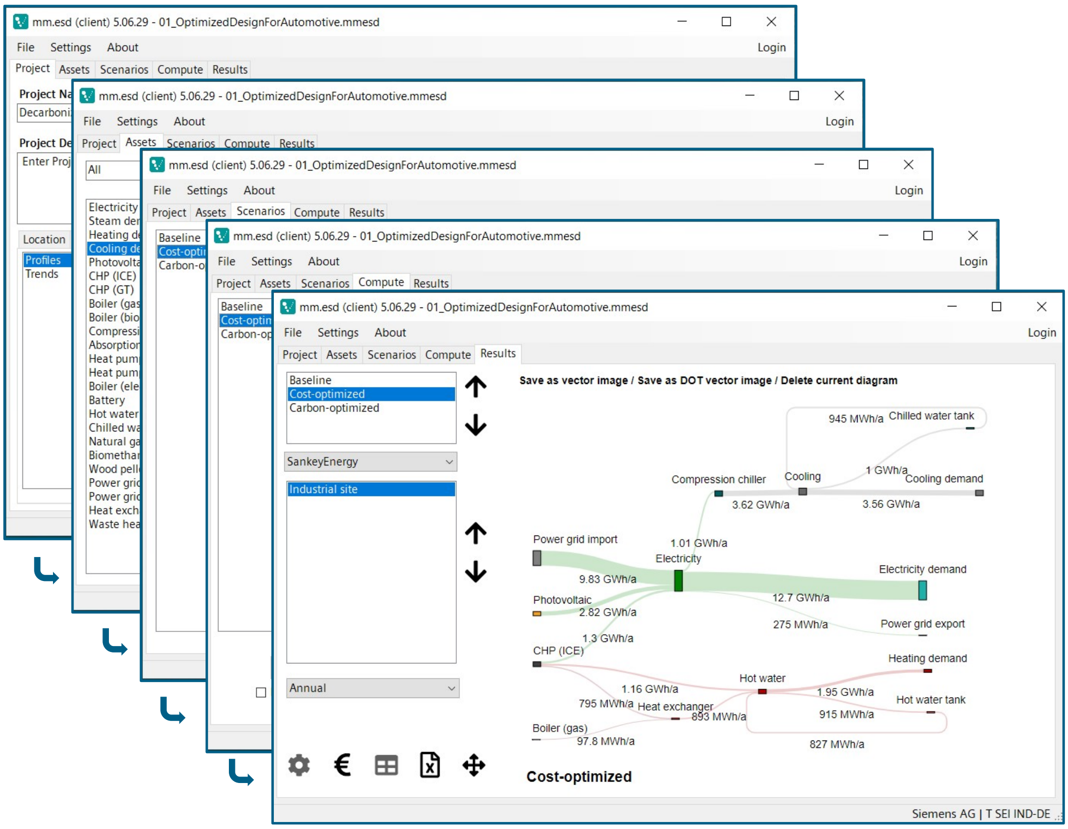

Figure 4.4.: Client application of the newly developed prototype tool *mm.esd* for multi-modal energy system design

worksheets for exchange with customers and other researchers. Moreover, technology and scenario names as well as colors can be dynamically updated. Input and result data are saved in a dedicated format. The optimization results for different projects can be merged. This enables a comparison of key performance indicators across multiple energy consultancy projects.

The introduced optimization framework is actively employed in commercial consultancy projects for more than two years. The user community counts for 30 energy experts in December 2022.

5. Results

Optimization-based design approaches enable energy system planners and consultants to make faster and more accurate decisions for sustainable industrial energy supply systems. This chapter highlights selected features of the newly developed optimization framework for three use cases derived from German industry. Energy supply systems of the brownfield sites are introduced in Section 5.1. Potential cost and carbon savings by optimization measures are calculated from an entire representative base year in Section 5.2. Calculations based on an entire representative year introduce significant computational complexity. Therefore, time series aggregation is applied in Section 5.3. Section 5.4 analyzes the robustness of the identified saving potentials to long-term changes in prices and demands. A detailed technical analysis including security of supply constraints for maintenance periods and unit failures is provided in Section 5.5. Finally, opportunities and limitations of the exemplary use cases are summarized in Section 5.6.

5.1. Use case descriptions

The suitability of the proposed methodology is highlighted by simulative evaluations of three use cases. The use cases illustrate production facilities from automotive, pharmaceutical and dairy industry in Southern Germany.[8] The use cases comprise multi-modal energy demands, which are supplied by existing gas-fired boilers and compression chillers. Existing supply concepts are optimized by investment in new supply equipment and adaptation of procurement tariffs. All optimization measures are summarized in a technical superstructure. The relevant input data for roadmap optimization is provided for the milestone years from 2023 to 2035. The design is optimized in each extension stage considering installed equipment from previous periods. The required investments are associated with an interest rate r of 7 %.

5.1.1. Energy demands

Industrial energy systems need to meet both production and building energy demands. These demands comprise electricity for drives and lightning, steam for sector specific processes, space heating in factory halls as well as cooling for building ventilation and process cooling. All energy demands in the three sites are represented by hourly load profiles. Temperature and pressure levels for steam, heating and cooling are assumed to be identical in all simulative evaluations. An exemplary weekly pattern of electricity demand is visualized in Figure 5.1. The production starts on Monday at 6 am and then continues till Friday 8 pm. Peak demands occur between 7 am and 4

[8] Case studies are derived from real-world sites in Germany. Energy demands and tariff details of the sites have been simplified and anonymized for the illustrative purpose of this work.

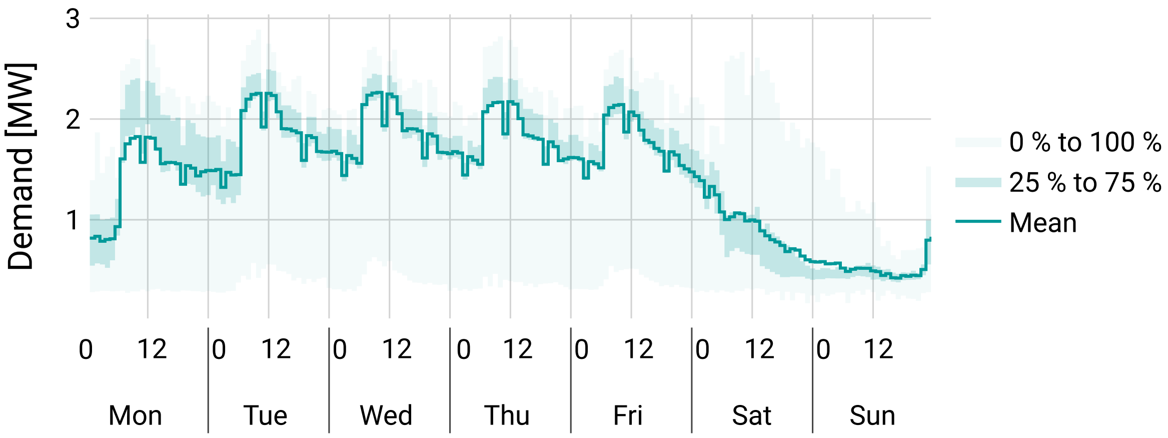

Figure 5.1.: Weekly pattern of electricity demand for automotive site in 2023

Table 5.1.: Multi-modal energy demands and projections for three industrial sites in Germany

Site	Electricity GWh/a	Steam GWh/a	Heating GWh/a	Cooling GWh/a	Change 2030 %
Automotive	12.7	-	2.0	3.6	-13.5
Pharma	14.9	9.0	0.7	7.8	- 3.2
Dairy	15.8	50.4	-	27.0	-2.0

pm. The electricity demand is significantly lower during the weekend. Production interruptions, e.g., due to plant holidays, occur only rarely for this site. The production is interrupted for two weeks in December only.

Total annual energy demands for the three sites are summarized in Table 5.1. Electricity demands range from 12 GWh/a to 16 GWh/a. Moreover, all sites comprise demands for process cooling which are not included in the electricity demands. The automotive and pharmaceutical site comprise additional demands for space heating with a seasonal pattern. The pharmaceutical and dairy sites require significant amounts of steam for production. Demand changes till 2030 are employed for roadmap optimization. Production volumes are assumed to remain constant along the planning horizon. Demand developments reflect the continuous implementation of energy efficiency measures based on the analysis in [146]. The automotive site is assumed to follow a progressive implementation of efficiency measures whereas the pharmaceutical site follows a moderate and the dairy a conservative implementation strategy.

5.1.2. Energy procurement

Industrial sites have typically higher on-site energy demands than on-site potential for renewable generation. Therefore, energy needs to be procured from energy markets. Energy procurement is technically feasible via the public power and natural gas grid connection. Solid fuels such as wood pellets are supplied via trucks. Different sources of energy procurement are implemented as grid technologies introduced in Section 3.2. The assumptions for costs and emission factors including

Table 5.2.: Price and carbon footprint projections for energy procurement based on [148]–[150] and own assumptions

Carrier	Unit	2023	2026	2029	2032	2035
Electricity	€/MWh (avr)	170	190	220	250	280
	€/kWp/a	97	100	103	106	110
	kgCO2/MWh	323	263	203	143	110
Natural gas	€/MWh	75	120	130	140	150
	kgCO2/MWh	210	210	210	210	210
Biomethan	€/MWh	105	150	165	180	195
Wood pellets	€/MWh	100	145	155	175	185
Carbon price	€/tCO2	70	90	120	170	200

long-term evolution are summarized in Table 5.2. Electricity procurement is based on an energy related Time of Use (ToU) tariff and a demand charge. Table 5.2 shows yearly average procurement costs. Following the approach of Bahl [92], the tariff is determined from a fixed proportion and the German spot market price. Spot market prices are extracted from the SMARD platform for 2020 [147] and adapted to projected increases in price levels. Periods with negative spot markt prices are set to zero to avoid strong incentives to waste electricity in the planning model. Demand charges reflect network costs and are calculated from the maximum power purchase. The German regulatory framework derives network charges depending on grid utilization [148]. Network charges for sites with constant grid utilization (> 2,500 h/a) are mostly based on demand charges. Demand charges are reduced by 87 % for low grid utilization (< 2,500 h/a) and replaced by energy related costs of 34 €/MWh. This regulatory framework condition is reflected by implementation of two tariffs which are mutually exclusive via the technology link concept introduced in Section 3.3. On-site generated electricity can be fed in the power grid and is rewarded by the hourly spot market price. Both power and natural gas procurement are associated with carbon footprints. A carbon price is considered for all on-site emissions from natural gas. The projected development is taken from the analysis in [149]. Biomethane and wood pellets can be procured at significantly higher costs. Their on-site use is not associated with carbon emissions.

5.1.3. Technical superstructure

The interface between energy procurement and energy demands is the on-site infrastructure for electricity, steam, heating, and cooling supply. Figure 5.2 shows the technical superstructure comprising the existing infrastructure equipment and possible technology extension options. The superstructure assumes that all equipment is installed in a central technical center which supplies the production facilities of the site. The existing energy supply concept of the three sites is based on central gas-fired boilers and compression chillers. These boilers and chillers are assumed to be at the end of lifetime and need to be replaced in three years. Steam and hot water systems are connected via local heat exchangers. A connection to the power grid ensures a secure supply with electricity.

The existing energy supply system can be extended by a set of possible technology options. Detailed assumptions for the technology extension options are summarized in the annex in Tables A.1 to A.3.

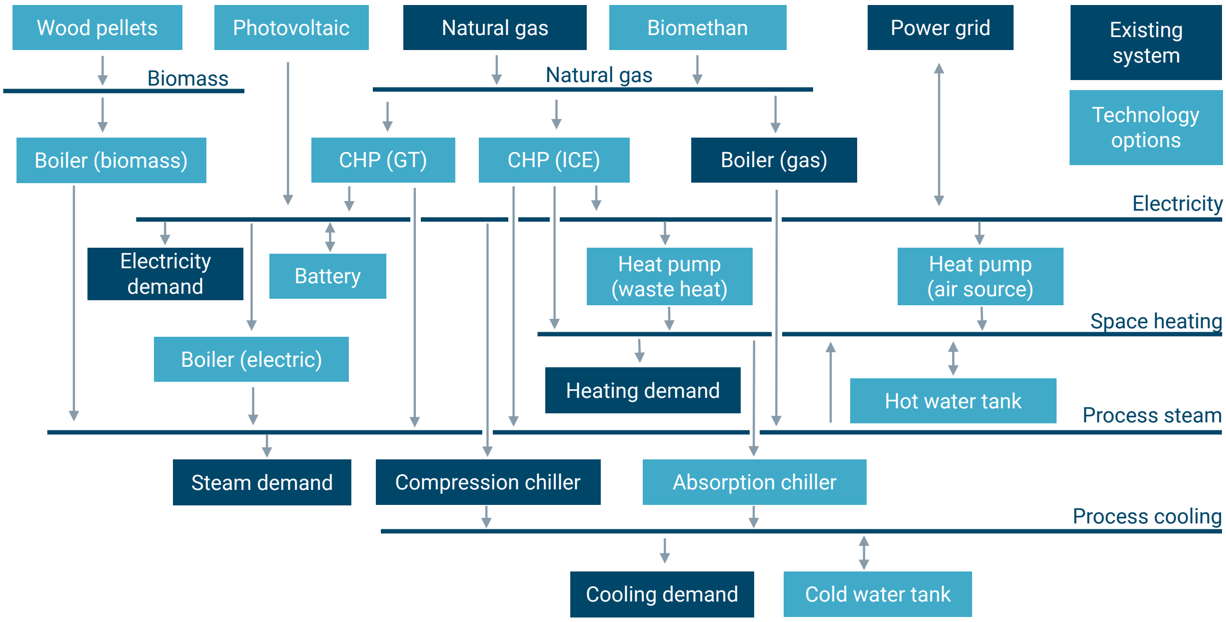

Figure 5.2.: Technical superstructure of multi-modal energy supply system. The existing equipment meets electricity, steam, heating, and cooling demands. The energy supply system can be extended by a variety of technology options.

New conversion and storage technologies are modeled with non-linear investment cost models. Delays for construction are not considered for the simulative evaluations in this work. Therefore, all options are immediately feasible. One technology option is the installation of a new combined heat-and-power (CHP) plant. The CHP can be installed with internal combustion engines (ICE) for small installations or with gas turbines (GT) for larger installations. Estimations for investment and maintenance costs are size dependent following the intercept-slope approach described in Section 2.3. Moreover, technology-specific minimum part-load ratios are considered. Simulative evaluations are conducted in hourly time steps. All technologies are assumed to ramp up and down significitantly faster. Therefore, ramping capabilities are not considered for this use case. The high-grade waste heat from the flue gases is integrated into the steam supply system. Low grade waste heat from engine cooling is used for space heating or process cooling by means of absorption chillers. Steam can be alternatively generated from boilers. Fuel for CHP and boilers can be selected from two gas tariffs with different costs and carbon emission factors.

Photovoltaic (PV) panels provide a renewable alternative for on-site electricity generation: Roof-top PV panels can be installed on production or logistic halls, on administrative buildings or in parking areas. Ground-mounted installations are built in the neighboring open spaces. Industrial sites are often historically grown. Space restrictions limit on-site installation of PV. These limitations require detailed on-site assessments and are not discussed in this Thesis. Consequently, potential for roof-top and ground-mounted PV is assumed to be unlimited for the conducted simulative evaluations. Hourly PV generation potentials are estimated based on the NASA climate reanalysis (MERRA-2) [151]. The employed photovoltaic model from Pfenninger [124] considers azimuth and tilt angle as well as system losses. The model has been validated for multiple sites. The time series is shown in Figure 5.3. Electricity from photovoltaic is available in particular during noon in summer. Generated electricity might exceed the demand of the factory during these times. Lithium-ion

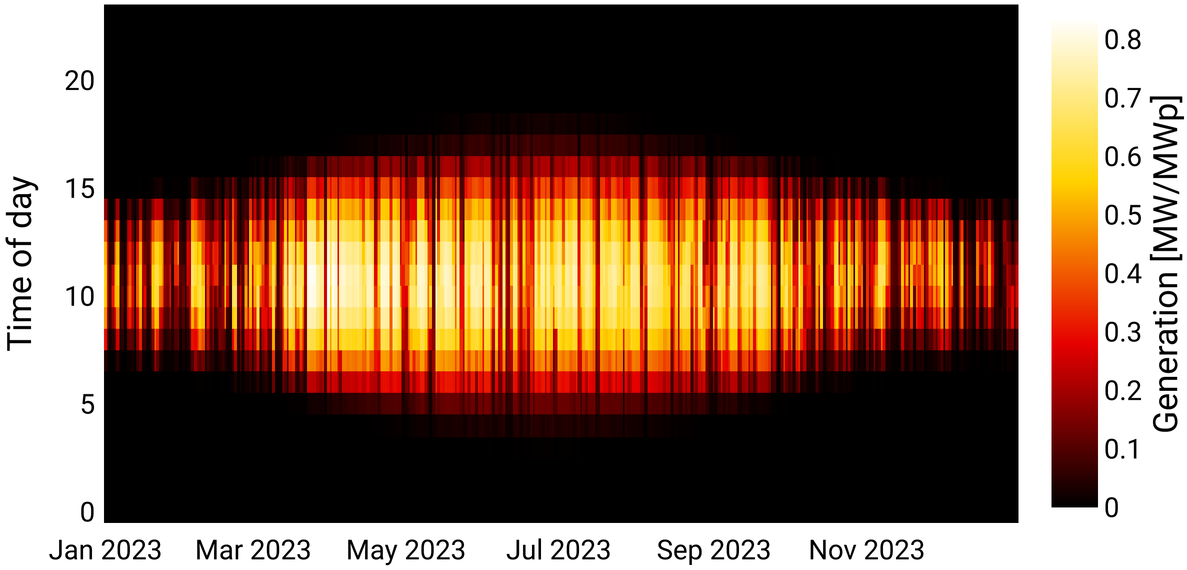

Figure 5.3.: Solar generation potential for a location in Southern Germany based on [124]

batteries help to increase the self-consumption rate of PV: They temporarily store excess electricity for use during evening and night hours. Beyond optimization of self-consumption, value streams for batteries include arbitrage trading and peak load management. Cost estimation for batteries comprise fixed proportions for planning and installation, power-related proportions for the inverter and capacity-related proportions for battery cells. Both investment and maintenance costs for photovoltaic and batteries are assumed to decline in the next years. The detailed assumptions for these trends are summarized in the annex in Table A.2.

Batteries are one technology option to decouple renewable generation and volatile demand. Hot and chilled water tanks are alternative sources for flexibility: They act as buffers to meet peak demands and integrate renewable excess energy. Power-to-heat technologies such as electric boilers and heat pumps are options to integrate renewable electricity in thermal supply systems. The coefficient of performance (COP) of the heat pumps is derived from the Carnot efficiency (η^{Carnot}) with an effective efficiency (η^{HP}) rate of 0.5 [152]: The COP is depending on the temperature ($\vartheta^{\text{Source}}$) of the heat source and the flow temperature ($\vartheta^{\text{Supply}}$) of the heating system.[9]

$$\eta^{\text{Carnot}} = \eta^{\text{HP}} \frac{\vartheta^{\text{Supply}}}{\vartheta^{\text{Supply}} - \vartheta^{\text{Source}}} \tag{5.1}$$

The heating system is assumed to be operated at constant flow temperatures $\vartheta^{\text{Supply}} = 75\,°C$ throughout the year. Low grade waste heat with $\vartheta^{\text{Source}} = 40\,°C$ is available during working shifts. Air source heat pumps use ambient air with varying temperatures as a heat source and thus have a seasonal depending COP. Energy efficiency ratios (EER) of the compression and absorption chillers are taken from the normative standard DIN 18599-7 [153].

[9]Temperatures ϑ for Carnot efficiencies refer to absolute temperatures in Kelvin.

5.2. Optimized energy supply

The proposed methodology derives key performance indicators for preliminary design variants of multi-modal coupled supply systems for electricity, steam, heating, and cooling. The following section shows exemplary results for the automotive site in the base year 2023. This discussion shall illustrate possible results during an early phase of a consultancy project. Moreover, it highlights the correct implementation of energy balances and technology models. The evaluation is conducted in three scenarios: a baseline scenario, a cost optimal scenario and carbon optimal scenario. The baseline scenario describes the existing concept for energy supply with a gas fired boiler for heating and a compression chiller for cooling demands. This concept is optimized in the cost optimal scenario by minimizing the total project costs. The carbon optimal scenario also minimizes total project costs while avoiding any emissions in Scope 1. The resulting design concept thus determines an optimal setup without on-site use of natural gas.

Key indicators for economic, ecological and energetic performance

Key performance indicators (KPIs) for the three scenarios are shown in Figure 5.4. The existing supply concept costs 2.8 M€/a and causes 4.9 kt/a of carbon emissions. An upgrade of the energy supply infrastructure significantly reduces both costs and emissions: The cost optimal scenario results in 6.4 % lower costs and 21 % lower carbon emissions. The carbon optimal scenario avoids any on-site use of fossil fuels and leads to even higher reductions of carbon emissions (26 %) compared to the baseline scenario. The upgrade of the energy supply concept requires investments which are estimated with 4.2 M€ and 5.1 M€ for the cost and carbon optimal scenario respectively.

Rated power and storage capacities are summarized in Table 5.3. The annual energy and peak flows of the cost optimal scenario are visualized in Figure 5.5. Storage losses and ambient heat sources or sinks are not shown in the Sankey diagram to enhance clarity of the economic relevant

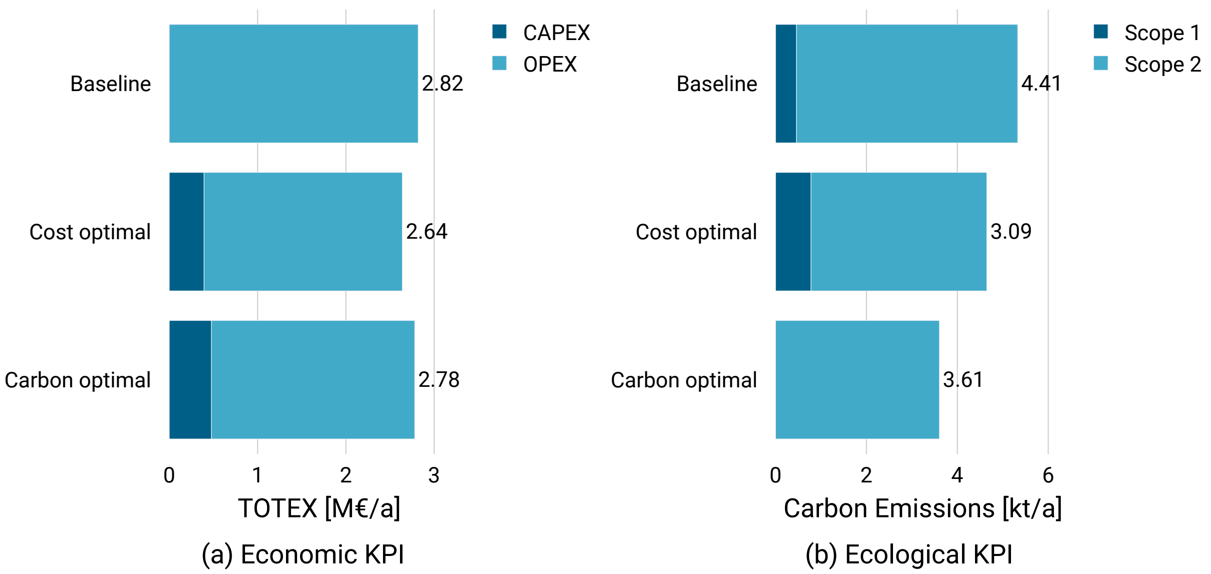

Figure 5.4.: Key performance indicators (KPIs) for three exemplary scenarios of a German automotive site

flows. The design of the baseline scenario is limited to installed equipment capacities with a 950 kW compression chiller and 1500 kW gas-fired boiler. The power grid provides electricity for on-site demands including compression chillers. The heating supply system is based on gas-fired boilers and meets the on-site heating demands. Auxiliary demands for boilers are not considered within this work. Therefore, the electricity and heating system are decoupled. In contrast, the energy supply systems for electricity, heating and cooling are strongly coupled in the optimized design scenario: The gas-fired boilers are only used as backup equipment in the optimized scenario: The utilization is reduced from 2.0 GWh/a to 0.1 GWh/a. Heat is generated by a newly installed CHP plant with internal combustion engine (ICE). Hot and cold water tanks provide sources of flexibility: Cold water tanks of 1.97 MWh enable a flexible operation of compression chillers during low electricity prices. Hot water tanks of 3.07 MWh balance waste heat from the CHP plant and heating demand. A photovoltaic plant of 2.3 MW provides renewable electricity to the system. The carbon optimal design comprises a slightly larger photovoltaic installation of 2.4 MW. The CHP plant is not part of the carbon optimal design concept. Heating demand is met by a 508 kW heat pump which uses the on-site waste heat potential. A biomass boiler with 637 kW capacity is used during cold periods with peaks in space heating demands. Additional details on the carbon optimal scenario are provided in Figure A.1. The optimization framework is able to automatically derive the economic, ecological and energetic KPIs for different design variants. Economic and ecological KPIs are directly visualized in bar charts enabling easy comparison of multiple scenarios. Sankey charts depict the energetic KPIs in hourly, monthly or annual aggregation. The developed visualizations clarify the value of multi-modal coupling in industrial energy supply systems for relevant stakeholders, e.g., factory management.

Table 5.3.: Rated power and storage capacities for the automotive site in three scenarios for the base year 2023

Technology	Unit	Baseline	Cost optimal	Carbon optimal
Photovoltaic	kW	-	2307	2353
CHP (ICE)	kW	-	632	0
Boiler (gas)	kW	1500	308	0
Boiler (biomass)	kW	-	0	637
Compression chiller	kW	950	744	786
Heat pump (waste heat)	kW	-	0	508
Hot water tank	kWh	-	3066	4152
Chilled water tank	kWh	-	1972	2486

Intradaily and seasonal dependence of energy demands and renewable generation

Industrial energy systems comprise intradaily and seasonal demand patterns as well as complex procurement tariffs. The following section highlights how these requirements are considered in the optimization for the example of the cost optimal scenario.

Solar generation from photovoltaic and space heating demands show a strong seasonal dependence. Heating demand accounts for 361 MWh in December compared to 36 MWh in July. In contrast, the solar plant generates only 2.5 % of its annual yield in December, but 13.4 % in July. The seasonal dependence is captured in the proposed optimization approach: The monthly energy balances for generation and supply with electricity, heating and cooling is shown in Figure 5.6

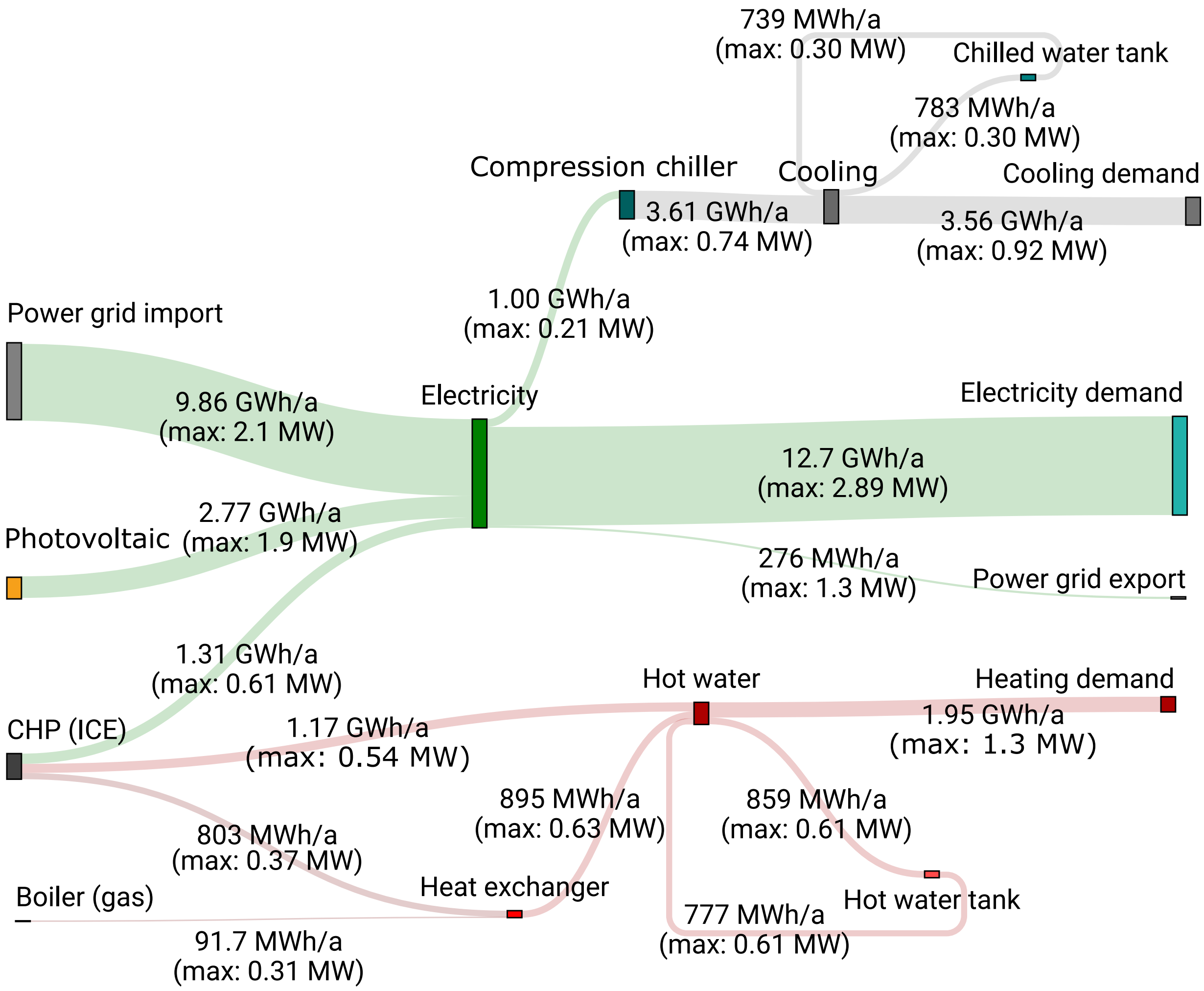

Figure 5.5.: Sankey charts for the cost optimal scenario of automotive site. The Sankey chart provides an overview of annual energy flows and peak utilization in a multi-modal coupled energy supply system.

for the optimized design scenario. The cooling demand is almost fully supplied by compression chillers. The compression chillers account for 9.0 % of electricity consumption. This share remains roughly constant throughout the year as the cooling demand is related to production processes. In contrast, the share of solar generation shows a yearly pattern: The photovoltaic plant delivers 32 % of electricity during July, but only for 8.2 % during December. The solar generation is thus complemented by the CHP plant which is almost not used during the summer months and generates 26 % of electricity in December. Waste heat from the CHP is sufficient to meet almost the entire heating demand during the winter season. Peak periods are supported by the existing gas-fired boilers. Understanding of seasonal variations in energy supply systems is crucial, in particular with increasing shares of renewable energy. The developed methodology helps to quantify the impact for energy system planners and consultants.

The cost optimal energy supply concept integrates renewable excess energy from photovoltaic and interacts with the energy markets via complex procurement tariffs. This requires a high temporal granularity with hourly time steps. Dispatch for electricity is shown in Figure 5.7 for

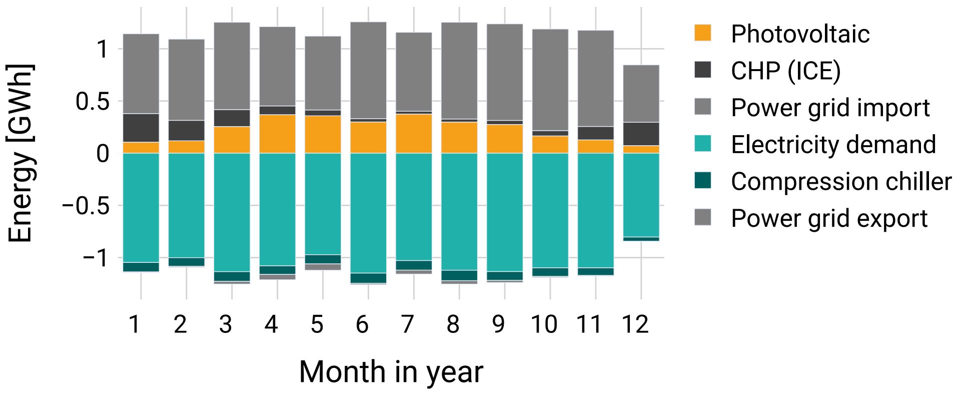

(a) Electricity generation (positive) and use (negative)

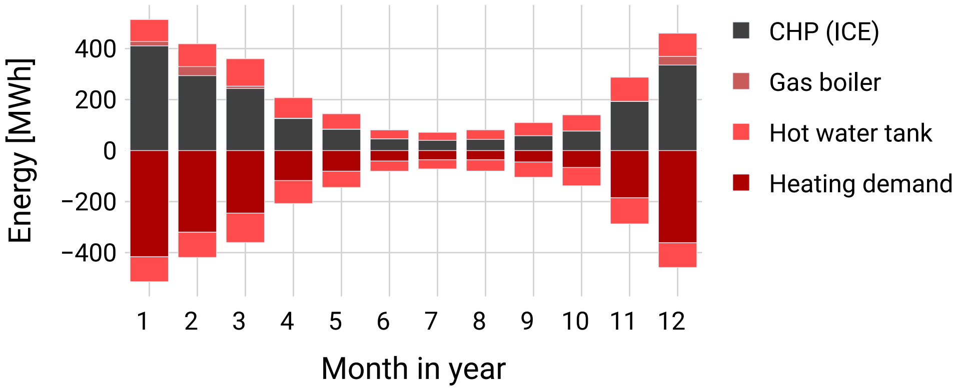

(b) Heat generation (positive) and use (negative)

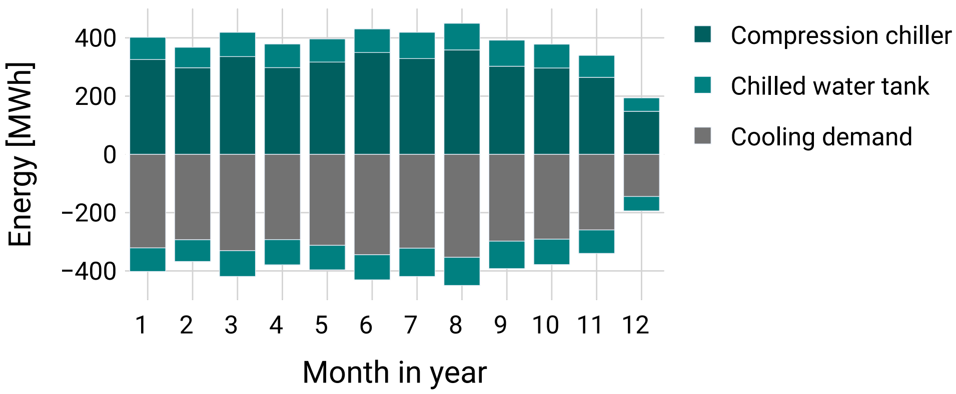

(c) Cold generation (positive) and use (negative)

Figure 5.6.: Monthly energy statistics for cost optimal design scenario of automotive site

an exemplary summer and winter week. To illustrate the impact of complex tariffs, the graph comprises the dynamic component of the ToU tariff which is based on German spot market prices. The electricity supply during noon in the summer week is dominated by solar generation. The generation correlates with peak demands during work days leading to high self-consumption rates. The generation exceeds the demand during weekends. The excess electricity is fed in the power

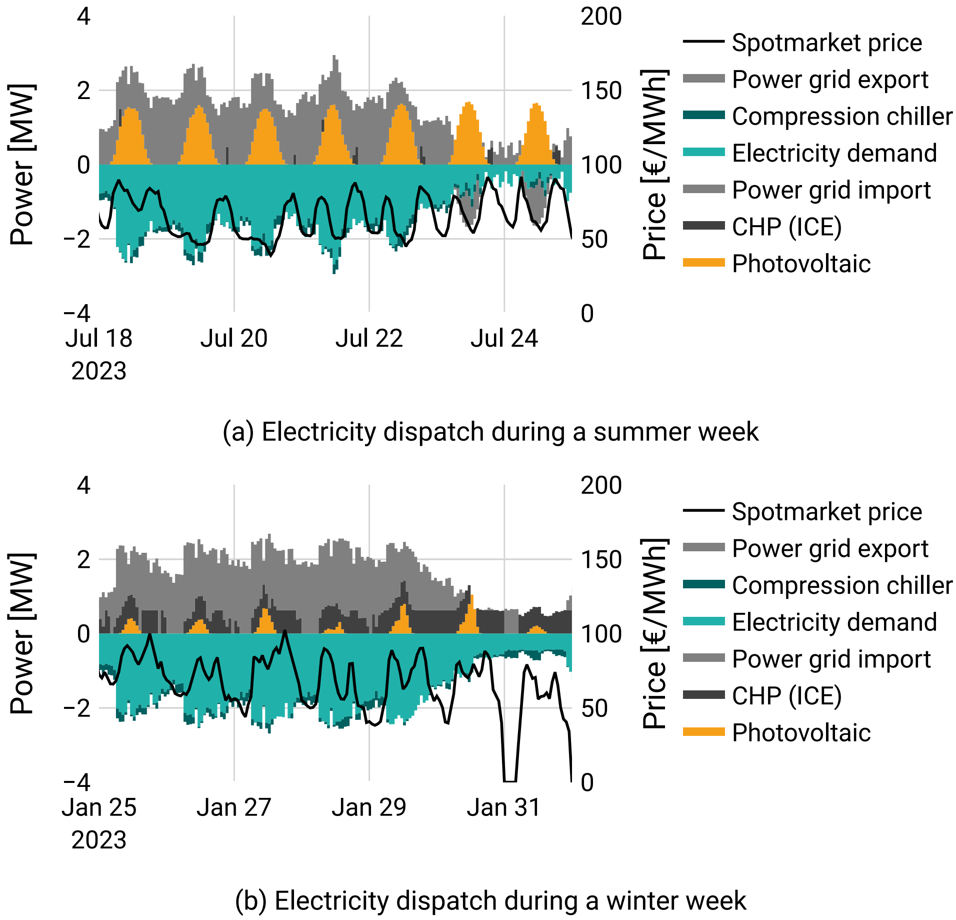

Figure 5.7.: Hourly generation (positive) and use (negative) of electricity in cost optimal scenario of automotive site

grid. However, potential revenues from feed-in are comparatively low during noon. Therefore, the excess electricity is used by compression chillers to meet cooling demand. In order to balance, generation and demand the installation of a tank for chilled water is required. In the winter week, solar generation is significantly lower. The CHP plant produces electricity during periods with both high spot market prices and sufficient on-site heating demands. The CHP generation is stopped during periods of extremely low spot market prices. Periods with low spot market prices are typically characterized by high shares of non-dispatchable renewable generation, e.g., from wind parks. The energy supply system adapts by advanced control schemas to market signals and procures its electricity from the power grid.

Compression chillers and cogeneration plants couple the on-site thermal supply systems with the electricity supply. Therefore, Figure 5.8 shows the heating and cooling dispatch for the summer and winter week. The compression chillers are preferably operated during periods with low electricity prices. This is obvious for those periods with excess electricity from on-site photovoltaic installations. Excess electricity is used to load chilled water tanks which serve cooling demands during peak periods. The flexible operation of CHP is enabled by a hot water tank. The storage ensures the supply of space heating demands when the operation of the CHP is not economically

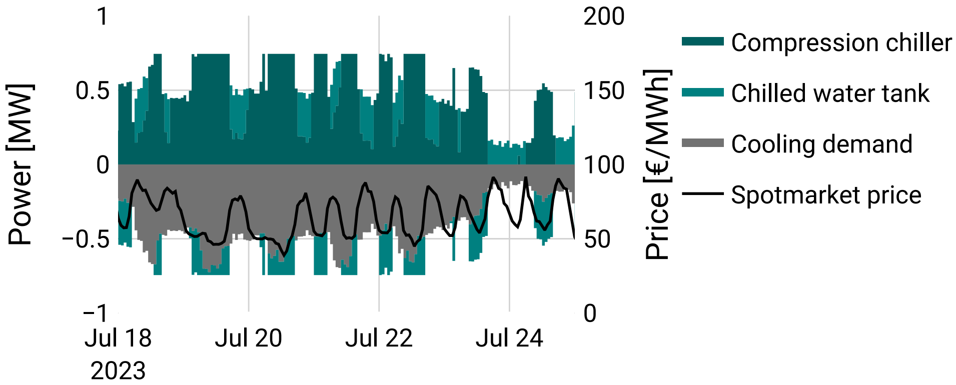

(a) Cooling dispatch during a summer week

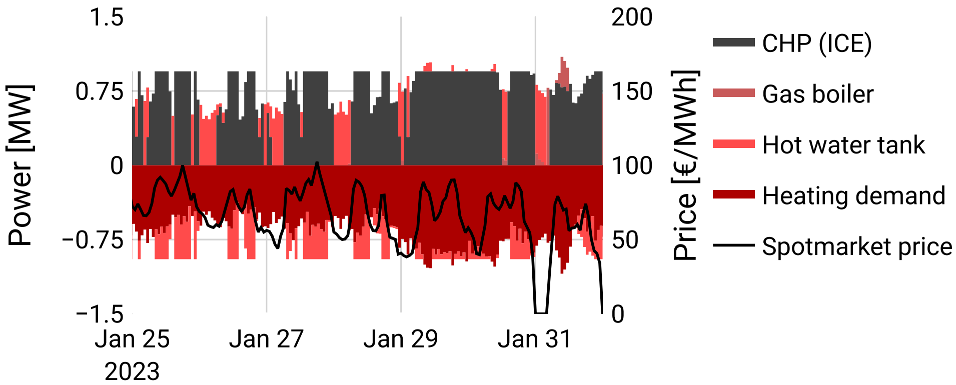

(b) Heating dispatch during a winter week

Figure 5.8.: Hourly generation (positive) and on-site use (negative) of heating and cooling in cost optimal scenario of automotive site

feasible due to low procurement prices. The value of flexibility from flexible operation of conversion and storage technologies is thus fully considered in the proposed modeling approach. Thereby, the methodology helps to integrate volatile generation in planning process of sustainable industrial energy supply systems.

Summary

The results highlight the suitability of the proposed modeling framework to design complex industrial energy supply systems. The model derives key performance indicators considering multi-modal coupling of energy supply systems and complex procurement tariffs for electricity. Thereby, the proposed methodology meets the requirements derived in Section 2.2. The presented optimization results have been computed based on an entire year with 8760 h. The computation of each scenario takes up to 71 minutes. The scenarios give a first understanding of the key performance indicators. During a course of an energy consultancy project, additional modeling details might be added to the problem formulation such as start-up costs, multi-year roadmaps or security of supply constraints. Solving times significantly increase with these modeling details. Higher solving times make it impossible to conduct extensive sensitivity analysis and identify

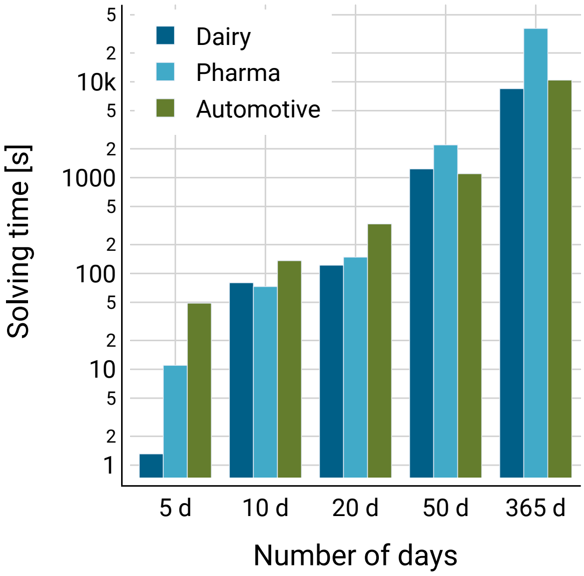

Figure 5.9.: Computation times for models with different aggregation levels. Representative days have been selected with OPS.

tipping points. Therefore, the following section discuss an efficient and robust approach to reduce computational complexity while maintaining the relevant characteristics of an full scale approach.

5.3. Time series aggregation

Time series aggregation reduces the number of time steps and thus the complexity of optimization models. Consequently, optimization models are more efficiently solved making them applicable in daily application of energy system planners and consultants. Figure 5.9 shows the computation time to build and solve the optimization model. The computational complexity strongly correlates with the number of representative periods in all examined use cases. Selection of representative periods reduces computation times by two orders of magnitudes. Full-scale models of an entire year take several hours to derive an optimized design concept. These model formulations are hardly applicable for extensive scenario analysis and dynamic integration of customer requirements in real-world projects. In contrast, planning models with less than 20 days are efficiently computed in less than 10 minutes.

Aggregation approaches need to capture the relevant statistical attributes of the full scale problem: Each time step in a representative period represents multiple time steps of the full scale problem. The representative periods need to be carefully selected in order to preserve the annual energy statistics and peak demands. Thereby, aggregation approaches lead to robust design concepts with significantly reduced computational effort. The two aggregation approaches introduced in Section 4.2 are benchmarked to the full scale problem with 8,760 h. The following section analyzes the required number of days to represent the on-site energy demands and to result in robust energy supply concepts.

Evaluation metrics

The two aggregation approaches SPS and OPS are evaluated regarding their suitability for design optimization of highly complex energy supply systems in industrial sites. Approaches are compared regarding two accuracy metrics: The first metric ΔE_n^{L} evaluates the accuracy of the approach to maintain the annual statistics of energy demands. It is derived for electricity, steam, heating, and cooling depending on the industrial site. Weight factors w_d for each representative period d are used to derive ΔE_n^{L}:

$$\Delta E_n^{\mathrm{L}} = \frac{\sum\limits_{d \in D^{\mathrm{Repr}}, t \in T_d} (w_d P_{n,t}^{\mathrm{L}} \Delta t) - \sum\limits_{t \in T} (P_{n,t}^{\mathrm{L}} \Delta t)}{\sum\limits_{t \in T} (P_{n,t}^{\mathrm{L}} \Delta t)} \cdot 100~\% \tag{5.2}$$

The second metric ΔTC analyzes the impact of time series aggregation on the optimization results: The total project costs (TC) indicate the economic feasibility of a design variant and are thus used to compare the optimization results of a full-scale problem (FSP) to those results obtained from SPS and OPS strategies.

$$\Delta TC^{\mathrm{i}} = \frac{TC^{\mathrm{i}} - TC^{\mathrm{FSP}}}{TC^{\mathrm{FSP}}} \cdot 100~\% \quad i = \{\mathrm{OPS}, \mathrm{SPS}\} \tag{5.3}$$

The robustness of the two aggregation approaches is analyzed in the following: The two strategies are applied to the three use cases with various patterns and demand relations. Moreover, the number of representative periods n^{Repr} is varied to determine the required temporal granularity to design highly complex industrial energy supply systems.

Aggregation results for 12 representative days

An adequate aggregation approach captures the relevant statistical attributes of the relevant time series. For instance, the energy demands are represented by hourly load profiles defining the required peak capacities and annual utilization of energy supply equipment. These static attributes are represented by the duration curves. The duration curves derived from the aggregated time series are thus compared to the duration curve of the FSP with 8760 steps. Figure 5.10 shows the curves for a selection of 12 representative days from SPS and OPS. The duration curve derived from the heuristic SPS approach shows significant deviations to the original load profiles. The annual heating demand is underestimated by 15 %, whereas the annual electricity and cooling demands are overestimated by 15 % and 8 % respectively. Moreover, peak demands are not included in the SPS approach. In contrast, the OPS strategy derives a set of representative periods which captures the relevant statistical attributes. The deviation in electricity, heating and cooling demand is below 3 %. Given the multi-year climate variability and uncertainty of long-term production forecasts, this small deviation appears clearly acceptable. Peak periods are enforced to be included in the approach ensuring feasibility of the design concept during the entire base year.

The OPS approach considers weight factors w_d for each selected representative period. Table 5.4 shows the selected representative periods including values of w_d for a selection of twelve representative periods. Periods with peak demands are highlighted in bold. These periods are enforced to be included in the optimized period set as demand peaks define the required maximum capacity,

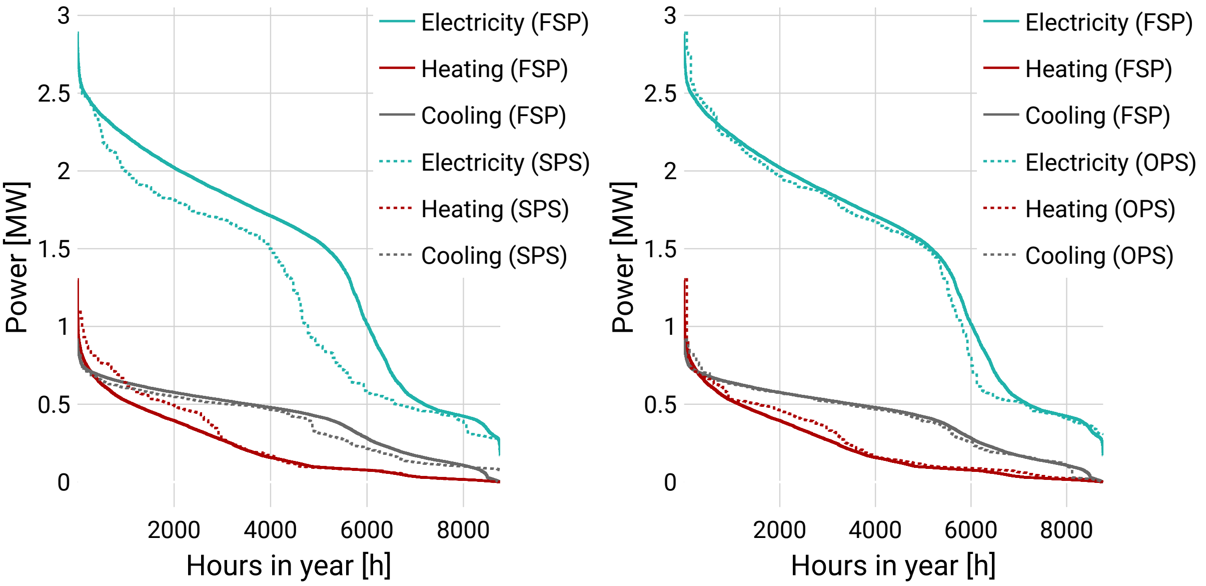

(a) Seasonal period selection (SPS)

(b) Optimized period selection (OPS)

Figure 5.10.: Duration curves of multi-modal energy demands based on annual load profile (FSP) and for twelve representative days based on seasonal and optimized period selection for the automotive site

which an energy supply system needs to provide. The pharmaceutical site comprises load profiles for electricity, steam, heating, and cooling. Therefore, four days are enforced to be included for the pharmaceutical site, whereas the models for automotive and dairy site include three periods with peak demands. The derived weight factors w_d vary between 1 and 51. This highlights that certain combinations of demands and renewable penetration occur more often than others. Representative periods with peak demands tend to have lower weight factors w_d. The operational costs during this period are thus less weighted in the objective function.

The number n^{Repr} of representative periods is a central parameter for practical application of aggregation strategies. A higher number of n^{Repr} can lead to higher modeling accuracies but results in higher computational complexity. Therefore, the trade-off between modeling accuracy and complexity is discussed in the following. The annual energy demands obtained from the aggregated time series with SPS and OPS are compared to the annual demands for 4 to 25 representative periods. The relative deviation ΔE^{L} of energy demands for electricity, steam, heating, and cooling is computed for the three industrial sites. The values obtained by OPS for pharmaceutical site are not shown for a selection of 4 representative days. In this case, the selection of days is not determined by the algorithm, but fully pre-defined by the periods with peak demands. Consequently, energy demands are strongly overestimated.

Representation of on-site energy demands in aggregated time series

The obtained deviations are summarized in Figure 5.11. The SPS approach leads to significant deviations in energy demands of up to 40 %. Energy demands are underestimated in some cases and overestimated in other cases. Moreover, the aggregation errors do not constantly reduce with increasing n^{Repr}: For more than 10 representative days, the average absolute deviation is 6.9 %

Table 5.4.: Selection of 12 representative days with OPS and derived weight factors w_d for three industrial sites. Periods with peak demands are highlighted in bold.

Automotive		Dairy		Pharma	
Date	w_d	Date	w_d	Date	w_d
17/01/2023	32	19/02/2023	34	**20/01/2023**	**6**
04/02/2023	28	08/03/2023	38	04/02/2023	48
10/04/2023	34	**26/03/2023**	**1**	06/03/2023	42
13/04/2023	35	20/04/2023	42	10/04/2023	30
10/05/2023	**45**	13/06/2023	69	04/05/2023	46
18/06/2023	**42**	**26/07/2023**	**7**	**08/06/2023**	**19**
23/06/2023	51	20/08/2023	55	17/06/2023	49
08/08/2023	24	**23/08/2023**	**4**	24/07/2023	50
29/09/2023	16	01/11/2023	42	02/08/2023	14
21/11/2023	22	21/11/2023	60	**25/08/2023**	**13**
25/11/2023	30	11/12/2023	6	25/11/2023	43
30/12/2023	**6**	30/12/2023	7	**05/12/2023**	**5**

for the automotive site, 3.1 % for the pharmaceutical site and 2.0 % for the dairy site. The OPS leads to significantly lower deviations of 2.2 %, 1.7 % and 0.8 % for the same range of n^{Repr}. A selection of more than 10 representative days with OPS results in deviations below 6 % for all use cases and energy demands. The OPS considers the hourly demand profiles in its selection of representative periods resulting in good approximations of regular operation and sporadic events such as plant shutdowns or extreme weather events. Energy demands are partly well captured by the SPS. However, certain values of n^{Repr} lead to inconvenient selections of representative periods. Such inconvenient selections estimate frequency of plant shutdowns or cold periods strongly wrong leading to significant deviations of more than 20 % in all energy demands. The analysis clearly highlights the robustness of the OPS aggregation approach compared to a heuristic approach with SPS: The newly developed aggregation strategy captures the annual statistics and peak values of load profiles.

The deviations obtained for the heating demands of the automotive and pharmaceutical sites show higher absolute deviations in the OPS than the other energy demands. In contrast to the other demands, the two load profiles show a strong seasonal dependence with demand peaks during the winter months and almost no demand in the summer. This behavior is difficult to obtain from a low number of representative periods. Deviations for energy demands of the dairy site are comparatively low. The production of the dairy is based on a three-shift operation for seven days a week. Consequently, the volatility of energy demands is lower than for the other two sites making it easier to be captured by an aggregation approach.

Accuracy of design concepts based on aggregated time series

Representative periods obtained on the SPS and OPS approaches are applied to the energy system design model. The weight factors w_d are included in the objective function of the optimization model to reflect the frequency of the operational conditions described by each period. The obtained values for the objective function are compared to the optimal solution of the FSP with 8760 h. The results are illustrated in Figure 5.12. The OPS strategy with more than 10 representative days

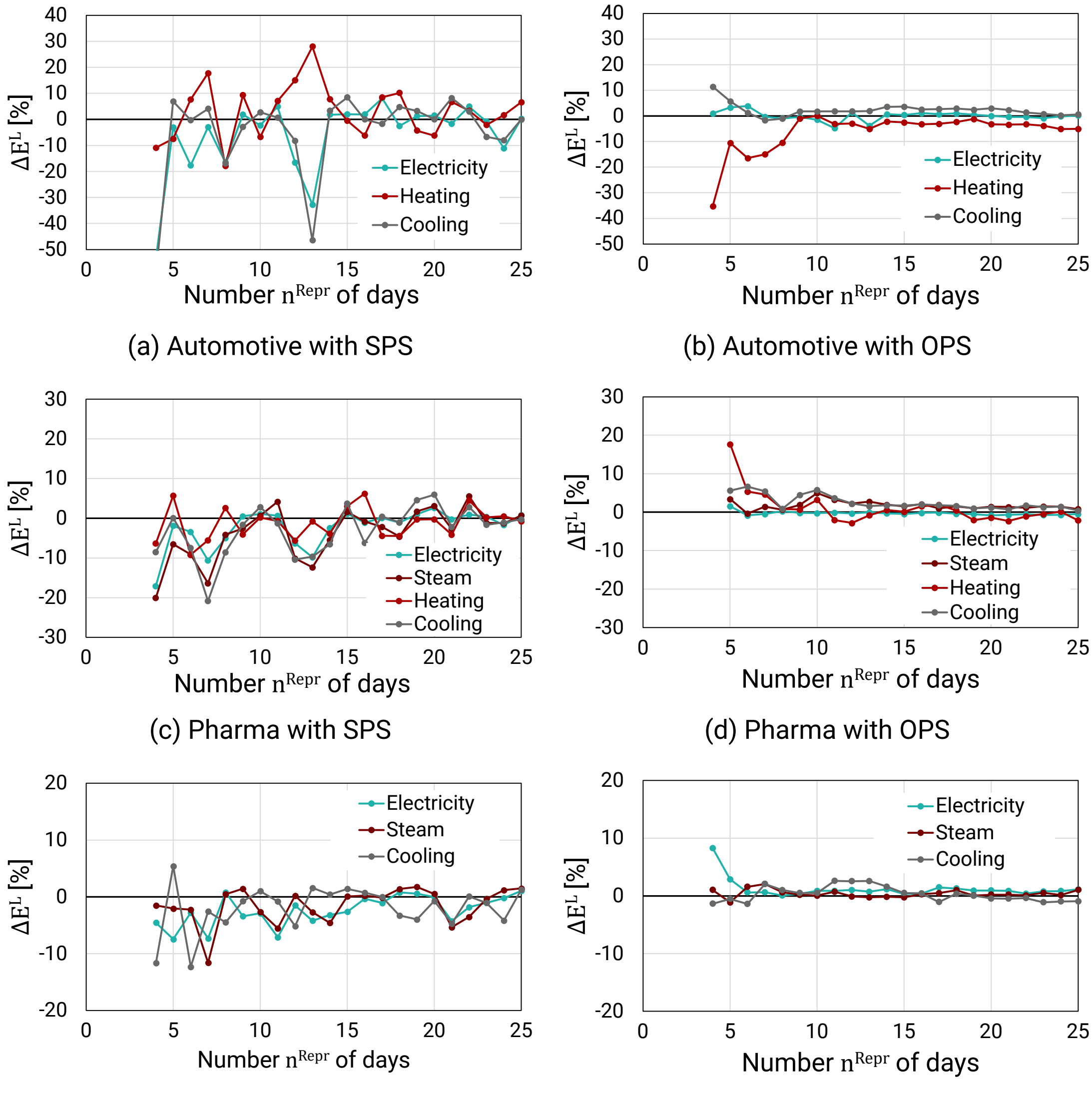

(a) Automotive with SPS

(b) Automotive with OPS

(c) Pharma with SPS

(d) Pharma with OPS

(e) Dairy with SPS

(f) Dairy with OPS

Figure 5.11.: Relative deviation ΔE^{L} of energy demands by time series aggregation with SPS (left) and OPS (right) depending on the number n^{Repr} of representative periods and three use cases

leads to highly accurate estimations of the objective with errors below 3 % for all three sites. In contrast, the optimization results obtained from SPS show significant deviations of up to 28 %. The average absolut deviation is also reduced by the optimized strategy for time series aggregation: from 5.4 % to 1.9 % for the automotive site, from 2.6 % to 0.8 % for the pharmaceutical site and from 1.9 % to 0.4 % for the dairy site. Like the demand analysis, deviations in total costs for the dairy use case are smaller than the other two cases.

Summary

An optimized strategy for the selection of representative periods has been developed in this Thesis.

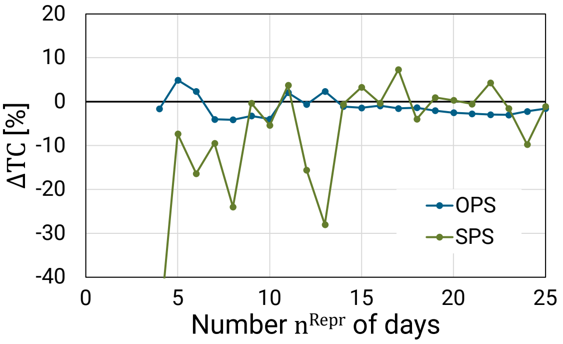

(a) Automotive

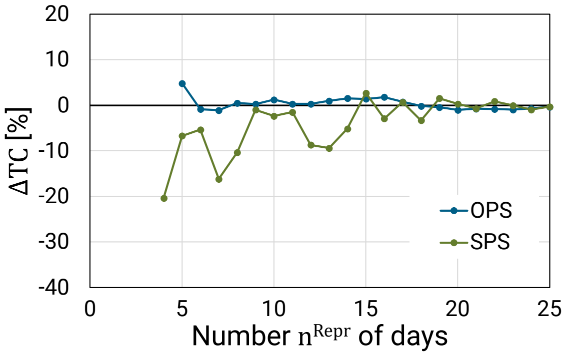

(b) Pharma

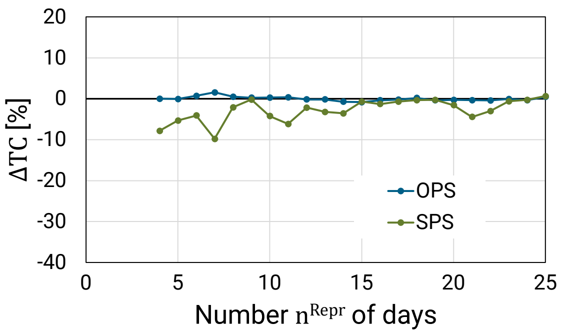

(c) Dairy

Figure 5.12.: Relative error of total costs (TC) depending on the number n^{Repr} of representative periods and the aggregation strategy for the three industrial sites

The suitability for complex energy supply systems is demonstrated for use cases of three industrial sites: The aggregation approach captures the annual statistics and peaks of energy demands and provides adequate estimations of the financial expenses. Simultaneously, the aggregation strategy leads to a reduction of solving times from more than 71 minutes for an entire year to below 30 s for 12 optimized days. Thereby, the developed model becomes applicable for computation of multiple design variants and extensive sensitivity analysis. The reduced computational complexity is now used to determine sustainable transformation roadmaps considering long-term trends in energy procurement and on-site demands.

5.4. Transformation roadmaps

Long-living character of energy supply equipment enforces an assessment of multi-decade project horizons to evaluate lifecycle costs of energy supply. Transformation roadmaps are a modeling technique to analyze the long-term evolution of an energy supply concept during these long planning horizons. Thereby, stakeholders gain clarity of cost and carbon saving potentials and the associated risks of their investments. Roadmaps enable the consideration of projected technology and price developments as well as the system's ability to adapt to these changes. The following case study applies a 15-year planning horizon to the three use cases. Energy supply concepts are optimized in each of the five extension stages considering investment decision from previous extension stages. Based on the results from the case studies, the value of foresight and adaptivity is analyzed. Moreover, the computational complexity is evaluated for the design of highly complex energy supply systems in industrial sites.

5.4.1. Roadmaps with perfect foresight

Transformation roadmaps can be derived from a single optimization run assuming perfect foresight on future developments and adaptive investment decisions at each extension stage. This approach is referred to as roadmap approach with perfect foresight (PERF) and has been introduced in Section 4.3. The following paragraph shows transformation roadmaps for the three use cases of industrial sites located in Southern Germany. Numerical values for KPIs, rated equipment capacities and tariff selection are summarized in Table 5.5. The following sections analyze the evolution of electricity supply concept with focus on the role of cogeneration plants. The optimized roadmaps for the three use cases are evaluated regarding their economic and ecological performance.

Evolution of electricity supply

Figure 5.13 shows the generation and use of electricity along the planning horizon. Continuous implementations of efficiency measures lead to a slight decrease in production related demands of 6 % for the dairy, 3 % for the pharmaceutical and 23 % for the automotive site till 2035. These effects are fully offset by electrification of process heating demands for the dairy and pharmaceutical use cases: The projected on-site use of electricity rises by 81 % to 43 GWh/a for the dairy and 26 % to 26 GWh/a for the pharmaceutical site. The automotive site does not comprise significant shares of thermal demands. The total electricity use thus slightly decreases.

Increasing energy carrier costs and a further decline in installation costs leads to a continuous expansion of PV from 2023 for the automotive and from 2026 for the two other use cases: Capacity expansions are conducted in each expansion stage. At the end of the planning horizon, share of PV in electricity mix accounts for 55 % for the automotive use case to 81 % for the dairy use case in 2035. The generated electricity is mostly directly consumed on-site: Self-consumption rates are above 65 % for the automotive site, above 75 % for the pharmaceutical site and above 85 % for the dairy site towards the end of the planning horizon. Remaining excess electricity is fed back to the power grid. High rates of self-consumption are effectively realized by power-to-heat technologies. Electric boilers with capacities of up to 6.8 MW serve on-site thermal demands for space heating and production during times of high PV generation. Thereby, they decarbonize thermal demands with low carbon electricity. Electric boilers account for 26 % and 21 % of steam generation for the

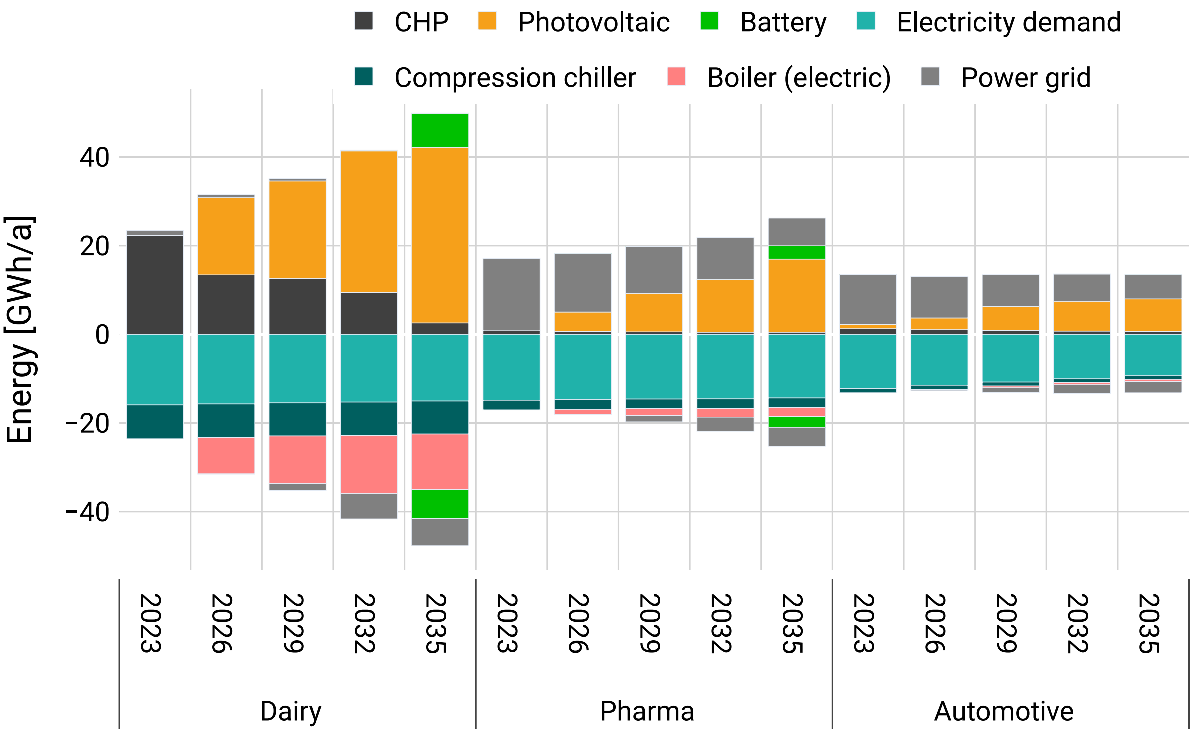

Figure 5.13.: Evolution of annual electricity generation (positive) and on-site use (negative) for three industrial sites based on the PERF strategy

dairy and pharmaceutical use case respectively. Additional tanks for hot and chilled water enable a flexible operation of boilers and chillers. The effective use of multi-modal coupling technologies makes battery storage technologies not economically viable for the examined use cases: Despite a significant decline in projected installation costs, the model recommends the installation of batteries only towards the end of the planning horizon for the pharmaceutical and dairy site with 2.2 MWh and 5.1 MWh capacity respectively. The proposed model considers value streams from both arbitrage and peak shaving. However, batteries can contribute also to short-term balancing services, which have not been included in this analysis. The influence will be discussed separately in Section 5.5.

Table 5.5.: Key performance indicators, equipment rated capacities and tariff selection derived by the roadmap approach with perfect foresight (PERF)

		Dairy					Pharma					Automotive				
	Unit	2023	2026	2029	2032	2035	2023	2026	2029	2032	2035	2023	2026	2029	2032	2035
TOTEX	M€/a	8.40	11.4	12.0	12.8	13.2	4.21	4.83	5.09	5.51	5.79	2.65	2.78	2.76	2.80	2.82
Investment	M€	2.00	18.8	4.60	10.1	11.7	0.33	5.67	4.27	3.04	5.71	1.53	2.04	2.62	0.95	0.41
OPEX	M€/a	8.21	9.41	9.58	9.36	8.50	4.18	4.26	4.12	4.25	3.92	2.51	2.44	2.17	2.12	2.10
CO_2	kt/a	18.4	13.6	9.77	6.74	1.40	7.80	5.66	2.52	1.42	0.63	4.39	3.05	1.73	1.03	0.71
CHP (ICE)	MW	0.0	0.0	0.0	0.0	0.0	0.26	0.26	0.26	0.26	0.26	0.37	0.37	0.37	0.37	0.37
CHP (GT)	MW	2.65	2.65	2.65	2.65	2.65	0.0	0.0	0.0	0.0	0.0	0.0	0.0	0.0	0.0	0.0
GB	MW	12.0	4.82	4.82	4.82	4.82	2.50	1.34	1.34	1.34	1.34	1.50	0.17	0.17	0.17	0.17
BB	MW	0.0	0.0	1.58	2.17	5.07	0.0	0.0	0.85	0.93	1.04	0.0	0.0	0.0	0.0	0.0
EB	MW	0.0	6.81	6.81	6.81	6.81	0.0	1.55	1.55	1.55	1.55	0.0	0.0	0.63	0.63	0.63
CC	MW	7.20	4.26	4.26	8.36	8.36	2.50	1.62	1.62	2.13	2.13	0.95	0.70	0.70	0.70	0.70
PV	MWp	0.0	13.1	16.6	24.1	29.8	0.0	3.59	7.18	9.83	13.6	0.77	2.10	4.34	5.36	5.81
BAT	MW	0.0	0.0	0.0	0.0	5.08	0.0	0.0	0.0	0.0	2.20	0.0	0.0	0.0	0.0	0.0
BAT	MWh	0.0	0.0	0.0	0.0	5.08	0.0	0.0	0.0	0.0	2.20	0.0	0.0	0.0	0.0	0.0
HWS	MWh	0.0	0.0	0.0	0.0	0.0	0.29	0.29	0.29	0.29	0.29	0.50	0.50	0.50	0.50	0.50
CWS	MWh	0.0	0.88	0.88	5.40	5.97	0.0	0.45	0.60	1.36	1.48	0.0	0.28	0.28	0.31	0.33
Power A [a]	GWh/a	1.18	0.64	0.53	0.18	0.07	0.0	0.0	0.0	0.0	0.0	0.0	0.0	0.0	0.0	0.0
Power B [b]	GWh/a	0.0	0.0	0.0	0.0	0.0	16.35	13.16	10.57	9.45	6.26	11.3	9.36	7.10	6.12	5.46
Natural gas	GWh/a	85.7	64.1	47.5	35.9	9.9	12.0	10.6	3.19	2.50	1.91	3.56	3.16	2.42	2.08	1.86
Wood pellets	GWh/a	0.0	0.0	11.1	14.8	30.4	0.0	0.0	6.19	6.30	6.67	0.0	0.0	0.0	0.0	0.0

[a] Electricity procurement from power grid with < 2,500 h/a
[b] Electricity procurement from power grid with > 2,500 h/a

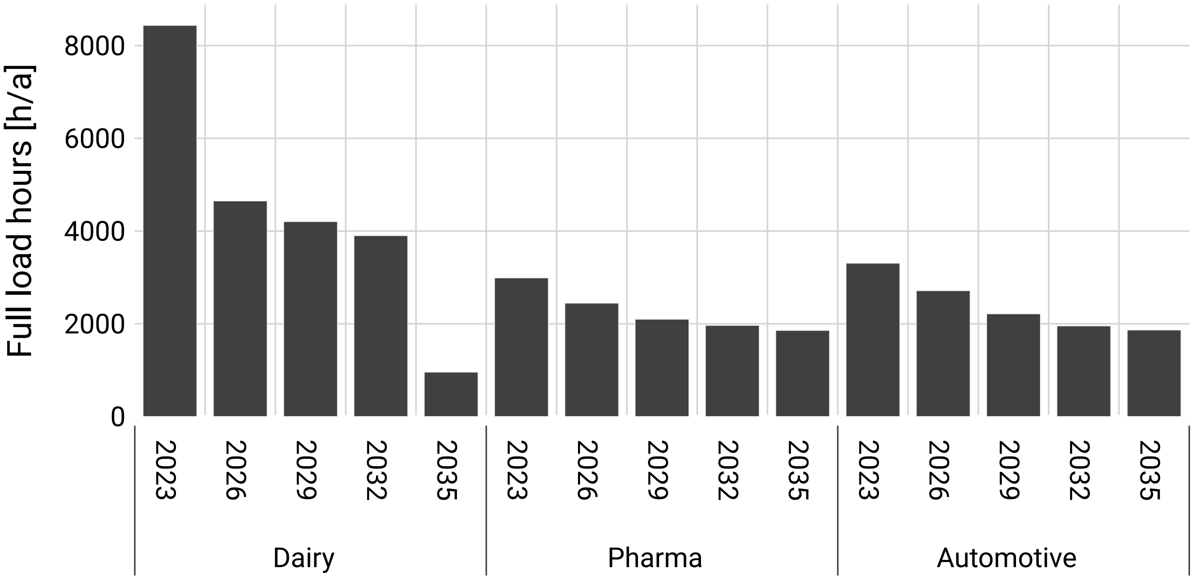

Figure 5.14.: Equivalent full load hours for CHP systems along the planning horizon derived by PERF strategy

Increasing shares of photovoltaic are integrated in industrial energy supply systems in all three examined use cases. However, additional sources for electricity generation are required to meet demands during days with low PV generation. For the pharmaceutical and automotive use case, the remaining electricity is mostly procured from the power grid. On-site generation from CHP accounts for 5 % (pharmaceutical) and 9 % (automotive) of total electricity use. The high utilization (> 2,500 h/a) of the power grid leads to a procurement tariff with high demand charges as outlined in Section 5.1. The cogeneration plant contributes to the active management of peak loads and thereby a reduction of these demand charges. In contrast, electricity generated by cogeneration plants makes 95 % of the on-site use in the dairy case. The power grid helps to meet peak demands. The selected procurement tariff for electricity (< 2,500 h/a) comprises reduced demand charges as outlined in Section 5.1. Therefore, the value of peak load management is limited in this use case. The example shows how the interaction of complex procurement tariffs and on-site equipment needs to be considered for design of industrial energy supply systems. Cogeneration plants are a central element in energy supply systems of many industrial sites as outlined in Section 2.1. Therefore, the role of CHP plants in the optimized technology roadmaps is analyzed in the following.

Role of cogeneration plants

Cogeneration plants are identified as part of an optimized design concept in all three examined cases. The model for the dairy site proposes a 2.6 MW gas turbine (GT). High temperature waste heat of the GT is effectively used for steam supply throughout the year. The CHP provides 95 % of electricity consumed in the simulative evaluations of the dairy use case. Practical shares might be slightly lower as maintenance periods for the GT have not been considered in the simulation. A secure supply with electricity and steam during maintenance periods is granted by the existing power grid connection and the gas-fired boilers. The impact of maintenance periods on system design is further discussed in Section 5.5. Use cases of pharmaceutical and automotive site comprise significant lower thermal demands: In these use cases, the installation of a CHP plant with internal combustion engines and capacities of 370 kW and 260 kW are identified as possible extension options. Low temperature waste heat serves as a source for space heating during winter. During these times, CHP plants can effectively generate electricity. The installation of the CHP plants is projected to remain along the entire planning horizon. The newly installed CHP plants will face changing boundary conditions during their technical lifetimes. Figure 5.14 shows the equivalent annual full load operating hours for the CHP units for the three examined use cases. The largest decline in utilization is observed in the use case for a dairy site: The projected full load hours decrease from 8,410 h/a in 2023 to 970 h/a in 2035. Among others, the decline is influenced by the limited part-load capabilities of the installed gas turbine: the gas turbine is assumed to be installed as a single module and cannot be operated below 50 % part-load. This operational constraint has been considered in the optimization. The part-load constraint prevents the operation at low load levels which occur more frequently with integration of photovoltaic and power-to-heat technologies. Similar declines of 40 % and 47 % are seen in the use cases of pharmaceutical and automotive sites.

The observations highlight the suitability of the methodology to analyze changing operating patterns along a multi-year planning horizon. The projected change in mode of cogeneration plants have been proposed in several studies, e.g., by Agora Energiewende[43], Fraunhofer ISE [154] or Prognos [44]. The developed methodology is able to determine the impact of these long-term developments for the on-site planning of industrial energy supply systems. Based on today's framework conditions, CHP plants might be designed for constant operating conditions with utilization of more than 8,000 h/a. These operating patterns are projected to change significantly with on-going decarbonization. Cogeneration plants are used less frequently which decreases their economic efficiency. Knowledge on the projected change in operating patterns can be used in later planning stages. Detailed specifications for technical capabilities of CHP plants should consider the projected changes. This example highlights how the proposed methodology enhances the planning process for the sustainable design of industrial energy supply systems.

Cost structure for energy supply

CHP plants are part of an optimized design concept which has been computed by minimizing the total project costs over the entire planning horizon. The employed model formulation accounts for procurement costs for electricity and fuels, costs for installation and maintenance of on-site equipment as well as capital costs for photovoltaic and battery installations. Progressive installations of PV plants and declining use of cogeneration change the cost structures for energy supply. Evolutions of capital and operational expenses are thus shown in Figure 5.15. Costs for energy supply are dominated by procurement costs for natural gas and electricity. These costs contribute for more than 92 % of total costs in the first extension stage. Costs for the dairy use case are mostly determined by natural gas purchase, whereas electricity procurement dominates expenses for pharmaceutical and automotive use cases. The shares of energy procurement constantly decrease in the subsequent extension stages with increasing shares of photovoltaic and batteries. All other supply equipment makes up less than 10 %. It is thus shown as aggregated values.

Capital costs are associated with the installations of PV starting from 2023 for the automotive site and from 2026 for the other use cases. The investments are depreciated over the entire technical lifetime of 20 years. Therefore, capital costs of previous installations are reflected in each following extension stage. The simulative evaluations in this work employ the linear estimation of investment

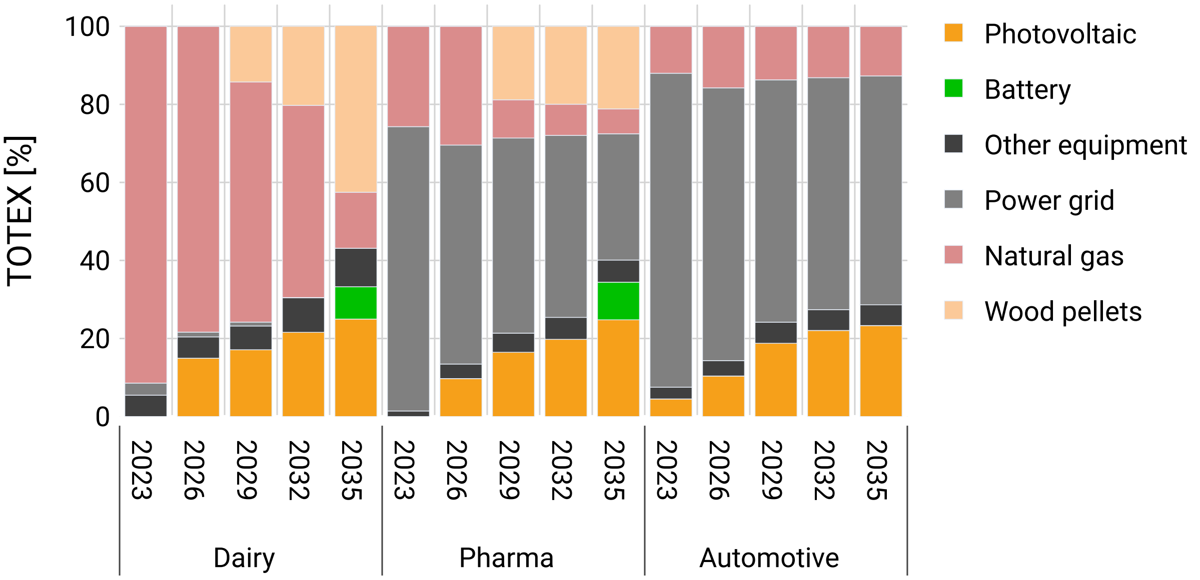

Figure 5.15.: Relative cost structure of energy supply for each extension stage in a multi-year planning horizon derived by PERF strategy

costs from the annual technology baseline (ATB) methodology of the national renewable energy laboratory (NREL) [155]. In contrast to non-linear investment cost estimations for CHP plants, PV installations are thus not associated with economies of scale: the specific investment costs are assumed to be independent of the installed capacity. The proposed model formulation thus tends to split PV investments in several smaller installations over the entire planning horizon rather than one large. The total capacity of PV is in the range of 6 MW to 30 MW. The continuous installations thus might reflect the installation of PV on different buildings of an industrial site. More detailed cost estimations might be considered in real-world applications with detailed knowledge of site conditions, planning efforts and risk margins for PV installations. These estimations probably comprise a fixed share for investments and thereby avoid recurrent planning efforts for PV projects. The simulative evaluations highlight the importance of adequate investment cost estimations to derive suitable equipment sizes in multi-year planning models.

Continuous integration of PV leads to significant capital costs and efforts for maintenance. PV generation exceeds on-site electricity demand during certain periods. Electric boilers use the renewable excess electricity and consequently reduce utilization of natural gas for steam generation. This increases the resilience of the energy supply system to increasing fuel and carbon prices.

Natural gas tariffs and carbon prices are projected to increase over the planning horizon. Assumptions are summarized in Table 5.1. These trends favor the on-site use of biomass: From 2029, biomass boilers of 1.6 MW and 0.9 MW generate steam in the dairy and pharmaceutical use cases. Biomass boilers account for 62 % (dairy) and 70 % (pharma) of total steam generation. The employment of biomass boilers results in significantly lower costs for natural gas purchase and increasing shares for procurement of wood pellets. The fuel switch is automatically determined by the proposed model formulation as a result of the projected price changes. These projections are known to comprise significant uncertainty, in particular on long time frames. The results of the optimization model should thus be considered as one possible future rather than a detailed working plan for the upcoming decade. Consequently, the replacement of biomass by natural gas needs to be interpreted as a reasonable option for the energy supply from today's point of knowledge. Based on the optimization results, energy system planners and consultants might evaluate space requirements to ensure that a biomass-based steam generation becomes feasible in a mid- to long-term future of an industrial site.

Analyzing the evolutions of cost structures helps to identify major drivers of costs and the associated risks resulting from capital intensive investment decisions. Increasing shares of renewable electricity from PV plants and renewable heat from biomass decreases dependence on natural gas and electricity procurement tariffs: Total costs for energy supply become less vulnerable to increases in tariffs. Beyond economic efficiency, environmental assessments are a central aspect for evaluation of energy supply concepts. Tightened regulatory framework and corporate decarbonization strategies encourage an evaluation of carbon footprints. Therefore, a detailed analysis is provided in the following.

Carbon footprint of optimized design concepts

Environmental assessments of energy supply have gained increasing attention as outlined in Section 1.1. The proposed optimization model considers carbon footprints from on-site use of natural gas (Scope 1) and indirect emissions from procurement of electricity (Scope 2). Excess electricity fed into the grid is remunerated by negative carbon emissions. Annual carbon footprints for each extension stage are visualized in Figure 5.16. Optimized design concepts have been determined by minimizing costs for energy supply along the entire project horizon. Optimization of design concepts does not only result in cost savings but also reduces carbon footprints of energy supply: projected carbon footprints decrease by 84 % for the automotive and 92 % for the dairy and pharmaceutical use cases along the planning horizon. The significant decreases are the result of multiple developments including model exogenous trends and optimization of energy supply infrastructure.

Declines of carbon emissions in the three use cases are partly caused by model exogenous trends. Two trends are considered in this work: the continuous implementation of efficiency measures and the reduction of carbon footprint in the power grid. They reduce the on-site energy demands for production and the specific emissions associated with electricity procurement. These carbon savings occur without additional investments in the on-site energy supply infrastructure. The model exogenous developments account for 69 % of carbon savings for the automotive, 44 % for the pharmaceutical and 30 % for the dairy use case. The analysis shows the impact of efficiency measures for decarbonization of energy supply in industrial sites. Low carbon pathways can only be achieved with adaptation of energy supply infrastructure in industrial sites.

All use cases show substantially higher carbon savings with optimized energy supply infrastructure derived by the newly developed PERF. Highest reductions are found for the dairy use case: Natural gas is mostly used for steam generation in this use case. In the base year, steam demand is mostly served from the CHP plant (76 %) and additional gas-fired boilers (24 %). This development changes along the planning horizon: 62 % of the steam is generated by biomass, 26 % by electric boilers in 2035. The change in energy supply infrastructure leads to significant decline in carbon emissions from 18.4 kt/a to 1.4 kt/a. Similar trends are observed for the pharmaceutical use case. The automotive use case is dominated by electricity procurement and comprises lower thermal demands. However, integration of PV reduces emissions from electricity procurement. The

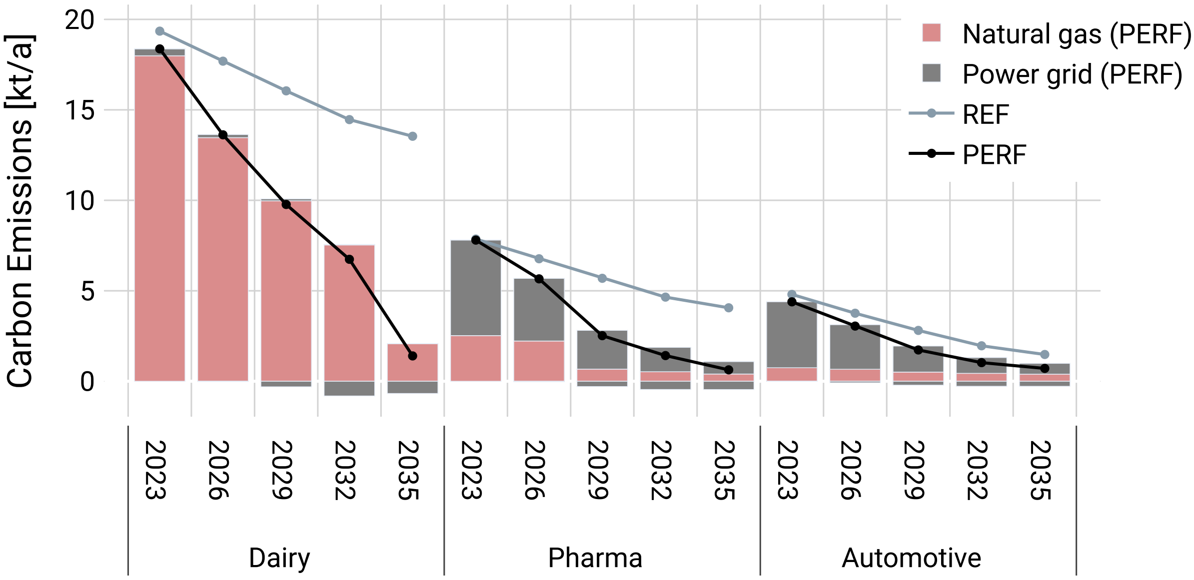

Figure 5.16.: Evolution of carbon footprint with existing energy supply system (REF) and with optimized energy supply concept (PERF). Bars indicate the composition of carbon emissions for the optimized energy supply concept (PERF)

integrated approach to design energy supply systems helps to identify sustainable and cost-efficient options to meet decarbonization targets.

Summary

Industrial energy supply systems comprise long-living equipment. Assessment of lifetime costs requires evaluation of multi-decade planning horizons. The proposed methodology accounts for the projected long-term trends, which are likely to influence the energy supply infrastructure: evolutions in energy markets (e.g., decline in carbon footprint of electricity procurement), trends in technology developments (e.g., cost degradation of photovoltaic and batteries) and changes in demands (e.g., due to implementation of efficiency measures) are fully considered in the proposed techno-economic planning model. Exemplary use cases from three industrial sectors have shown multiple benefits of integrating long-term trends in planning process:

- **Replacement of existing equipment:** The methodology automatically considers the remaining lifetime of existing energy supply infrastructure. Roadmap optimization enables to use the existing equipment till the end of lifetime and accounts for the necessity of replacement. Thereby, the model can be applied to challenging design studies of historically grown brownfield sites.

- **Integration of volatile renewable generation:** Decline in investment costs makes on-site integration of renewables economically more attractive. Integration decreases dependence of fossil fuels and thereby reduces associated risks. If the integration potential for renewables exceeds the on-site potential, e.g., due to space limitations, power purchase agreements (PPA) can be evaluated.

- **Flexibility from power-to-heat:** Excess electricity becomes available with continuous expansion of volatile renewable generation. Energy supply systems in industrial sites can effectively use this excess electricity by power-to-heat technologies such as electric boilers. Thereby, the use of fossil fired boilers is reduced leading to lower annual carbon emissions.

- **Changing role of cogeneration plants:** CHP plants have been traditionally designed for constant operation modes. Provided analysis underlines that the operation strategies might significantly change towards lower full load hours and increasing shares of part-load operation. Projected change of operational patterns can be considered in the specification of technical requirements for newly installed CHP plants.

- **Long-term options for fuel switch:** The model accounts for fuel switch options, e.g., wood pellets for steam generation. Investment decisions are strongly dependent on future procurement costs and thus cannot be answered based on today's knowledge. However, the optimization results provide valuable input for spatial planning within a factory: Energy system planners can ensure the feasibility of a possible future fuel switch by considering space requirements for on-site storages of wood pellets.

The above mentioned benefits of transformation roadmaps help decision makers to gain clarity on the impact of future evolutions on their energy supply infrastructure. Presented results have been determined with the PERF approach with perfect foresight over entire planning horizon and adaptive investment decision in each extension stage. This approach determines a transformation roadmap for the entire planning horizon. However, long-term projections are known to suffer from uncertainty. Even leading institutions in energy economics cannot reliably forecast trends for more than five years [109]. Consequently, transformation roadmaps need to be regularly updated considering the latest developments of energy demands and procurement costs. The PERF adds computational complexity to the model formulation. Therefore, the following section will discuss the impact of adaptivity and foresight on accuracy and complexity of techno-economic planning models.

5.4.2. Adaptivity and foresight

Transformation roadmaps have been determined based on the roadmap approach with perfect foresight (PERF) on future developments of demands and energy procurements. These projections are known to comprise uncertainty [109]. Their integration adds computational complexity to techno-economic optimization models. Therefore, the added value of adaptivity and foresight is analyzed for the complex design of industrial energy supply systems. Additional transformation roadmaps for the three use cases are determined with the forward-looking design approach (FLA) and roadmap approach with myopic foresight (MYOP) introduced in Section 4.3. These strategies are compared to the reference (REF) roadmap based on the existing energy supply system and required one-to-one replacements. Optimization results are analyzed regarding three metrics: First, the total cost over the planning horizon is used to evaluate the global economic performance of the obtained design concepts. Second, technology selection and sizing in the first extension stage are analyzed regarding possible lock-in effects. Finally, all strategies are compared regarding the computational complexity.

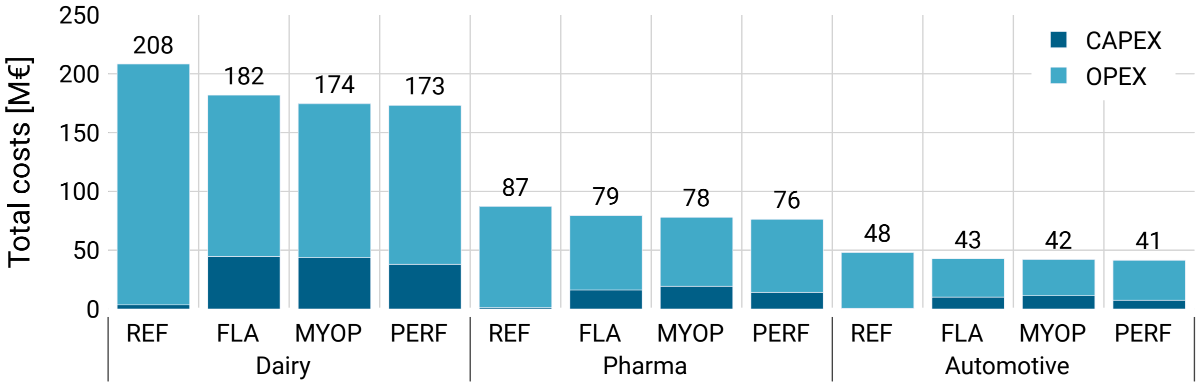

Figure 5.17.: Total costs along 15 year planning horizon derived by FLA, MYOP and PERF strategies

Global economic performance

Figure 5.17 summarizes the total project costs along the 15 years planning horizon. The dairy use case comprises highest costs due to high thermal demands for production processes. The reference (REF) case results in total expenses of 209 M€. Existing boilers and chillers are replacement at the end of their lifetime. The required capital costs of 3.52 M€ for replacements are comparatively small to the operational expenses of 206 M€. Additional investments are not allowed in the reference system. In contrast, the design of energy supply system is optimized by the FLA with perfect knowledge of future energy demands and procurement costs. OPEX are reduced to 137 M€. The required investments are associated with 45 M€ of capital costs. Thereby, the FLA promise a sustainable saving potential of 12.5 % compared to the reference roadmap. The PERF optimizes design decisions at each extension stage and thus account for the value of adaptivity. Thereby, the approach results in the cost-optimal roadmap with 173 M€ (-16.8 %). The MYOP optimizes each extension stage sequentially. The investment strategy assumes only limited foresight on future developments: MYOP considers only those information available in the respective extension stage to derive investment decisions. However, the total project costs are almost identical with 174 M€.

Similar trends can be observed for the pharmaceutical and automotive use cases: The reference (REF) system results in a solution with low capital expenditures. Capital intensive investments in energy supply infrastructure significantly reduces total costs for energy supply by 9 % to 13 % for the pharmaceutical case and 10 % to 15 % for the automotive case. Highest saving potentials are identified for the PERF whereas the FLA accounts for lowest saving potentials. Results highlight the value of adaptive investment decisions: Energy supply systems are likely to change with projected long-term trends. Simulative evaluations find a fixed design concept over the entire planning horizon to be not beneficial. Consequently, FLA result in slightly higher costs for energy supply. An adaptive investment strategy based on MYOP or PERF leads to highest saving potentials.

Relative differences in total project costs are in the same order of magnitude for the three roadmap strategies. Simulative evaluations have shown that even these small deviations result in additional savings of several million euros along the planning horizon. Therefore, technology selection and sizing of the computed design concepts are analyzed in the following.

Equipment selection and sizing

The identified saving potentials are the result of adapted energy supply concepts. These concepts comprise an updated set of technologies. The selection and sizing in the first extension stage is particularly relevant for energy system planners to determine the immediately required measures. The resulting measures remain in the following extension stages ("lock-in" effect). Figure 5.18 shows the selection and sizing of newly installed equipment for the first extension stage (2023) in the three use cases. The reference (REF) system is limited to existing boilers and chillers and thus not discussed here. Technology selection and sizing shows clear differences between the FLA, MYOP and PERF. These differences are discussed in the following.

All optimized design concepts comprise CHP plants. Sizes for gas turbines range from 2.23 MW to 2.68 MW for the dairy use case. CHPs with ICEs are selected for the pharmaceutical and automotive use cases. MYOP identifies a trigeneration system with an absorption chiller (AC) as an optimal supply concept. Consequently, the size of 1.16 MW for the CHP is significant larger than in the FLA (0.31 MW) and PERF (0.26 MW). For the pharmaceutical site with FLA, heating supply is supported by an additional heat pump. As a result, the derived CHP size of 0.21 MW is lower than those obtained with MYOP (0.41 MW) and PERF (0.37 MW). Moreover, the optimized designs with the FLA comprise additional biomass and electric boilers for the dairy and pharmaceutical site. Selection and sizing of renewable and storage technologies is also influenced by the selection of roadmap strategies: Models based on FLA show largest photovoltaic plants with up to 16 MW capacity. Renewable excess electricity is integrated by chilled water tanks of up to 26 MWh. Renewable and storage technologies are part of optimized solutions with the MYOP, but sized significantly smaller. A chilled water tank is not part of the optimized concept. Transformation roadmaps obtained with PERF comprise smaller PV installations. A PV plant is only selected in the automotive use case. In this use case, renewable electricity is directly used for own site demands. Therefore, chilled water storages are not selected in the first extension stage for the PERF.

Selection of roadmap strategies strongly influences the technology selection and sizing. Concepts derived by FLA strategy target at a single optimized design along the entire planning horizon. Investment decisions cannot be delayed in this modeling concept. Therefore, design concepts in the first extension stage comprise more technologies (e.g., biomass boilers and heat pumps) and larger equipment sizes (e.g., photovoltaic or chilled water tank) than the other roadmap strategies. Investment decisions are prioritized without urgent need for actions as FLA does not account for the value of adaptivity in a transformation roadmap. This drawback is overcome by the MYOP. The approach sequentially derives design decisions based on the respective prices of the extension stage. Results show many similarities with the PERF, e.g., the selection and sizing of the CHP plant in the dairy and automotive use cases. However, results substantially differ for the pharmaceutical use case. Extrapolation of low fuel prices in the first extension stage result in an investment decision for a trigeneration system with CHP plant and AC. Total investment efforts are estimated with 1.5 M€. The installation remains in the following extension stages ("lock in" effect). Changing commodity prices counteract further utilization of the trigeneration system ("stranded investment") in the second extension stage: full load hours of the CHP strongly decrease by 87 % (5,170 h/a to 738 h/a). Consequently, utilization of the AC declines by 90 % (5380 h/a to 551 h/a). Similar dramatic declines are avoided by the PERF with foresight on the energy carrier price development. The CHP plant is sized significantly smaller. Waste heat is not integrated to supply cooling demands. Instead, existing compression chillers meet process demands in the PERF. Beyond the selection of conversion technologies, the PERF derives a different selection and sizing of renewable and storage technologies. PERF accounts for the option to delay investment decisions ("wait and see"). For instance, investment costs for PV are projected to decline which favors a subsequent investment in later extension stages. Thereby, PV capacities are installed with lower

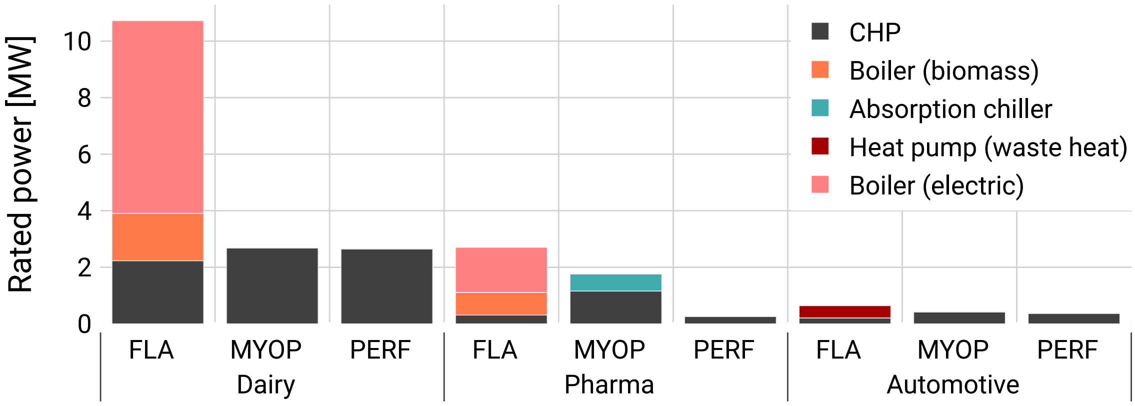

(a) Conversion technologies

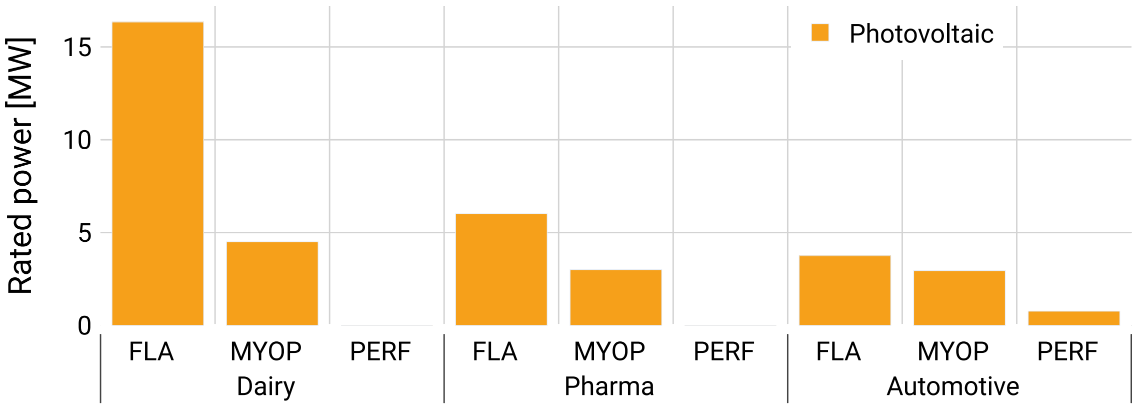

(b) Renewable technologies

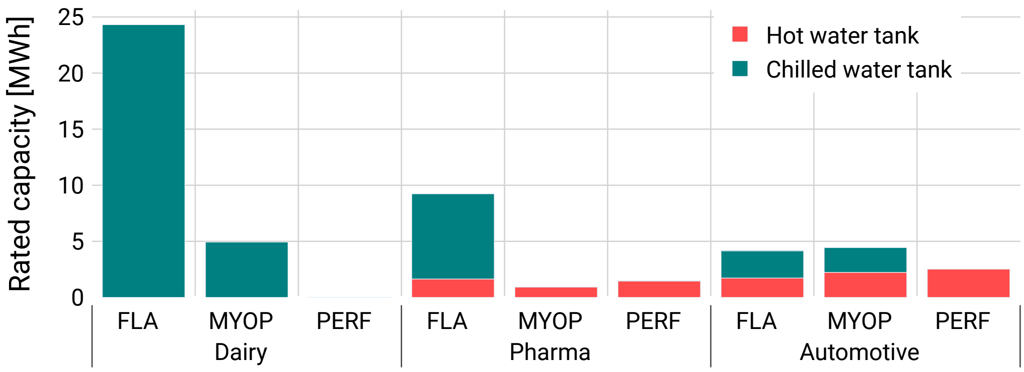

(c) Storage technologies

Figure 5.18.: Newly installed equipment capacities in first extension stage (2023) derived by FLA, MYOP and PERF strategies

specific investment costs. Both example of the CHP and PV highlight the value of foresight for the complex design of industrial energy supply systems. The knowledge of future trends leads to lower costs for energy supply as outlined in the previous section. However, formulation of the PERF enforces complex modeling strategies. The computational complexity added by these strategies is

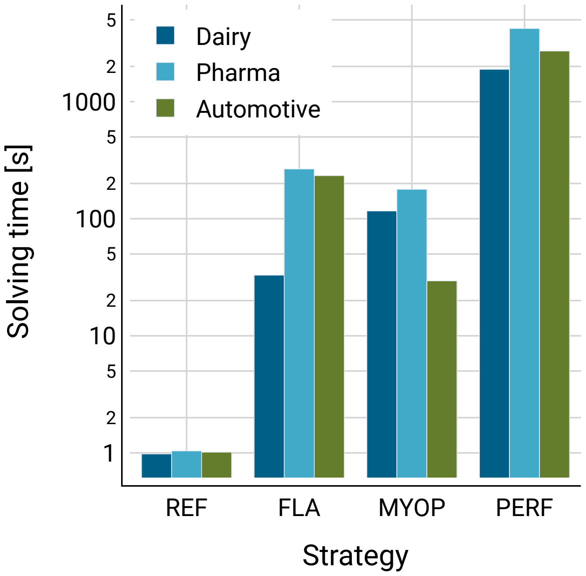

Figure 5.19.: Computation times to determine transformation roadmaps derived by FLA, MYOP and PERF strategies

evaluated in the next section.

Computational complexity

Transformation roadmaps are derived by three modeling strategies. These strategies add different computational complexity to the proposed model formulation. Figure 5.19 summarizes computation times for all strategies and use cases discussed in the previous paragraphs. Computation times comprise both time to build and solve the mathematical optimization model with Gurobi. Highest computation times are observed for the use case of the pharmaceutical site. In contrast to the automotive and dairy site, four types of energy demands are considered here leading to more complex interconnections in the on-site energy supply system. The reference approach takes approximately one second to determine the dispatch for the existing energy supply equipment with on-site compression chillers and gas-fired boilers. In contrast, the FLA accounts for extension options from a variety of conversion, storage and renewable technologies. Consequently, computation times of 33 s (dairy) to 266 s (pharma) are significantly higher. Similar order of magnitude can be observed for the MYOP which accounts for adaptive investment decisions with myopic foresight. Computation times range from 30 s (automotive) to 178 s (pharma). The sequential solving process indicates a linear time increase with increasing number of extension stages. In contrast, the PERF comprises highest modeling accuracy with adaptive decisions and perfect foresight in all extension stages. Computation times exceed 1,900 s for the dairy, 2,700 s for the automotive and 4200 s for the pharmaceutical use case. The MYOP requires more than one order of magnitude more computation time than the other modeling strategies. This needs to be considered in the right choice of a modeling strategy for feasibility studies.

Summary

Three pathway strategies have been applied to the complex design of industrial energy supply systems. Simulative evaluations highlight the value of adaptivity and foresight to identify non-regret investment decisions under changing boundary conditions. The forward-looking design approach (FLA) identifies saving potentials compared to a reference approach. However, investment decisions are moved up in the planning horizon, e.g., biomass boilers are installed a long time before it becomes economically attractive to use them. Given the uncertainty of long-term projections in energy demands and commodity prices, this strategy leads to undesirable design decisions. This highlights the value of adaptivity in investment decisions which is captured in a transformation roadmap derived by MYOP and PERF strategies. Commercially available simulation software includes multi-year simulation models [70]. These modules simulate an initial design over multi-decade project horizons [109]. The value of adaptivity is omitted in these types of simulations.

Adaptive investment decisions in both MYOP and PERF have led to several small investment decisions for those technologies with linear cost estimations, particulary PV investments. For instance, a continuous expansion of photovoltaic is simulated for all use cases along the planning horizon. Energy planners typically avoid recurring planning efforts. Non-linear investment estimations reflect efforts for recurring planning and thereby avoid investment splits. These types of estimations have been applied for majority of technologies in this work.

The roadmap approach with perfect foresight (PERF) results in a cost optimal roadmap due to perfect foresight whereas the roadmap approach with myopic foresight (MYOP) derives a near optimal roadmap in significantly shorter computation times. The near optimal roadmap might include stranded investment decisions which turn out to be economically unviable with projected long-term trends. For instance, simulations have shown that investment in trigeneration systems might be stranded if fuel and carbon prices significantly increase along the project horizon. These stranded investments need to be identified and ruled out manually by an energy system consultant. In contrast, the PERF accounts for perfect foresight which targets at non-regret investment decisions for a given set of input parameters. Consequently, the PERF shows a cost saving potential of up to 1.69 M€ in the pharmaceutical use case compared to MYOP. However, the accuracy of long-term projections is known to suffer from significant uncertainty. In this light, one might argue that the MYOP results in more robust design decisions as future projections are omitted for today's investment decisions. The choice between MYOP and PERF should thus consider the accuracy of long-term projections.

All transformation pathways have been derived assuming reliability of all equipment over the entire planning horizon, e.g., periods of maintenance work for the CHP or short-term balancing for PV have been omitted. However, unavailabilities occur in practical applications and might lead to severe interruptions of production processes. Therefore, the following section will evaluate concepts to guarantee sufficient levels for security of supply.

5.5. Security of supply

Optimization results in the previous sections have indicated high saving potentials to reduce costs and carbon footprints. The evaluations of these saving potentials have not considered limited technology availabilities due to maintenance work, equipment failures or short-term fluctuations. Therefore, three reserve concepts will be discussed in the following. These concepts allow to include preliminary security of supply considerations in the techno-economic model formulation. Simulative evaluations are conducted based on the cost optimal scenario of the automotive use case for an entire year introduced in Section 5.2. If not explicitly mentioned, technologies which have not been part of the optimized design concept are excluded from the solution space. The derived design concept can be extended by additional equipment capacities of selected technologies to ensure security of supply.[10]

Maintenance scheduling

Regular maintenance work is required for all on-site equipment. For instance, small CHP plants with ICE typically require one week of annual maintenance [156]. Costs for equipment maintenance are considered as part of the objective function as outlined in Section 3.5. Beyond costs, equipment maintenance causes planned unavailabilities of technologies which have been omitted in the previous analysis. Planned unavailabilities can be scheduled. Their impact is considered as part of the optimization formulation by setting the maximum part-load ratio ($\overline{u}_{CHP,t}$) to zero for the scheduled maintenance periods. The following simulations outline impact of maintenance scheduling for the cost optimal scenario of the automotive use case. Maintenance periods are defined in spring (11.04. - 17.04), summer (18.07. - 24.07.), autumn (10.10. - 16.10.) and winter (25.01. - 31.01.). Figure 5.20 shows the impact of maintenance scheduling on the total costs.

The existing energy supply system can meet the energy demands any time. Consequently, no additional equipment capacities are required to serve energy demands during maintenance work of the CHP. Costs for planned unavailabilities occur as CHP plant cannot be operated and electricity needs to be procured during these times. The highest cost increase of 36 k€/a occur if power needs to be procured in peak periods during winter. Waste heat from CHP plant can be effectively used to meet space heating demands in this season. During the summer months, the CHP plant is mostly shut down. Consequently, maintenance scheduling in these periods causes almost no additional costs (+0.2 k€/a) favoring a scheduling of maintenance work in this season.

The simulation results prove that the proposed methodology can capture the impact of maintenance scheduling. The examined case study comprises sufficient backup capacities from existing boilers and chillers. Maintenance scheduling thus results only in incremental increases of up to 1.3 % of total costs. The impact of maintenance scheduling becomes more relevant for use cases with high equipment utilization and with longer maintenance periods. The proposed optimization framework supports evaluation and analysis of maintenance scheduling implications for these types of energy supply systems.

Maintenance work causes regular and planned unavailabilities of on-site supply equipment. Unavailabilities can be scheduled in periods with low demands reducing their impact. Equipment unavailabilities are also caused by technical failures. In contrast to maintenance work, technical failures can occur any time. Therefore, redundant equipment is required to avoid costly production interruptions in industrial sites.

Redundancy allocation

Technical failures result in unplanned unavailabilities of on-site equipment. Risks from technical failures can be mitigated by allocation of redundancies, e.g., backup boilers. Existing approaches

[10] Integration of outage costs ("Value of Lost Load") is one approach to analyze reinforcement investments in distribution grids and reduce impact of grid failures. They can be considered as curtailment costs in the objective function of the proposed model introduced in Section 3.5. Authors work in [49] finds only limited impact of outage costs for sites in countries with high reliability of power supply. Outage costs are thus not discussed in this Thesis.

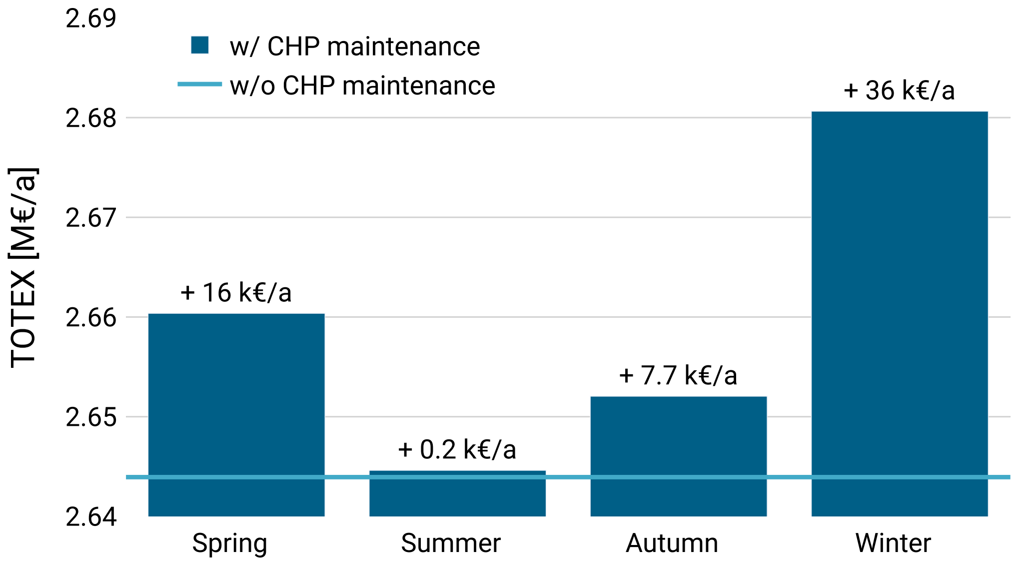

Figure 5.20.: Cost increases from CHP maintenance scheduling in different seasons for the cost-optimized scenario of the automotive use case

in literature focus either on the electrical supply system [136], [137] or the thermal supply system [102]. This work proposes a holistic redundancy concept for all energy demands within an industrial site as introduced in Section 3.4.2. The allocated additional equipment capacities serve as backup during technical equipment failures of single units of a technology. A comprehensive database on equipment reliability is provided in IEEE Standard 3006.8 [157]. The database is based on an extensive survey of nearly 400 sites and evaluates 900,000 technical failure events. Survey results indicate that failures of compression chillers (0.35/a), steam boilers (0.58/a) and engines (1.8/a) of CHP plants are likely to occur multiple times during planning horizon. Energy supply systems need to continue serving the energy demands during these unexpected equipment failures. Mean time to repair equipment failures is up to 48 hours [157]. Storage technologies with hourly charging cycles cannot meet these long-term backup requirements. Backup is thus fully provided by additional capacities of conversion technologies.

For redundancy allocation, conversion technologies are installed in multiple smaller units rather than in one large unit. Consequently, models of conversion technologies need to consider the unit sizing constraints introduced in Section 3.4. For the illustrative purpose of this work, the existing energy supply system is assumed to comprise 4 units of 240 kW compression chillers and three units of 500 kW gas boilers. Capacity additions are possible by adding unit capacities, e.g., 240 kW for a compression chiller. This assumption reflects energy planers policy to reduce maintenance efforts by standardization of on-site equipment. The effect of redundancy allocation is analyzed in three scenarios for economic optimal selection, moderate N-1 constraints and conservative N-1 constraints. Parameters for N-1 secured loads are summarized in Table 5.6. The economic scenario considers no backup requirements whereas the two N-1 scenarios ensure security of supply for certain critical loads. In contrast, the conservative approach ensures backup even during rarely occurring demand peaks. Peaks of different demand types (electricity, steam, heating, cooling) typically occurs during different times. Moreover, storage technologies and thermal inertia from distribution systems may support remaining conversion technologies to provide a sufficient level

Table 5.6.: Assumptions for critical load ($p^{\mathrm{RED,L}}$) secured by redundant backup equipment

Mode	Unit	Economic	N-1 (moderate)	N-1 (conservative)
Electricity	MW	-	2.4	2.9
Heating	MW	-	0.69	1.3
Cooling	MW	-	0.71	0.92

of energy supply. Therefore, the moderate scenario guarantees energy supply only outside peak periods. 300 h of each energy demand are thus not secured with backup capacities.

Introducing redundancy requirements causes slightly higher objective values of 0.1 % for the moderate N-1 scenario and 0.5 % for the conservative N-1 scenario. The impact of redundancy allocation on the sizing of conversion and storage technologies is summarized in Figure 5.21. Backup for electricity supply system is provided by the grid connection which is assumed to provide reliable backup. Therefore, the introduction of redundancy constraints has only minor impact on the sizing of the CHP plant. Security of supply for heating and cooling demands are ensured by backup boilers and chillers. In the moderate N-1 scenario, one additional boiler of 0.5 MW and one additional chiller of 0.24 MW are installed. In contrast, the conservative N-1 scenario results in two additional units of both gas boilers and chillers. The additional capacities only serve as backup for rarely occurring peak demands.

Increasing peak-load capacities from boilers and chillers have an impact on the sizing of hot and chilled water tanks. The computed capacities of the hot water tanks decrease by 10.4 % in the conservative N-1 scenario. Backup boilers can serve peak demands in this scenario. In contrast, capacity of the chilled water tank is increased by 38 % (moderate) and 48 % (conservative). The additional capacities of compression chillers enable a flexible charging during times with low electricity prices.

The developed redundancy allocation concept enables energy system planners to include site-specific backup requirements for technical equipment failures. The integration of redundancy constraints shows only minor impact on total costs for the considered use case. However, consideration of backup equipment has a clear impact on sizing of peak-load conversion and storage technologies. Backup equipment capacities in combination with storage technologies allow for a flexible operation and better integration of renewable energy sources. The proposed model formulation accounts for discrete unit characteristics for chillers and boilers. Computation times of the resulting combinatoric optimization model are significantly higher (817 s to 2763 s) than for the model without discrete unit characteristics (333 s). One might argue that the additional capacities for backup equipment might be allocated in a post-processing routine rather than in the formulation of the techno-economic planning model. However, a post-processing routine would omit the impact of backup equipment on sizing of storages. The proposed formulation accounts for this impact on storage sizing. Therefore, the optimization framework enables the computation of optimal design concept which mitigate risks from equipment failures.

Equipment failures cause unavailabilities at any time and remain for hours to days. In contrast to long-term equipment failures, integration of photovoltaic plants introduces short-term fluctuations. These short-term fluctuations need to be balanced by the energy supply infrastructure. The following section applies an operating reserve which considers a reserve margin to mitigate risks from sudden and temporarily changes in energy demands and renewable generation.

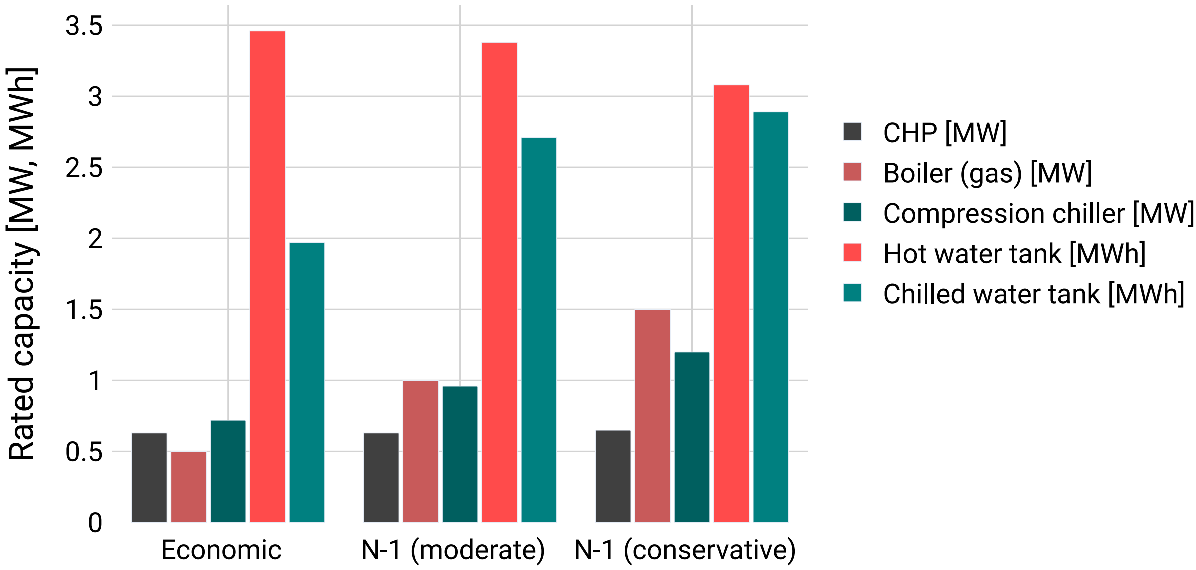

Figure 5.21.: Conversion and storage capacities for the automotive site considering discrete unit sizes for boilers and chillers and three types of redundancy requirements

Short-term balancing

Operational reserve margins are required to reliably operate energy supply systems during sudden drops in renewable generation (e.g., cloud movement over PV plant) or demand peaks (e.g., start-up demands of large motors). Sustainable design concepts comprise sufficient equipment capacities to meet the required reserve margins. The following paragraph analyzes the impact of operating reserves introduced in Section 3.4. Assumptions of reserve margins are based on a conventional control schema described in [158]:[11] margins ($a_t^{\mathrm{L,OR,rel}}$) of 10 % for electricity and cooling demands as well as 80 % of photovoltaic generation are considered as constraints in the dispatch formulation. The required duration ($T^{\mathrm{OR,D}}$) is selected with 30 minutes. The CHP plant can contribute to the reserve by adapting its set point if switched on ($B_{\mathrm{CHP},t}^{\mathrm{Opr}} = 1$). Temporarily overloading of the CHP is omitted which limits the contribution of the CHP to its rated capacity. Beyond the CHP, batteries and the power grid contribute to operating reserve requirements. Table 5.7 summarizes parameters for operating reserve requirements. The analysis is conducted for a grid-connected and a self-sufficient scenario. In contrast to the grid-connected scenario, the energy supply system of the automotive site is operated independently from the power grid in the self-sufficient scenario. This scenario reflects basic requirements for remote sites which are connected to no or a highly unreliable power system.

The self-sufficient scenario results in total expenditures between 3.5 M€/a to 3.6 M€/a which is 36 % higher than the grid-connected scenario. Share of PV generation increases from 21 % to 32 %. Moreover, a battery stores excess electricity and provides 3.6 % to the electricity mix. The remaining electricity is generated by the CHP plant with a rated capacity of 2.1 MW. Figure 5.22 shows the dispatch for a summer week in this scenario. PV generation meets most of the demand during noon. The CHP plant is shut down during these hours and thus cannot contribute to the

[11] Required operating reserve margins for PV can be reduced by advanced control schemas with local weather sensors, particulary during clear-sky conditions. The interested reader is guided to [158] for additional information.

Table 5.7.: Operating reserve requirements for electric and cooling loads ($\alpha^{\mathrm{OR,L,rel}}$) as well as PV generation ($a^{\mathrm{OR,Ren}}$)

	None	Load	Load + PV
$\alpha^{\mathrm{OR,L,rel}}$	0	0.1	0.1
$a^{\mathrm{OR,Ren}}$	0	0	0.8

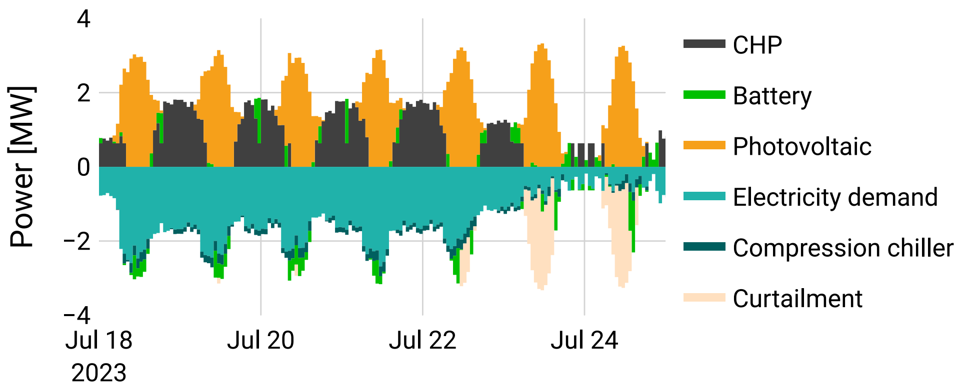

Figure 5.22.: Electricity dispatch during a summer week in the self-sufficient scenario with operating reserve for short term fluctuations of load and PV

reserve. The operating reserve during these hours is provided by the battery storage. During the weekends, the PV generation is partly curtailed as excess electricity can no longer be fed in the power grid. Curtailment energy accounts for 17 % of annual PV generation.

Figure 5.23 summarizes the electric generation capacities for the conducted analysis. The operating reserve is provided by the power grid in the grid-connected scenario. Therefore, the introduction of reserve constraints shows no impact in these scenarios. In contrast, the sizing of the battery storage is highly dependent on the assumed reserve parameters in the self-sufficient scenario. The consideration of a load and PV reserve increases the optimized battery capacity from 1.03 MWh to 1.15 MWh (+ 12 %) and 2.53 MWh (+ 145 %). The battery provides operating reserves and simultaneously store renewable excess energy. The proposed formulation derives an optimal capacity sizing considering both revenue streams.

Optimization results highlight the value of a reliable connection to a power system for the energy supply systems of industrial sites. Design of stand-alone systems requires consideration of short-term balancing constraints to provide sufficient reserve for sudden and temporary disturbances of power balances, in particular due to volatile PV generation. The proposed operating reserve concept enables the computation of self-sufficient design concepts with reliable cost and equipment estimations. The comparison of the grid-connected and the self-sufficient scenario clearly indicates that industrial sites profit from a reliable connection to the power grid.

Summary

Security of supply considerations are successfully integrated in the techno-economic planning model. Their integration strengthens stakeholders' confidence in the feasibility of the derived

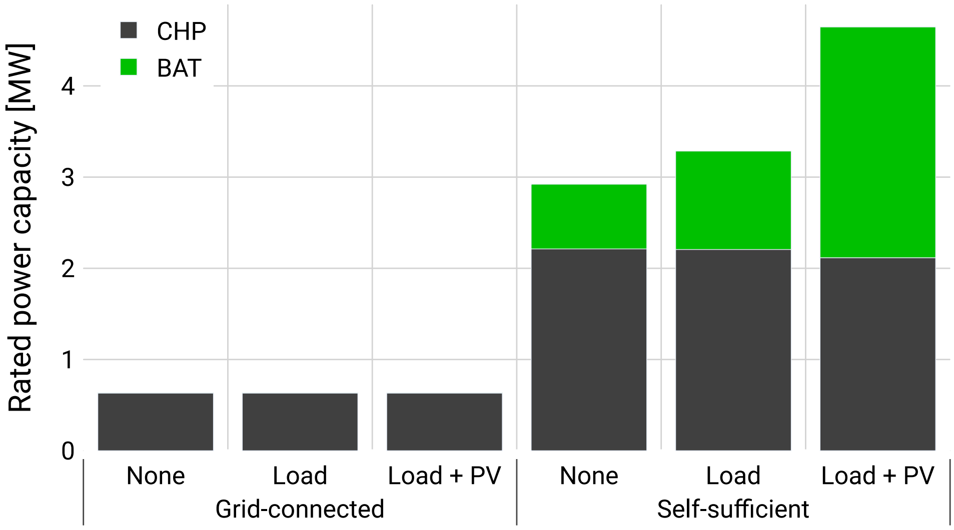

Figure 5.23.: Dispatchable electricity generation capacities for a grid-connected and a self-sufficient energy supply system depending on the short term balancing services

preliminary design concepts and thus increase chances of project realization. Simulative evaluations for the use case of an automotive site underline the ability to account for maintenance scheduling, redundancy allocation and short-term balancing services.

- **Maintenance scheduling:** Maintenance periods of equipment are effectively scheduled in periods of low demands, e.g., during summer time for heating demands. If maintenance work can be scheduled in these periods, the impact of planned unavailabilities has only minor impact on the design concept.
- **Redundancy allocation:** Allocation of redundancies mitigates risks of equipment failures. Therefore, the model captures discrete unit characteristics of conversion technologies. The consideration of redundancies is in particular relevant for sizing of peak load technologies such as backup boilers.
- **Short-term balancing:** Operating reserves for short-term changes in electric demands and PV generation require additional equipment installations if short-term balancing needs to be provided by the on-site energy supply system. However, industrial sites in Europe are typically connected to reliable power grids which ensure electricity supply at any time.

Feasibility studies select an optimal design concept by comparison of multiple design variants regarding their economic, ecological and energetic KPIs. Primary objective of techno-economic planning models is thus the optimization under normal operational conditions [109]. In contrast, security of supply considerations focus on challenging extreme situations. Energy supply concepts need to comprise sufficient equipment to handle these extreme situations. The consideration of security of supply constraints shows only minor impact on the KPIs for the considered use case of a German industrial site. However, both operating reserves and redundancy allocation significantly increase model complexity. Therefore, these concepts should be only employed if a use case desires security of supply considerations. Importance of security of supply rises if sites cannot procure electricity from a reliable power grid connection, e.g., mining industry in remote locations or sites in countries with weak power grids. Similar recommendations are given by the National Renewable Energy Agency (NREL) in their recently released manual for a design web tool [159].

5.6. Discussion

This section discusses the results of the presented use cases regarding the requirements derived in Section 2.2 and critically assesses limitations. Suggested improvements for practical applications and future research can be directly handled within the newly developed optimization framework

Exemplary use cases from three industrial sectors have illustrated multiple features of the newly developed optimization framework. The proposed model derives economic, ecological and energetic KPIs for multiple scenarios considering non-linear technology models and time-dependent procurement tariffs in multi-modal coupled energy supply systems. The techno-economic model is integrated in an optimization framework enabling a computationally effective solving process by optimized period selection (OPS) and a roadmap approach with myopic foresight (MYOP). Stakeholders' confidence in the robustness of the derived design concepts is strengthened by identifying non-regret decisions in multi-year transformation roadmaps, e.g., to analyze the changing role of cogeneration plants. Moreover, the framework can derive robust design concepts which guarantee security of supply during maintenance work, technical failures and short-term imbalances for all production related energy demands. The newly developed framework provides valuable insights to identify non-regret design decisions and meet decarbonization targets.

Models for the three examplary use cases have been simplified for the illustrative purpose of this Thesis. The following four paragraphs give modeling guidance for real-world applications and future research with the newly developed optimization framework.

Cost estimations and regulatory boundary conditions: Cost estimations for the three use cases are mostly based on open source databases [155], [156]. Real-world applications should consider more detailed cost estimations considering planning efforts, assembly costs and risks margins. Moreover, subsidies and network charges have not been fully reflected in the presented use cases. The use cases do not included subsidies offered by German local or national authorities. Practical applications need to account for these subsidies, which make business cases for low carbon technologies even more viable. For instance, author's analysis in [50] have discussed full-load dependent CHP promotions in combination with additional technical constraints for high-efficiency criterion. Revenue streams from network charge incentives are also simplified. Network charges are modelled by a composite electricity tariff structure depending on the grid utilization rate. Reduction of network charges for atypical or intensive grid usage incentivizes a grid friendly electricity procurement and offers additional saving potentials for industrial stakeholders. The interested reader is guided to author's work in [49], which has discussed these options for a real-world use case from non-ferrous metal industry. Regulatory boundary conditions are continuously revised by regional and national authorities. The proposed cost parameters and linking concept in the newly developed optimization framework provide a solid basis to model a variety of existing and future boundary conditions.

Technology characteristics: The technical superstructure for the presented use cases includes the most relevant technology options for industrial sites. Practical applications may adapt technology parameters according to site specific characteristics. Constant temperature and pressure levels have been assumed for all three use cases, e.g., 80 °C for space heating. Lower temperatures for space heating increase COP values of heat pumps and encourage their use. Temperature levels of waste heat should also be included. Depending on the required temperature levels, free cooling or reversible heat-pumps may be applicable to reduce use of compression chillers. Beyond flow temperature dependence, the model of CHP may also account for start-up costs to penalize wear and tear from frequent start up and shut down processes. Emission factors of electricity procurement have been considered as constant for the three use cases. Future work might also consider time dependent emission factors from macro-economic models to reflect the changes in power grid more accurately. All of the above-mentioned suggestions require only updates of model parameters and can be handled within the proposed technical superstructure.

Demand-side measures: The three use cases have strongly focused on supply-side decarbonization measures linked to on-site generation and energy procurement. Demand-side measures have been accounted for by model exogenous annual changes of load profiles according to analysis in [146]. Data-driven decision support for demand-side measures might become more relevant in the near future as increasing monitoring of large energy consumers brings additional transparency in energy use, in contrast to today's practice to measure only the point of common coupling. Future research could thus extend the technical superstructure by demand-side measures. Demand-side measures include capital-intensive measures such as the installation of new highly efficient vents and heat exchangers in HVAC systems. Other demand-side measures might be linked to employment of advanced control schemas. Demand-driven controls avoid high standby consumptions of industrial processes. Other control schemas might exploit flexibility potentials of demands for peak-load management. Author's work in [49] has considered flexibility from on-site air separation plants and electrical furnaces. The mentioned demand-side measures can be formulated with the proposed generic technology model as a combination of grid, load, and conversion technologies.

Uncertainty handling: The above mentioned suggestions refer to an extension of the technical superstructure and refinement of techno-economic model parameters. These suggestions assume that data is available in a sufficient coverage and quality. Input data is known to comprise significant uncertainty during early project phases, as outlined in Section 3.1. Projected electricity and gas prices have dynamically evolved during the course of this Thesis. Future work should thus employ extensive sensitivity analysis and quantify the impact of single measures. Sensitivity analysis allows to identify tipping points when investments reach the threshold of economic viability. They thus assess trade-offs between multiple capital-intensive investment decisions. The presented use cases have compared scenarios which result from multiple measures. Future work should also compute the impact of each measure seperately, e.g., the payback period of a PV installation. This gives stakeholders the option to derive action plans with priorities on those measures with the highest cost and carbon saving potential.

6. Conclusion and Outlook

Optimization-based design approaches support strategic planning of industrial energy supply systems. This Thesis has developed a novel optimization framework which effectively generates transformation roadmaps with non-regret decarbonization measures. The chapter highlights the main achievements, followed by perspectives for future research.

6.1. Thesis achievements

This work has developed and applied a comprehensive decision support tool to design highly complex multi-modal energy supply systems in industrial sites. The key contributions regarding the four focus research questions are summarized in the following.

Energy supply systems define the on-site infrastructure to serve multi-modal demands of buildings and production processes within industrial sites. Chapter 2 has derived requirements for feasibility studies and reviewed existing research work. MILP-based optimization models are found to capture the relevant techno-economic characteristics of on-site infrastructure and procurement tariffs. The generic formulation with technology base classes of Thiem [27] accounts for the diverse requirements typically found in industrial sites, e.g., general purpose and sector specific technologies. The mathematical formulation from Thiem is thus re-implemented and extended for multi-node, multi-stakeholder and multi-year system analysis. The optimization functionality of the framework is provided as a scalable sizing service, which can be accessed by several users simultaneously. Moreover, the framework includes a client application which allows experienced energy consultants to easily access the sizing service. The client application comprises extensive functionality for input data checking and immediate result analysis, e.g., an automatic generation of interactive topology and sankey diagrams. The client application is frequently employed in research and consulting projects since October 2020.

The techno-economic planning model has been formulated in Chapter 3. The model comprises two newly developed deterministic reserve concepts to guarantee highly reliable supply of production related demands in industrial sites. The operating reserve concept ensures system's ability to dynamically respond to short-term imbalances resulting from demand peaks, grid failures or renewable generation drops. These short-term imbalances are handled by a reliable connection to the power grid or installation of on-site battery storages. The redundancy allocation concept mitigates risks from technical failures which last for several hours to days. Both concepts allocate additional equipment capacities which can promote an integration of renewable excess generation. Security of supply constraints can strengthen stakeholders' confidence in the feasibility of the derived transformation roadmaps. However, both reserve concepts add significant complexity to the model formulation: additional dispatch constraints for each time step are required for the operating reserve concept, the redundancy concept enforces a modeling of discrete unit characteristics for conversion technologies.

Beyond security of supply, the framework allows to compute transformation roadmaps, as described in Chapter 4. These roadmaps integrate projected long-term trends in decision process and highlight the evolution of an energy supply system. The computational feasibility is ensured by the newly developed optimized period selection (OPS) approach for time series aggregation. Based on an integer program, the OPS approach derives a robust selection of representative days capturing the multi-modal energy demands of the entire base year. Computation times are reduced from 71 minutes to 30 s for a base year model. Solving times of multi-year models are further reduced by the roadmap approach with myopic foresight (MYOP). Examined models are solved between 93 % to 98 % faster compared to the roadmap approach with perfect foresight (PERF). The sequential solving process of MYOP strategy accounts for adaptive decisions along a roadmap offering stakeholder a clear view on a sustainable evolution of their energy supply systems. However, the MYOP strategy might identify stranded investments as promising options due to lock-in effects of long-living energy supply equipment. This drawback is overcome by a strategic planning strategy with perfect foresight (PERF).

Three exemplary use cases from automotive, pharmaceutical, and dairy industry in Southern Germany have demonstrated the suitability of the methodology developed in this Thesis. Results have been presented in Chapter 5. The use cases optimize supply concepts for electricity, steam, space heating and process cooling. Optimization results indicate that cogeneration plants might be an attractive investment option if waste heat can be efficiently used within the factory site. However, the role of CHP plants is projected to change significantly along the 15-year planning horizon. For instance, the equivalent annual full load hours of a CHP in the dairy use case decrease from 8,410 h/a to 970 h/a. This long-term development challenges the economic feasibility of an investment. High carbon and gas prices as well as the availability of renewable excess electricity from PV favor the electrification of thermal demands. The electrification leads to significant increases of on-site electricity use despite implementation of efficiency measures. The remaining steam demands are supplied by biomass in the conducted use case. Optimization results strongly depend on the projected fuel and electricity price developments. Projected developments have dynamically evolved during this Thesis, giving the high uncertainty in the European electricity and gas markets. The proposed setup allows to easily repeat design calculations with updated projections on procurement costs and energy demands. Thereby, it supports energy system planners and consultants in identifying non-regret decarbonization strategies for highly complex industrial sites.

6.2. Future perspectives

Previous chapters have described the newly developed optimization framework to design highly complex energy supply systems in industrial sites. This section critically assesses limitations of the derived methodology and provides perspectives for future research. Shortcomings of the three exemplary use cases have been discussed in Section 5.6. The discussion of this shortcomings gives clear modeling guidelines for future work within the newly developed framework. The techno-economic planning model is based on several key assumptions outlined in Section 3.6. Among others, these key assumptions offer perspectives for future research.

Control strategies: The results presented have been derived under the assumption of perfect foresight and full controllability of all assets. However, these assumptions omit limitations of real-world controllers. Consequently, the proposed methodology overestimates potentials for flexibility. Realistic control strategies should account for forecasting uncertainties. Modeling of realistic control strategies might also account for flexibility options from shifting energy-intensive processes in production planning. An application-oriented summary of experiences from coupling of material and energy simulations is provided by Köberlein in [67]. Simulations of control strategies enable more accurate estimations of cost and carbon saving potentials.

Enterprise perspectives: Focus of this Thesis has been the computation of technical energy supply concepts for single sites. Ownership structures and procurement strategies have been simplified for the simulative evaluations in this Thesis. Real-world applications should consider bankability of investments. Bankability poses a major hurdle for practical implementation in companies [138]. A comprehensive review on this topic is provided by Ioannou in [160]. Beyond bankability of investments, procurement strategies often include hedging strategies with long-term supply contracts or power-purchase agreements (PPA). These procurement strategies may also be optimized across multiple sites of a company to reach corporate decarbonization targets.

Coupling to physical models: Techno-economic planning models are clearly valuable for feasibility studies, e.g., to engage non-technical management stakeholders. However, these models basically omit underlying physical properties such as voltages for electrical supply systems and temperatures for heating networks [74]. These physical properties become more relevant in later project stages. Therefore, the design concepts derived with the proposed methodology could be refined by simulation models for building performance [161] and network flows [162]. Network simulations require detailed knowledge of topology structures which can be generated based on an economic optimization approach [163].

Comprehensible results: Practical acceptance of the proposed methodology is closely linked to consultants' ability to explain the optimization results. This Thesis provides a comprehensive user interface with interactive visualizations of results. Future work could link input and result data to create an even deeper understanding of the highly complex interactions in industrial energy supply systems. Moreover, costs and carbon emissions might be interlinked with energy demands by tracing algorithms, giving stakeholders additional clarity on the most relevant measures to transform existing energy supply concepts into sustainable solutions.

Bibliography

[1] C. A. Frangopoulos, “Recent developments and trends in optimization of energy systems”, *Energy*, vol. 164, pp. 1011–1020, 2018, ISSN: 03605442. DOI: 10.1016/j.energy.2018.08.218. [Online]. Available: https://doi.org/10.1016/j.energy.2018.08.218.

[2] P. Lopion, P. Markewitz, M. Robinius, and D. Stolten, “A review of current challenges and trends in energy systems modeling”, *Renewable and Sustainable Energy Reviews*, vol. 96, pp. 156–166, 2018, ISSN: 1364-0321. DOI: 10.1016/j.rser.2018.07.045. [Online]. Available: https://doi.org/10.1016/j.rser.2018.07.045.

[3] O. D. Doleski, T. Kaiser, M. Metzger, S. Niessen, and S. Thiem, *Digitale Dekarbonisierung*. Springer Vieweg, 2021, ISBN: 9783658329334. DOI: 10.1007/978-3-658-32934-1_3.

[4] Boston Consulting Group, “Klimapfade 2.0 Ein Wirtschaftsprogramm für Klima und Zukunft”, Bundesverband der Deutschen Industrie, Tech. Rep., 2021.

[5] Agora Energiewende und Wuppertal Institut, “Klimaneutrale Industrie - Schlüsseltechnologien und Politikoptionen für Stahl, Chemie und Zement”, 2019.

[6] United Nations, “Global Impact of war in Ukraine on food, energy and finance system”, 2022. [Online]. Available: https://news.un.org/pages/wp-content/uploads/2022/04/UN-GCRG-Brief-1.pdf.

[7] S. M. Buettner, C. Schneider, W. König, H. M. Nulty, C. Piccolroaz, and A. Sauer, “How Do German Manufacturers React to the Increasing Societal Pressure for Decarbonisation?”, *Applied Sciences (Switzerland)*, vol. 12, no. 2, 2022, ISSN: 20763417. DOI: 10.3390/app12020543.

[8] Siemens AG, *Siemens is leading the way towards carbon neutrality*. [Online]. Available: new.siemens.com/global/en/company/sustainability/carbonneutral.html (visited on 05/19/2021).

[9] RWE, *Klimaschutz*. [Online]. Available: https://www.group.rwe/verantwortung-und-nachhaltigkeit/umweltschutz/klimaschutz (visited on 01/02/2021).

[10] Thyssenkrupp, *Klimastrategie thyssenkrupp Steel*. [Online]. Available: https://www.thyssenkrupp-steel.com/de/unternehmen/nachhaltigkeit/klimastrategie/ (visited on 01/02/2021).

[11] Nestle, *Klimaschutz*. [Online]. Available: https://www.nestle.de/klimaschutz (visited on 06/12/2022).

[12] T. Bründlinger, J. Elizalde-König, O. Frank, and D. Gründig, “Integrated Energy Transition - Impulses to shape the energy system up to 2050”, Deutsche Energie-Agentur GmbH (dena), Tech. Rep., 2018.

[13] International Renewable Energy Agency (IRENA), "Global Energy Transformation: A roadmap to 2050," International Renewable Energy Agency, Abu Dhabi, Tech. Rep., 2018, p. 12. [Online]. Available: www.irena.org/publications.

[14] B. C. Ram M., Bogdanov D., Aghahosseini A., Oyewo A.S., Gulagi A., Child M., Fell H.-J., *Global Energy System based on 100 Power, Heat, Transport and Desalination Sectors*. Lappeenranta, Berlin: Lappeenranta University of Technology and Energy Watch Group, 2019, ISBN: 9789523353398. [Online]. Available: http://energywatchgroup.org/new-study-global-energy-system-based-100-renewable-energy.

[15] International Renewable Energy Agency (IRENA), *Renewable Power Generation Costs in 2020*. Abu Dhabi: International Renewable Energy Agency, 2021, p. 160, ISBN: 978-92-9260-348-9. [Online]. Available: https://www.irena.org/-/media/Files/IRENA/Agency/Publication/2018/Jan/IRENA_2017_Power_Costs_2018.pdf.

[16] A. Sauer, E. Abele, and H. U. Buhl, "Energieflexibilität in der Deutschen Industrie", Fraunhofer Verlag, Tech. Rep., 2019.

[17] Deutsches Institut für Normung (DIN), *Energetische Bewertung von Gebäuden – Berechnung des Nutz-, End- und Primärenergiebedarfs für Heizung, Kühlung, Lüftung, Trinkwarmwasser und Beleuchtung (DIN 18599) - Teil 1: Allgemeine Bilanzierungsverfahren, Begriffe, Zonierung und Bewertung der Energie*, Berlin, 2018.

[18] P. Voll, "Automated optimization based synthesis of distributed energy supply systems", PhD Thesis, RWTH Aachen, 2013, ISBN: 978-3-86130-474-6. DOI: urn:nbn:de:hbz:82-opus-49136.

[19] Umweltbundesamt, *Umwelt- und Energiemanagementsysteme*, 2022. [Online]. Available: https://www.umweltbundesamt.de/themen/wirtschaft-konsum/wirtschaft-umwelt/umwelt-energiemanagement#wozu-dient-ein-umwelt-und-energiemanagement (visited on 06/16/2022).

[20] J. Shalf, "The future of computing beyond Moore ' s Law Subject Areas :" *Philosophical Transactions Royal Society*, vol. 378, no. 20190061, pp. 1–14, 2020.

[21] Gurobi, *Gurobi Optimizer Reference Manual*, 2020. [Online]. Available: http://www.gurobi.com.

[22] IBM Corporation, "CPLEX Optimization Studio 12.10 Performance improvements", 2020.

[23] C. Gamarra and J. M. Guerrero, "Computational optimization techniques applied to microgrids planning: A review", *Renewable and Sustainable Energy Reviews*, vol. 48, pp. 413–424, 2015, ISSN: 18790690. DOI: 10.1016/j.rser.2015.04.025. [Online]. Available: http://dx.doi.org/10.1016/j.rser.2015.04.025.

[24] E. A. Martínez Ceseña, N. Good, A. L. Syrri, and P. Mancarella, "Techno-economic and business case assessment of multi-energy microgrids with co-optimization of energy, reserve and reliability services", *Applied Energy*, vol. 210, no. August 2017, pp. 896–913, 2018, ISSN: 03062619. DOI: 10.1016/j.apenergy.2017.08.131. [Online]. Available: https://doi.org/10.1016/j.apenergy.2017.08.131.

[25] C. Marnay, G. Venkataramanan, M. Stadler, A. S. Siddiqui, and R. Firestone, "Optimal Technology Selection and Operation of Commercial-Building Microgrids", vol. 23, no. 3, pp. 975–982, 2008.

[26] L. Kotzur, "Future Grid Load of the Residential Building Sector", PhD Thesis, RWTH Aachen, 2018, ISBN: 9783958063709. DOI: 10.18154/RWTH-2018-231872.

[27] S. M. Thiem, “Multi-modal on-site energy systems Development and application of a superstructure-based optimization method for energy system design under consideration of part-load efficiencies”, PhD Thesis, TU Munich, 2017.

[28] G. Mavromatidis, “Model-based Design of Distributed Urban Energy Systems Under Uncertainty”, PhD Thesis, ETH Zurich, 2017. DOI: 10.3929/ethz-b-000182697.

[29] T. Schütz, “Optimal Design of Energy Conversion Units and Building Envelopes for Residential Neighborhoods”, PhD Thesis, RWTH Aachen, 2018. DOI: 10.18154/RWTH-2019-02124.

[30] A. S. Wallerand, “Integration of solar energy with industrial processes”, PhD Thesis, EPFL Lausanne, 2018. DOI: 10.5075/epfl-thesis-8635.

[31] International Renewable Energy Agency (IRENA), “A background paper to Renewable Energy in Manufacturing”, International Renewable Energy Agency, Abu Dhabi, Tech. Rep., 2015, p. 94.

[32] M. Blesl and A. Kessler, *Energieeffizienz in der Industrie*. Springer Vieweg, 2017, vol. 55, ISBN: 9783662559987. DOI: 10.1007/978-3-662-55999-4.

[33] M. Dehli, *Energieeffizienz in Industrie, Dienstleistung und Gewerbe*. Springer Vieweg, 2020, ISBN: 9783658232030. DOI: 10.1007/978-3-658-23204-7.

[34] The Energy Efficiency Financial Institutions Group, *De-risking Energy Efficiency Platform*. [Online]. Available: https://deep.eefig.eu/ (visited on 06/11/2022).

[35] C. Lauterbach, B. Schmitt, U. Jordan, and K. Vajen, “The potential of solar heat for industrial processes in Germany”, *Renewable and Sustainable Energy Reviews*, vol. 16, no. 7, pp. 5121–5130, 2012, ISSN: 13640321. DOI: 10.1016/j.rser.2012.04.032. [Online]. Available: http://dx.doi.org/10.1016/j.rser.2012.04.032.

[36] Clemens Rohde, “Erstellung von Anwendungsbilanzen für die Jahre 2018 bis 2020 für die Sektoren Industrie und GHD. Studie für die Arbeitsgemeinschaft Energiebilanzen e.V. (AGEB)”, *Fraunhofer ISI*, no. September, pp. 1–64, 2020. [Online]. Available: https://ag-energiebilanzen.de/wp-content/uploads/2020/10/isi_anwendungsbilanz_industrie_2020_20210903.pdf.

[37] P. Mancarella and G. Chicco, “Global and local emission impact assessment of distributed cogeneration systems with partial-load models”, *Applied Energy*, vol. 86, no. 10, pp. 2096–2106, 2009, ISSN: 0306-2619. DOI: 10.1016/j.apenergy.2008.12.026. [Online]. Available: http://dx.doi.org/10.1016/j.apenergy.2008.12.026.

[38] E. Carpaneto, G. Chicco, P. Mancarella, and A. Russo, “Cogeneration planning under uncertainty Part I : Multiple time frame approach”, *Applied Energy*, vol. 88, no. 4, pp. 1059–1067, 2011, ISSN: 0306-2619. DOI: 10.1016/j.apenergy.2010.10.014. [Online]. Available: http://dx.doi.org/10.1016/j.apenergy.2010.10.014.

[39] V. Andiappan, R. R. Tan, K. B. Aviso, and D. K. S. Ng, “Synthesis and optimisation of biomass-based tri-generation systems with reliability aspects”, *Energy*, vol. 89, pp. 803–818, 2015, ISSN: 0360-5442. DOI: 10.1016/j.energy.2015.05.138. [Online]. Available: http://dx.doi.org/10.1016/j.energy.2015.05.138.

[40] Statistisches Bundesamt (Destatis), *Produzierendes Gewerbe - Stromerzeugungsanlagen der Betriebe im Verarbeitenden Gewerbe sowie im Bergbau und in der Gewinnung von Steinen und Erden*. 2019, ISBN: 2040640187004.

[41] Verein Deutscher Ingenieure (VDI), *Wirtschaftlichkeit gebäudetechnischer Anlagen Grundlagen und Kostenberechnung (VDI 2067)*, Düsseldorf, 2012.

[42] Agora Energiewende and Wuppertal Institute, "Breakthrough strategies for climate-neutral industry in Europe : policy and technology pathways for raising EU climate ambition", Tech. Rep., 2021. [Online]. Available: http://nbn-resolving.de/urn:nbn:de:bsz:wup4-opus-77513.

[43] LBD Beratungsgesellschaft mbH, "Die Rolle der Kraft-Wärme-Kopplung in der Energiewende", *Agora Energiewende*, 2015.

[44] M. Wünsch, B. Eikmeier, S. Gores, M. Gailfuß, and O. Antoni, "Evaluierung der Kraft-Wärme-Kopplung - Analysen zur Enwicklung der Kraft-Wärme-Kopplung in einem Energiesystem mit hohem Anteil erneuerbarer Energien", *PROGNOS, Fraunhofer IFAM, Öko-Institut e.V., Stiftung Umweltenergierecht, BHKW-Infozentrum*, 2019. [Online]. Available: https://www.bmwi.de/Redaktion/DE/Publikationen/Studien/evaluierung-der-kraft-waerme-kopplung.pdf?__blob=publicationFile&v=6.

[45] International Renewable Energy Agency (IRENA), "A background paper to "Renewable Energy in Manufacturing"", IRENA, Abu Dhabi, Tech. Rep., 2015. [Online]. Available: www.irena.org/remap..

[46] M. F. U. Guminski, Andrej; Schimmel, "Energiewende in der Industrie - Potenziale und Wechselwirkungen mit dem Energiesektor", Tech. Rep. 42, 2019, pp. 115–145. DOI: 10.1007/978-3-658-09852-0_6.

[47] T. Fleiter, A. Herbst, M. Rehfeldt, and M. Arens, "Industrial Innovation: Pathways to deep decarbonisation of Industry. Part 2: Scenario analysis and pathways to deep decarbonisation", Fraunhofer ISI, Tech. Rep., 2019, p. 95.

[48] M. R. Hennen, "Decision Support for the Synthesis of Energy Systems by Analysis of the Near-Optimal Solution Space", PhD Thesis, RWTH Aachen, 2019, ISBN: 9783958862777.

[49] L. Hoettecke, S. Thiem, J. Schäfer, and S. Niessen, "Resilience optimization of multi-modal energy supply systems: Case study in German metal industry", *Computers and Chemical Engineering*, vol. 162, p. 107 824, 2022, ISSN: 00981354. DOI: 10.1016/j.compchemeng.2022.107824. [Online]. Available: https://doi.org/10.1016/j.compchemeng.2022.107824.

[50] L. Hoettecke, T. Schuetz, S. Thiem, and S. Niessen, "Technology pathways for industrial cogeneration systems : Optimal investment planning considering long-term trends", *Applied Energy*, vol. 324, p. 119 675, 2022, ISSN: 0306-2619. DOI: 10.1016/j.apenergy.2022.119675. [Online]. Available: https://doi.org/10.1016/j.apenergy.2022.119675.

[51] L. Hoettecke, S. Thiem, and S. Niessen, "Enhanced time series aggregation for long-term investment planning models of energy supply infrastructure in production plants", *4th International Conference on Smart Energy Systems and Technologies*, pp. 1–6, 2021. DOI: 10.1109/SEST50973.2021.9543162.

[52] Verein Deutscher Ingenieure (VDI), *Energy consultancy – Energy consultancy pro- cess and methods (VDI 3922 Blatt 1)*, Düsseldorf, 2019.

[53] A. S. Wallerand, M. Kermani, R. Voillat, I. Kantor, and F. Maréchal, "Optimal design of solar-assisted industrial processes considering heat pumping: Case study of a dairy", *Renewable Energy*, vol. 128, pp. 565–585, 2018, ISSN: 18790682. DOI: 10.1016/j.renene.2017.07.027.

[54] P. H. Tiemann, A. Bensmann, V. Stuke, and R. Hanke-Rauschenbach, “Electrical energy storage for industrial grid fee reduction – A large scale analysis”, *Energy Conversion and Management*, vol. 208, no. November 2019, p. 112 539, 2020, ISSN: 01968904. DOI: 10.1016/j.enconman.2020.112539. [Online]. Available: https://doi.org/10.1016/j.enconman.2020.112539.

[55] F. Zimmerman, D. Pottmeier, A. Emde, and A. Sauer, “Comparison of Peak Shaving and Atypical Grid Usage Application for Energy Storage Systems in the German Industrial Sector”, in *16. Symposium Energieinnovation*, Graz, 2020, pp. 4–5.

[56] Danish Energy Agency and Energinet, “Technology Data Energy storage”, Tech. Rep., 2020. [Online]. Available: http://www.ens.dk/teknologikatalog.

[57] Z. Wang, F. Gao, Q. Zhai, X. Guan, K. Liu, and D. Zhou, “An integrated optimization model for generation and batch production load scheduling in energy intensive enterprise”, *IEEE Power and Energy Society General Meeting*, pp. 1–8, 2012, ISSN: 19449925. DOI: 10.1109/PESGM.2012.6345296.

[58] Verein Deutscher Ingenieure (VDI), *Energy consultancy - Competence assessment of energy consultants (VDI 3922 Blatt 2)*, Düsseldorf, 2019.

[59] K. Fahy, M. Stadler, Z. K. Pecenak, and J. Kleissl, “Input data reduction for microgrid sizing and energy cost modeling: Representative days and demand charges”, *Journal of Renewable and Sustainable Energy*, vol. 11, no. 6, 2019, ISSN: 19417012. DOI: 10.1063/1.5121319.

[60] G. Cusano, M. R. Gonzalo, F. Farrell, R. Remus, S. Roudier, and L. D. Sancho, *Best Available Techniques (BAT) Reference Document for the Non-Ferrous Metals Industries*. 2017, p. 1233, ISBN: 9789279696558. DOI: 10.2760/8224. [Online]. Available: http://eippcb.jrc.ec.europa.eu/reference/BREF/NFM/JRC107041_NFM_Bref_2017.pdf.

[61] Verein Deutscher Ingenieure (VDI), *Economy calculation systems for capital goods and plants (VDI 6025)*, Düsseldorf, 2012.

[62] G. Mavromatidis, K. Orehounig, and J. Carmeliet, “A review of uncertainty characterisation approaches for the optimal design of distributed energy systems”, *Renewable and Sustainable Energy Reviews*, vol. 88, pp. 258–277, 2018, ISSN: 18790690. DOI: 10.1016/j.rser.2018.02.021. [Online]. Available: https://doi.org/10.1016/j.rser.2018.02.021.

[63] G. Mavromatidis and I. Petkov, “MANGO: A novel optimization model for the long-term, multi-stage planning of decentralized multi-energy systems”, *Applied Energy*, vol. 288, p. 116 585, 2021, ISSN: 03062619. DOI: 10.1016/j.apenergy.2021.116585. [Online]. Available: https://linkinghub.elsevier.com/retrieve/pii/S030626192100129X.

[64] L. Kriechbaum, G. Scheiber, and T. Kienberger, “Grid-based multi-energy systems-modelling, assessment, open source modelling frameworks and challenges”, *Energy, Sustainability and Society*, vol. 8, no. 1, 2018, ISSN: 21920567. DOI: 10.1186/s13705-018-0176-x.

[65] J. A. Schachter and P. Mancarella, “A critical review of Real Options thinking for valuing investment flexibility in Smart Grids and low carbon energy systems”, *Renewable and Sustainable Energy Reviews*, vol. 56, pp. 261–271, 2016, ISSN: 18790690. DOI: 10.1016/j.rser.2015.11.071. [Online]. Available: http://dx.doi.org/10.1016/j.rser.2015.11.071.

[66] S. Thiem, V. Danov, M. Metzger, J. Schäfer, and T. Hamacher, “Project-level multi-modal energy system design - Novel approach for considering detailed component models and example case study for airports”, *Energy*, vol. 133, pp. 691–709, 2017, ISSN: 03605442. DOI: 10.1016/j.energy.2017.05.159.

[67] J. Köberlein, L. Bank, S. Roth, E. Köse, T. Kuhlmann, B. Prell, M. Stange, M. Münnich, D. Flum, D. Moog, S. Ihlenfeldt, A. Sauer, M. Weigold, and J. Schilp, “Simulation Modeling for Energy-Flexible Manufacturing: Pitfalls and How to Avoid Them”, *Energies*, vol. 15, no. 10, 2022, ISSN: 19961073. DOI: 10.3390/en15103593.

[68] M. Philipp, G. Schumm, R. H. Peesel, T. G. Walmsley, M. J. Atkins, F. Schlosser, and J. Hesselbach, “Optimal energy supply structures for industrial food processing sites in different countries considering energy transitions”, *Energy*, vol. 146, pp. 112–123, 2018, ISSN: 03605442. DOI: 10.1016/j.energy.2017.05.062. [Online]. Available: https://doi.org/10.1016/j.energy.2017.05.062.

[69] EMD International, *energyPRO*. [Online]. Available: www.emd-international.com/energypro/ (visited on 10/10/2022).

[70] Homer Software, *HOMER Pro*. [Online]. Available: https://www.homerenergy.com/products/pro/index.html (visited on 10/10/2022).

[71] Gesellschaft zur Förderung angewandter Informatik e. V. (GFaI), *TOP-Energy®*. [Online]. Available: https://www.top-energy.de/en/ (visited on 10/10/2022).

[72] J. C. Bruno, F. Fernandez, F. Castells, and I. E. Grossmann, “A rigorous minlp model for the optimal synthesis and operation of utility plants”, *Chemical Engineering Research and Design*, vol. 76, no. 3, pp. 246–258, 1998, ISSN: 02638762. DOI: 10.1205/026387698524901.

[73] Z. K. Pecenak, M. Stadler, and K. Fahy, “Efficient multi-year economic energy planning in microgrids”, *Applied Energy*, vol. 255, no. April 2019, p. 113 771, 2019, ISSN: 03062619. DOI: 10.1016/j.apenergy.2019.113771. [Online]. Available: https://doi.org/10.1016/j.apenergy.2019.113771.

[74] J. Dorfner, “Open Source Modelling and Optimisation of Energy Infrastructure at Urban Scale”, PhD Thesis, TU Munich, 2016.

[75] J. Kallrath, *Gemischt-ganzzahlige Optimierung: Modellierung in der Praxis*. Springer Fachmedien Wiesbaden, 2013, ISBN: 9783658006891.

[76] S. Sass, T. Faulwasser, D. E. Hollermann, C. D. Kappatou, D. Sauer, T. Schütz, D. Y. Shu, A. Bardow, L. Gröll, V. Hagenmeyer, D. Müller, and A. Mitsos, “Model compendium, data, and optimization benchmarks for sector-coupled energy systems”, *Computers and Chemical Engineering*, vol. 135, 2020, ISSN: 00981354. DOI: 10.1016/j.compchemeng.2020.106760.

[77] P. Mancarella, “MES (multi-energy systems): An overview of concepts and evaluation models”, *Energy*, vol. 65, pp. 1–17, 2014, ISSN: 03605442. DOI: 10.1016/j.energy.2013.10.041. [Online]. Available: http://dx.doi.org/10.1016/j.energy.2013.10.041.

[78] L. Kotzur, L. Nolting, M. Hoffmann, T. Groß, A. Smolenko, J. Priesmann, H. Büsing, R. Beer, F. Kullmann, B. Singh, A. Praktiknjo, D. Stolten, and M. Robinius, “A modeler’s guide to handle complexity in energy systems optimization”, *Advances in Applied Energy*, vol. 4, no. August, p. 100 063, 2021, ISSN: 26667924. DOI: 10.1016/j.adapen.2021.100063. arXiv: 2009.07216. [Online]. Available: https://doi.org/10.1016/j.adapen.2021.100063.

[79] Arbeitsgemeinschaft für sparsamen und umweltfreundlichen Energieverbrauch (ASUE), “BHKW-Kenndaten 2014/15 Module, Anbieter, Kosten”, Tech. Rep.

[80] T. Schütz, M. H. Schraven, M. Fuchs, P. Remmen, and D. Müller, “Comparison of clustering algorithms for the selection of typical demand days for energy system synthesis”, *Renewable Energy*, vol. 129, pp. 570–582, 2018, ISSN: 0960-1481. DOI: 10.1016/j.renene.2018.06.028. [Online]. Available: https://doi.org/10.1016/j.renene.2018.06.028.

[81] E. Klotz and A. M. Newman, “Practical guidelines for solving difficult mixed integer linear programs”, *Surveys in Operations Research and Management Science*, vol. 18, no. 1, pp. 18–32, 2013, ISSN: 18767354. DOI: 10.1016/j.sorms.2012.12.001. [Online]. Available: http://dx.doi.org/10.1016/j.sorms.2012.12.001.

[82] S. A. Papoulias and I. E. Grossmann, “A structural optimization approach in process synthesis I: Utility systems”, *Computers and Chemical Engineering*, vol. 7, no. 6, pp. 695–706, 1983, ISSN: 0098-1354. DOI: https://doi.org/10.1016/0098-1354(83)85022-4. [Online]. Available: https://www.sciencedirect.com/science/article/pii/0098135483850224.

[83] R. Yokoyama, Y. Hasegawa, and K. Ito, “A MILP decomposition approach to large scale optimization in structural design of energy supply systems”, *Energy Conversion and Management*, vol. 43, no. 6, pp. 771–790, 2002, ISSN: 01968904. DOI: 10.1016/S0196-8904(01)00075-9.

[84] R. Yokoyama, Y. Shinano, S. Taniguchi, M. Ohkura, and T. Wakui, “Optimization of energy supply systems by MILP branch and bound method in consideration of hierarchical relationship between design and operation”, *Energy Conversion and Management*, vol. 92, pp. 92–104, 2015, ISSN: 0196-8904. DOI: 10.1016/j.enconman.2014.12.020. [Online]. Available: http://dx.doi.org/10.1016/j.enconman.2014.12.020.

[85] P. Voll, C. Klaffke, M. Hennen, and A. Bardow, “Automated superstructure-based synthesis and optimization of distributed energy supply systems”, *Energy*, vol. 50, no. 1, pp. 374–388, 2013, ISSN: 03605442. DOI: 10.1016/j.energy.2012.10.045. [Online]. Available: http://dx.doi.org/10.1016/j.energy.2012.10.045.

[86] V. Andiappan and D. K. Ng, “Synthesis of tri-generation systems: Technology selection, sizing and redundancy allocation based on operational strategy”, *Computers and Chemical Engineering*, vol. 91, pp. 380–391, 2016, ISSN: 00981354. DOI: 10.1016/j.compchemeng.2016.04.003. [Online]. Available: http://dx.doi.org/10.1016/j.compchemeng.2016.04.003.

[87] M. Stadler, G. Cardoso, S. Mashayekh, T. Forget, N. Deforest, A. Agarwal, and A. Schönbein, “Value streams in microgrids : A literature review”, *Applied Energy*, vol. 162, pp. 980–989, 2016, ISSN: 0306-2619. DOI: 10.1016/j.apenergy.2015.10.081. [Online]. Available: http://dx.doi.org/10.1016/j.apenergy.2015.10.081.

[88] M. Stadler, Z. Pecenak, P. Mathiesen, K. Fahy, and J. Kleissl, “Performance Comparison between Two Established Microgrid Planning MILP Methodologies Tested On 13 Microgrid Projects”, *Energies*, 2020.

[89] P. Gabrielli, M. Gazzani, E. Martelli, and M. Mazzotti, “Optimal design of multi-energy systems with seasonal storage”, *Applied Energy*, vol. 219, no. July 2017, pp. 408–424, 2018, ISSN: 0306-2619. DOI: 10.1016/j.apenergy.2017.07.142. [Online]. Available: https://doi.org/10.1016/j.apenergy.2017.07.142.

[90] P. Gabrielli, A. Poluzzi, G. J. Kramer, C. Spiers, M. Mazzotti, and M. Gazzani, “Seasonal energy storage for zero-emissions multi-energy systems via underground hydrogen storage”, *Renewable and Sustainable Energy Reviews*, vol. 121, p. 109 629, 2020, ISSN: 18790690. DOI: 10.1016/j.rser.2019.109629. [Online]. Available: https://doi.org/10.1016/j.rser.2019.109629.

[91] B. Bahl, M. Lampe, P. Voll, and A. Bardow, “Optimization-based identification and quantification of demand-side management potential for distributed energy supply systems”, *Energy*, vol. 135, pp. 889–899, 2017, ISSN: 03605442. DOI: 10.1016/j.energy.2017.06.083.

[92] B. Bahl, “Optimization-Based Synthesis of Large-Scale Energy Systems by Time-Series Aggregation Strukturoptimierung von Energiesystemen durch Zeitreihenaggregation”, PhD Thesis, RWTH Aachen, 2018, ISBN: 9783958862401.

[93] B. Bahl, T. Söhler, M. Hennen, and A. Bardow, “Typical periods for two-stage synthesis by time-series aggregation with bounded error in objective function”, *Frontiers in Energy Research*, vol. 5, no. January, pp. 1–13, 2018, ISSN: 2296598X. DOI: 10.3389/fenrg.2017.00035.

[94] T. Schütz, X. Hu, M. Fuchs, and D. Müller, “Optimal design of decentralized energy conversion systems for smart microgrids using decomposition methods”, *Energy*, vol. 156, pp. 250–263, 2018, ISSN: 03605442. DOI: 10.1016/j.energy.2018.05.050. [Online]. Available: https://doi.org/10.1016/j.energy.2018.05.050.

[95] A. S. Wallerand, M. Kermani, I. Kantor, and F. Maréchal, “Optimal heat pump integration in industrial processes”, *Applied Energy*, vol. 219, no. March, pp. 68–92, 2018, ISSN: 03062619. DOI: 10.1016/j.apenergy.2018.02.114. [Online]. Available: https://doi.org/10.1016/j.apenergy.2018.02.114.

[96] L. Urbanucci, J. C. Bruno, and D. Testi, “Thermodynamic and economic analysis of the integration of high-temperature heat pumps in trigeneration systems”, *Applied Energy*, vol. 238, no. August 2018, pp. 516–533, 2019, ISSN: 03062619. DOI: 10.1016/j.apenergy.2019.01.115. [Online]. Available: https://doi.org/10.1016/j.apenergy.2019.01.115.

[97] L. Urbanucci, F. D’Ettorre, and D. Testi, “A comprehensive methodology for the integrated optimal sizing and operation of cogeneration systems with thermal energy storage”, *Energies*, vol. 12, no. 5, 2019, ISSN: 19961073. DOI: 10.3390/en12050875.

[98] H. Teichgraeber and A. R. Brandt, “Clustering methods to find representative periods for the optimization of energy systems: An initial framework and comparison”, *Applied Energy*, vol. 239, no. February, pp. 1283–1293, 2019, ISSN: 03062619. DOI: 10.1016/j.apenergy.2019.02.012. [Online]. Available: https://doi.org/10.1016/j.apenergy.2019.02.012.

[99] M. Bohlayer, A. Bürger, M. Fleschutz, M. Braun, and G. Zöttl, “Multi-period investment pathways - Modeling approaches to design distributed energy systems under uncertainty”, *Applied Energy*, vol. 285, no. 285, p. 116 368, 2021.

[100] M. Bohlayer, “Investment and Operating Strategies for Distributed Energy Systems”, Ph.D. dissertation, Friedrich-Alexander-Universität Erlangen-Nürnberg, 2020.

[101] D. E. Hollermann, “Reliable and Robust Optimal Design of Sustainable Energy Systems Zuverlässige und robuste optimale Auslegung von nachhaltigen Energiesystemen”, PhD Thesis, RWTH Aachen, 2020, ISBN: 9783958863460.

[102] D. E. Hollermann, D. F. Hoffrogge, F. Mayer, M. Hennen, and A. Bardow, “Optimal reliable design of distributed energy supply systems”, *Computers and Chemical Engineering*, vol. 121, pp. 317–326, 2019, ISSN: 00981354. DOI: 10.1016/j.compchemeng.2018.09.029. [Online]. Available: https://doi.org/10.1016/j.compchemeng.2018.09.029.

[103] I. Petkov, G. Mavromatidis, C. Knoeri, J. Allan, and V. H. Hoffmann, "MANGOret: An optimization framework for the long-term investment planning of building multi-energy system and envelope retrofits", *Applied Energy*, vol. 314, no. March, 2022, ISSN: 03062619. DOI: 10.1016/j.apenergy.2022.118901.

[104] J. Richarz, S. Henn, T. Osterhage, and D. Müller, "Optimal scheduling of modernization measures for typical non-residential buildings", *Energy*, vol. 238, p. 121 871, 2022, ISSN: 03605442. DOI: 10.1016/j.energy.2021.121871. [Online]. Available: https://doi.org/10.1016/j.energy.2021.121871.

[105] P. Gabrielli, F. Fürer, P. Murray, K. Orehounig, J. Carmeliet, M. Gazzani, and M. Mazzotti, "A Time-series-based approach for robust design of multi-energy systems with energy storage", *Computer Aided Chemical Engineering*, vol. 43, no. 2016, pp. 525–530, 2018, ISSN: 15707946. DOI: 10.1016/B978-0-444-64235-6.50093-0.

[106] H. Teichgraeber, L. Kuepper, and A. Brandt, "TimeSeriesClustering: An extensible framework in Julia", *Journal of Open Source Software*, vol. 4, no. 41, p. 1573, 2019, ISSN: 2475-9066. DOI: 10.21105/joss.01573.

[107] A. J. Conejo, L. Baringo, S. Jalal Kazempour, and A. S. Siddiqui, *Investment in electricity generation and transmission: Decision making under uncertainty*. Springer, 2016, pp. 1–384, ISBN: 9783319295015. DOI: 10.1007/978-3-319-29501-5.

[108] M. Chang, J. Zink, B. Zakeri, B. Pickering, S. Pfenninger, H. Lund, and P. Alberg, "Trends in tools and approaches for modelling the energy transition", *Applied Energy*, vol. 290, 2021. DOI: 10.1016/j.apenergy.2021.116731.

[109] Z. K. Pecenak, M. Stadler, and K. Fahy, "Efficient multi-year economic energy planning in microgrids", *Applied Energy*, vol. 255, p. 113 771, 2019, ISSN: 0306-2619. DOI: 10.1016/j.apenergy.2019.113771. [Online]. Available: https://doi.org/10.1016/j.apenergy.2019.113771.

[110] M. Hennen, S. Postels, P. Voll, M. Lampe, and A. Bardow, "Multi-objective synthesis of energy systems: Efficient identification of design trade-offs", *Computers and Chemical Engineering*, vol. 97, pp. 283–293, 2017, ISSN: 00981354. DOI: 10.1016/j.compchemeng.2016.10.010. [Online]. Available: http://dx.doi.org/10.1016/j.compchemeng.2016.10.010.

[111] K.-k. Cao, K. V. Krbek, M. Wetzel, F. Cebulla, and S. Schreck, "Classification and evaluation of concepts for improving the performance of applied energy system optimization models", *Energies*, 2019. DOI: 10.3390/en12244656.

[112] C. Milan, M. Stadler, G. Cardoso, and S. Mashayekh, "Modeling of non-linear CHP efficiency curves in distributed energy systems", *Applied Energy*, vol. 148, pp. 334–347, 2015, ISSN: 03062619. DOI: 10.1016/j.apenergy.2015.03.053.

[113] R. Yokoyama, Y. Shinano, Y. Wakayama, and T. Wakui, "Model reduction by time aggregation for optimal design of energy supply systems by an MILP hierarchical branch and bound method", *Energy*, vol. 181, pp. 782–792, 2019, ISSN: 03605442. DOI: 10.1016/j.energy.2019.04.066. [Online]. Available: https://doi.org/10.1016/j.energy.2019.04.066.

[114] D. E. Hollermann, D. F. Hoffrogge, F. Mayer, M. Hennen, and A. Bardow, "Optimal reliable design of distributed energy supply systems", *Computers and Chemical Engineering*, vol. 121, pp. 317–326, 2019, ISSN: 00981354. DOI: 10.1016/j.compchemeng.2018.09.029. [Online]. Available: https://doi.org/10.1016/j.compchemeng.2018.09.029.

[115] J. Priesmann, L. Nolting, and A. Praktiknjo, "Are complex energy system models more accurate? An intra-model comparison of power system optimization models", *Applied Energy*, vol. 255, pp. 1–28, 2019, ISSN: 03062619. DOI: 10.1016/j.apenergy.2019.113783.

[116] G. M. Kopanos, D. P. Xenos, M. Cicciotti, E. N. Pistikopoulos, and N. F. Thornhill, "Optimization of a network of compressors in parallel: Operational and maintenance planning - The air separation plant case", *Applied Energy*, vol. 146, pp. 453–470, 2015, ISSN: 03062619. DOI: 10.1016/j.apenergy.2015.01.080. [Online]. Available: http://dx.doi.org/10.1016/j.apenergy.2015.01.080.

[117] J. F. Marquant, G. Mavromatidis, R. Evins, and J. Carmeliet, "Comparing different temporal dimension representations in distributed energy system design models", *Energy Procedia*, vol. 122, pp. 907–912, 2017, ISSN: 18766102. DOI: 10.1016/j.egypro.2017.07.403. [Online]. Available: https://doi.org/10.1016/j.egypro.2017.07.403.

[118] L. Kotzur, P. Markewitz, M. Robinius, and D. Stolten, "Impact of different time series aggregation methods on optimal energy system design", *Renewable Energy*, vol. 117, pp. 474–487, 2018, ISSN: 0960-1481. DOI: 10.1016/j.renene.2017.10.017. [Online]. Available: https://doi.org/10.1016/j.renene.2017.10.017.

[119] M. Hoffmann, L. Kotzur, D. Stolten, and M. Robinius, "A review on time series aggregation methods for energy system models", *Energies*, vol. 13, no. 3, 2020, ISSN: 19961073. DOI: 10.3390/en13030641.

[120] Verein Deutscher Ingenieure (VDI), *Referenzlastprofile von Wohngebäuden für Strom, Heizung und Trinkwarmwasser sowie Referenzerzeugungsprofile für Fotovoltaikanlagen (VDI 4655)*, Düsseldorf, 2019.

[121] P. Gabrielli, M. Gazzani, E. Martelli, and M. Mazzotti, "Optimal design of multi-energy systems with seasonal storage", *Applied Energy*, vol. 219, no. June 2017, pp. 408–424, 2018, ISSN: 03062619. DOI: 10.1016/j.apenergy.2017.07.142. [Online]. Available: https://doi.org/10.1016/j.apenergy.2017.07.142.

[122] L. Kotzur, P. Markewitz, M. Robinius, and D. Stolten, "Time series aggregation for energy system design: Modeling seasonal storage", *Applied Energy*, vol. 213, no. January, pp. 123–135, 2018, ISSN: 03062619. DOI: 10.1016/j.apenergy.2018.01.023. arXiv: 1710.07593. [Online]. Available: https://doi.org/10.1016/j.apenergy.2018.01.023.

[123] K. Poncelet, H. Hoschle, E. Delarue, A. Virag, and W. Drhaeseleer, "Selecting representative days for capturing the implications of integrating intermittent renewables in generation expansion planning problems", *IEEE Transactions on Power Systems*, vol. 32, no. 3, pp. 1936–1948, 2017, ISSN: 08858950. DOI: 10.1109/TPWRS.2016.2596803.

[124] S. Pfenninger and I. Staffell, "Long-term patterns of European PV output using 30 years of validated hourly reanalysis and satellite data", *Energy*, vol. 114, pp. 1251–1265, 2016, ISSN: 03605442. DOI: 10.1016/j.energy.2016.08.060. [Online]. Available: http://dx.doi.org/10.1016/j.energy.2016.08.060.

[125] S. Fazlollahi, S. L. Bungener, P. Mandel, G. Becker, and F. Maréchal, "Multi-objectives, multi-period optimization of district energy systems: I. Selection of typical operating periods", *Computers and Chemical Engineering*, vol. 65, pp. 54–66, 2014, ISSN: 00981354. DOI: 10.1016/j.compchemeng.2014.03.005.

[126] R. Yokoyama, K. Takeuchi, Y. Shinano, and T. Wakui, "Effect of model reduction by time aggregation in multiobjective optimal design of energy supply systems by a hierarchical MILP method", *Energy*, vol. 228, p. 120 505, 2021, ISSN: 03605442. DOI: 10.1016/j.energy.2021.120505. [Online]. Available: https://doi.org/10.1016/j.energy.2021.120505.

[127] M. Zatti, M. Gabba, M. Freschini, M. Rossi, A. Gambarotta, M. Morini, and E. Martelli, "k-MILP: A novel clustering approach to select typical and extreme days for multi-energy systems design optimization", *Energy*, vol. 181, pp. 1051–1063, 2019, ISSN: 03605442. DOI: 10.1016/j.energy.2019.05.044. [Online]. Available: https://doi.org/10.1016/j.energy.2019.05.044.

[128] I. V. Beuzekom, J. Fraiture, B.-m. Hodge, and H. Slootweg, "Mixed-integer optimization model for long-term investment planning of integrated urban energy", *Applied Energy*, vol. 292, no. February, p. 116 880, 2021, ISSN: 0306-2619. DOI: 10.1016/j.apenergy.2021.116880. [Online]. Available: https://doi.org/10.1016/j.apenergy.2021.116880.

[129] J. F. Marquant, R. Evins, and J. Carmeliet, "Reducing computation time with a rolling horizon approach applied to a MILP formulation of multiple urban energy hub system", *Procedia Computer Science*, vol. 51, no. 1, pp. 2137–2146, 2015, ISSN: 18770509. DOI: 10.1016/j.procs.2015.05.486. [Online]. Available: http://dx.doi.org/10.1016/j.procs.2015.05.486.

[130] I. Staffell and S. Pfenninger, "Using bias-corrected reanalysis to simulate current and future wind power output", *Energy*, vol. 114, pp. 1224–1239, 2016, ISSN: 03605442. DOI: 10.1016/j.energy.2016.08.068. [Online]. Available: http://dx.doi.org/10.1016/j.energy.2016.08.068.

[131] M. R. Haghifam and M. Manbachi, "Reliability and availability modelling of combined heat and power (CHP) systems", *International Journal of Electrical Power and Energy Systems*, vol. 33, no. 3, pp. 385–393, 2011, ISSN: 01420615. DOI: 10.1016/j.ijepes.2010.08.035. [Online]. Available: http://dx.doi.org/10.1016/j.ijepes.2010.08.035.

[132] H. Sabouhi, A. Abbaspour, M. Fotuhi-Firuzabad, and P. Dehghanian, "Reliability modeling and availability analysis of combined cycle power plants", *International Journal of Electrical Power and Energy Systems*, vol. 79, pp. 108–119, 2016, ISSN: 01420615. DOI: 10.1016/j.ijepes.2016.01.007. [Online]. Available: http://dx.doi.org/10.1016/j.ijepes.2016.01.007.

[133] Y. Ye, I. E. Grossmann, J. M. Pinto, and S. Ramaswamy, "Integrated optimization of design, storage sizing, and maintenance policy as a Markov decision process considering varying failure rates", *Computers and Chemical Engineering*, vol. 142, p. 107 052, 2020, ISSN: 00981354. DOI: 10.1016/j.compchemeng.2020.107052. [Online]. Available: https://doi.org/10.1016/j.compchemeng.2020.107052.

[134] R. Chakrabarti, P. K. Chattopadhyay, and C. K. Panigrahi, "A review of recent advances in economic dispatch", *IEEE Transactions on Power Systems*, pp. 1248–1255, 1990, ISSN: 00203386.

[135] N. Yang, Z. Dong, L. Wu, L. Zhang, X. Shen, D. Chen, B. Zhu, and Y. Liu, "A Comprehensive Review of Security-constrained Unit Commitment", *Journal of Modern Power Systems and Clean Energy*, vol. 10, no. 3, pp. 562–576, 2022, ISSN: 21965420. DOI: 10.35833/MPCE.2021.000255.

[136] S. Mashayekh, M. Stadler, G. Cardoso, M. Heleno, S. C. Madathil, H. Nagarajan, R. Bent, M. Mueller-Stoffels, X. Lu, and J. Wang, “Security-Constrained Design of Isolated Multi-Energy Microgrids”, *IEEE Transactions on Power Systems*, vol. 33, no. 3, pp. 2452–2462, 2018, ISSN: 08858950. DOI: 10.1109/TPWRS.2017.2748060.

[137] S. Chalil Madathil, E. Yamangil, H. Nagarajan, A. Barnes, R. Bent, S. Backhaus, S. J. Mason, S. Mashayekh, and M. Stadler, “Resilient off-grid microgrids: Capacity planning and N-1 security”, *IEEE Transactions on Smart Grid*, vol. 9, no. 6, pp. 6511–6521, 2018, ISSN: 19493053. DOI: 10.1109/TSG.2017.2715074.

[138] Z. K. Pecenak, P. Mathiesen, K. Fahy, C. Cannon, E. Ayandele, T. J. Kirk, and M. Stadler, “The impact of project financing in optimizing microgrid design”, *Journal of Renewable and Sustainable Energy*, vol. 12, no. 6, 2020, ISSN: 19417012. DOI: 10.1063/5.0026187.

[139] M. Di Somma, B. Yan, N. Bianco, G. Graditi, P. B. Luh, L. Mongibello, and V. Naso, “Multi-objective design optimization of distributed energy systems through cost and exergy assessments”, *Applied Energy*, vol. 204, pp. 1299–1316, 2017, ISSN: 03062619. DOI: 10.1016/j.apenergy.2017.03.105. [Online]. Available: http://dx.doi.org/10.1016/j.apenergy.2017.03.105.

[140] V. Oree, S. Z. Sayed Hassen, and P. J. Fleming, “A multi-objective framework for long-term generation expansion planning with variable renewables”, *Applied Energy*, vol. 253, no. March, p. 113 589, 2019, ISSN: 03062619. DOI: 10.1016/j.apenergy.2019.113589. [Online]. Available: https://linkinghub.elsevier.com/retrieve/pii/S0306261919312632.

[141] M. Hennen, M. Lampe, P. Voll, and A. Bardow, “SPREAD – Exploring the decision space in energy systems synthesis”, *Computers and Chemical Engineering*, vol. 106, pp. 297–308, 2017, ISSN: 00981354. DOI: 10.1016/j.compchemeng.2017.06.002. [Online]. Available: http://dx.doi.org/10.1016/j.compchemeng.2017.06.002.

[142] K. Anderson, D. Olis, B. Becker, L. Parkhill, N. Laws, X. Li, and S. Mishra, “REopt Lite User Manual”, National Renewable Energy Laboratory, Tech. Rep., 2021. [Online]. Available: https://reopt.nrel.gov/tool/REoptLiteWebToolUserManual.pdf#page=5.

[143] R. Fourer, D. M. Gay, and B. W. Kernighan, “AMPL: A Mathematical Programing Language”, in *Algorithms and Model Formulations in Mathematical Programming*, S. W. Wallace, Ed., Berlin, Heidelberg: Springer Berlin Heidelberg, 1989, ISBN: 978-3-642-83724-1. DOI: 10.1007/978-3-642-83724-1_12.

[144] Siemens, *Siemens AutoLP*, 2020. [Online]. Available: autolp.ct@siemens.com.

[145] Zuse Institute Berlin, *The SCIP Optimization Suite 7.0*, 2020.

[146] Y. Chan and R. Kantamaneni, “Study on Energy Efficiency and Energy Saving Potential in Industry and on Possible Policy Mechanisms”, *ICF Consulting Limited*, no. December, pp. 1–461, 2015. [Online]. Available: https://ec.europa.eu/energy/sites/ener/files/documents/151201DGENERIndustrialEEstudy-finalreport_clean_stc.pdf.

[147] Bundesnetzagentur, *SMARD*, 2022. [Online]. Available: https://www.smard.de//en/ (visited on 09/19/2022).

[148] Erlanger Stadtwerke, “Preisblatt Netznutzungsentgelte für die Nutzung der Stromversorgungsnetze der Erlanger Stadtwerke AG”, 2022.

[149] A. Kemmler, A. Kirchner, A. Maur, F. Ess, S. Kreidelmeyer, A. Piégsa, T. Spillmann, M. Wünsch, and I. Ziegenhagen, "Energiewirtschaftliche Projektionen und Folgeabschätzungen 2030/2050", *Prognos AG*, 2020. [Online]. Available: https://www.bmwi.de/Redaktion/DE/Publikationen/Wirtschaft/klimagutachten.pdf?__blob=publicationFile&v=8.

[150] P. Sterchele, J. Brandes, J. Heilig, and D. Wrede, "Wege zu einem klimaneutralen Energiesystem - Die deutsche Energiewende im Kontext gesellschaftlicher Verhaltensweisen. Anhang zur Studie", *Fraunhofer ISE*, 2020.

[151] R. Gelaro, W. McCarty, M. J. Suárez, R. Todling, A. Molod, L. Takacs, C. A. Randles, A. Darmenov, M. G. Bosilovich, R. Reichle, K. Wargan, L. Coy, R. Cullather, C. Draper, S. Akella, V. Buchard, A. Conaty, A. M. da Silva, W. Gu, G. K. Kim, R. Koster, R. Lucchesi, D. Merkova, J. E. Nielsen, G. Partyka, S. Pawson, W. Putman, M. Rienecker, S. D. Schubert, M. Sienkiewicz, and B. Zhao, "The modern-era retrospective analysis for research and applications, version 2 (MERRA-2)", *Journal of Climate*, vol. 30, 2017, ISSN: 08948755. DOI: 10.1175/JCLI-D-16-0758.1.

[152] O. Walter, "Hybrid Energy Storage in Future Energy Systems Hybride Energiespeicherung in zukünftigen Energiesystemen", *Dissertation an der Technischen Fakultät der Friedrich-Alexander-Universität Erlangen-Nürnberg*, p. 225, 2021. [Online]. Available: https://opus4.kobv.de/opus4-fau/frontdoor/index/index/docId/16997.

[153] Deutsches Institut für Normung (DIN), *Energetische Bewertung von Gebäuden – Berechnung des Nutz-, End- und Primärenergiebedarfs für Heizung, Kühlung, Lüftung, Trinkwarmwasser und Beleuchtung (DIN 18599) – Teil 7: Endenergiebedarf von Raumlufttechnik- und Klimakältesystemen für den Nichtwohnun*, Berlin, 2018.

[154] T. Hübner, A. Guminski, B. Kleinartz, and S. von Roon, "Die Rolle von Kraft - Wärme - Kopplung im zukünftigen Energiesystem", *BWK – Das Energie Fachmagazin*, p. 15, 2019.

[155] L. Vimmerstedt, S. Akar, B. Mirletz, A. Sekar, D. Stright, C. Augustine, P. Beiter, P. Bhaskar, N. Blair, S. Cohen, W. Cole, P. Duffy, D. Feldman, P. Gagnon, P. Kurup, C. Murphy, V. Ramasamy, J. Robins, T. Stehly, J. Zuboy, G. Oladosu, and J. Hoffmann, "Annual Technology Baseline: The 2022 Electricity Update", [Online]. Available: https://www.osti.gov/biblio/1875073.

[156] Danish Energy Agency and Energinet, "Technology Data - Generation of Electricity and District heating", Tech. Rep., 2022. [Online]. Available: http://www.ens.dk/teknologikatalog.

[157] IEEE Industry Applications Society, "IEEE Recommended Practice for Analyzing Reliability Data for Equipment Used in Industrial and Commercial Power Systems Pressure", New York, Tech. Rep., 2018.

[158] B. H. Vu and I. Y. Chung, "Optimal generation scheduling and operating reserve management for PV generation using RNN-based forecasting models for stand-alone microgrids", *Renewable Energy*, vol. 195, pp. 1137–1154, 2022, ISSN: 18790682. DOI: 10.1016/j.renene.2022.06.086. [Online]. Available: https://doi.org/10.1016/j.renene.2022.06.086.

[159] K. Anderson, D. Olis, B. Becker, L. Parkhill, N. Laws, X. Li, S. Mishra, T. Kwasnik, A. Jeffery, E. Elgqvist, K. Krah, D. Cutler, A. Zolan, N. Muerdter, R. Eger, A. Walker, C. Hampel, G. Tomberlin, and A. Farthing, "The REopt Web Tool User Manual", Tech. Rep., 2023. [Online]. Available: https://reopt.nrel.gov/tool/reopt-user-manual.pdf.

[160] A. Ioannou, A. Angus, and F. Brennan, "Risk-based methods for sustainable energy system planning: A review", *Renewable and Sustainable Energy Reviews*, vol. 74, no. February, pp. 602–615, 2017, ISSN: 18790690. DOI: 10.1016/j.rser.2017.02.082. [Online]. Available: http://dx.doi.org/10.1016/j.rser.2017.02.082.

[161] A. Foucquier, S. Robert, F. Suard, L. Stéphan, and A. Jay, "State of the art in building modelling and energy performances prediction: A review", *Renewable and Sustainable Energy Reviews*, vol. 23, pp. 272–288, 2013, ISSN: 13640321. DOI: 10.1016/j.rser.2013.03.004.

[162] D. Lohmeier, D. Cronbach, S. R. Drauz, M. Braun, and T. M. Kneiske, "Pandapipes: An open-source piping grid calculation package for multi-energy grid simulations", *Sustainability*, vol. 12, no. 23, 2020. DOI: 10.3390/su12239899.

[163] Y. Wack, M. Baelmans, R. Salenbien, and M. Blommaert, "Economic Topology Optimization of District Heating Networks using a Pipe Penalization Approach", *Energy*, vol. 264, no. October 2022, 2022, ISSN: 0360-5442. DOI: 10.1016/j.energy.2022.126161. arXiv: 2205.12019.

[164] International Energy Agency (IEA), "Technology Brief E04 - Combined Heat and Power", *Energy Technology System Analysis Programme*, 2010. [Online]. Available: http://www.iea-etsap.org/web/e-techds/pdf/e04-chp-gs-gct_adfinal.pdf.

A. Appendix

A.1. Linearization schemas

The model equations introduced in Chapter 3 comprises non-linear constraints to simplify understanding of the correlations. The introduction of non-linear constraints adds significant computational complexity. In the implemented model formulation, the non-linear constraints are thus reformulated in mixed-integer formulations using two different linearization schemas.

Equations 3.19, 3.22, 3.28 and 3.29 comprise bilinear terms with one factor being a binary variable. The explanation below applies Glover's reformulation to Equation 3.29. The approach is applied to the other equations analogously. Following Glover's linearization schema, the product of binary variable ($B^{\text{Opr}}_{k,t}$) and a sum term ($\xi_{k,y} = c^{\text{OM,run,fix}}_{k,y} + c^{\text{OM,run,var}}_{k,y} P^{\text{R}}_{k,y}$) is replaced by a continuous helper variable $H_{k,t} \in \mathbb{R}^{+}$. The value of this helper variable is constraint by three mixed integer inequality constraints. The parameter m_k describes a sufficiently high number with $m_k \gg \xi_{k,y}$.

$$H_{k,t} \leq \xi_{k,y} \quad \forall k \in \mathcal{K}_C, y \in \mathcal{Y}, t \in \mathcal{T}_y \tag{A.1}$$

$$H_{k,t} \leq m_k \cdot B^{\text{Opr}}_{k,t} \quad \forall k \in \mathcal{K}_C, t \in \mathcal{T} \tag{A.2}$$

$$m_k \cdot (B^{\text{Opr}}_{k,t} - 1) + \xi_{k,y} \leq H_{k,t} \quad \forall k \in \mathcal{K}_C, y \in \mathcal{Y}, t \in \mathcal{T}_y \tag{A.3}$$

Constraints with products of two continous variables occur in Equations 3.32 and 3.39. The linearization of these equations requires the introduction of an additional helper binary variable $B^{H}_{k,t} \in \{0,1\}$. The reformulation is shown for Equation 3.39. The parameter m_k describes a sufficiently high number with $m_k \gg P^{\text{In}}_{k,t}$ and $m_k \gg P^{\text{Out}}_{k,t}$. The value of m_k is chosen sufficiently low to keep the optimization model numerically stable. The two inequality constraints ensure that only one of two continuous variable can take a non-zero value.

$$P^{\text{In}}_{k,t} \leq m_k \cdot B^{H}_{k,t} \quad \forall k \in \mathcal{K}_S, t \in \mathcal{T} \tag{A.4}$$

$$P^{\text{Out}}_{k,t} \leq m_k \cdot (1 - B^{H}_{k,t}) \quad \forall k \in \mathcal{K}_S, t \in \mathcal{T} \tag{A.5}$$

A.2. Techno-economic assumptions

Table A.1.: Assumptions on technical and economic characteristics of renewable and storage technologies

Technology	Parameter	Value	Unit	Source
Photovoltaic	Investment	1448	€/kWp	[155]
	O&M	17	€/kWp/a	[155]
Battery	Investment	349	k€	[155]
		183	€/kWh	[155]
		268	€/kW	[155]
	O&M	40	€/kW/a	[155]
	Efficiency	85	%	[155]
	Lifetime	12	a	[155]
Hot water tank	Investment	10	k€	[27]
		20	€/kWh	[27]
	O&M	0.1025	€/kWh/a	[27]
	Self-discharge	0.5	%/h	[27]
	Charging efficiency	98	%	[27]
	Discharg efficiency	98	%	[27]
Chilled water tank	Investment	11	k€	[27]
		77	€/kWh	[27]
	O&M	0.1025	€/kWh/a	[27]
	Self-discharge	0.334	%/h	[27]
	Charging efficiency	98	%	[27]

Table A.2.: Projected evolution of photovoltaic and battery prices based on [155]

	Unit	2023	2026	2029	2032	2035
Photovoltaic, Investment	€/kWp	1448	1224	1001	905	873
Photovoltaic, O&M	€/kW/a	17	14	12	11	11
Battery, Investment	k€	349	318	298	285	274
	€/kWh	183	134	115	107	103
	€/kW	268	219	196	185	178
Battery, O&M	€/kW/a	40	32	29	27	26

Table A.3.: Assumptions on technical and economic characteristics of conversion technologies

Technology	Parameter	Value	Unit	Source
CHP (ICE)	Investment	121	k€	[79]
(< 4 MW)		650	€/kW	[79]
	O&M	8	€/kW/a	Assumption
		15	€/MWh	Assumption
	Electric efficiency	36	%	[164]
	Heat efficiency	22	%	[164]
	Steam efficiency	32	%	[164]
	Minimum part load	30	%	[156]
CHP (GT)	Investment	750	€/kW	[156]
(> 2.0 MW)	O&M	7	€/kW/a	Assumption
		8	€/MWh	Assumption
	Electric efficiency	31	%	[113]
	Steam efficiency	53	%	[113]
	Minimum part load	50	%	[156]
Boiler (gas)	Investment	60	€/kW	[156]
	O&M	1.1	€/kW/a	[156]
	Efficiency	90	%	Assumption
Boiler (biomass)	Investment	690	€/kW	[156]
	O&M	2.72	€/MWh	[156]
	Efficiency	97	%	Assumption
Boiler (electric)	Investment	343	k€	[156]
		36	€/kW	[156]
	O&M	0.9	€/kW/a	[156]
	Efficiency	98	%	[156]
Heat pump	Investment	713	k€	[156]
(air source)		714	€/kW	[156]
	O&M	2.69	€/kW/a	[156]
	COP	2.2	-	[156]
Heat pump	Investment	571	k€	[156]
(waste heat)		666	€/kW	[156]
	O&M	3	€/kW/a	[156]
	COP	4.5	-	[156]
Compression chiller	Investment	21	k€	[27]
		329	€/kW	[27]
	O&M	8.8	€/kW/a	[27]
	EER	3.6	-	[153]
Absorption chiller	Investment	63	k€	[27]
		588	€/kW	[27]
	O&M	2.5	€/kW/a	[27]
	EER	0.69	€/kW/a	[153]

A.3. Optimization results

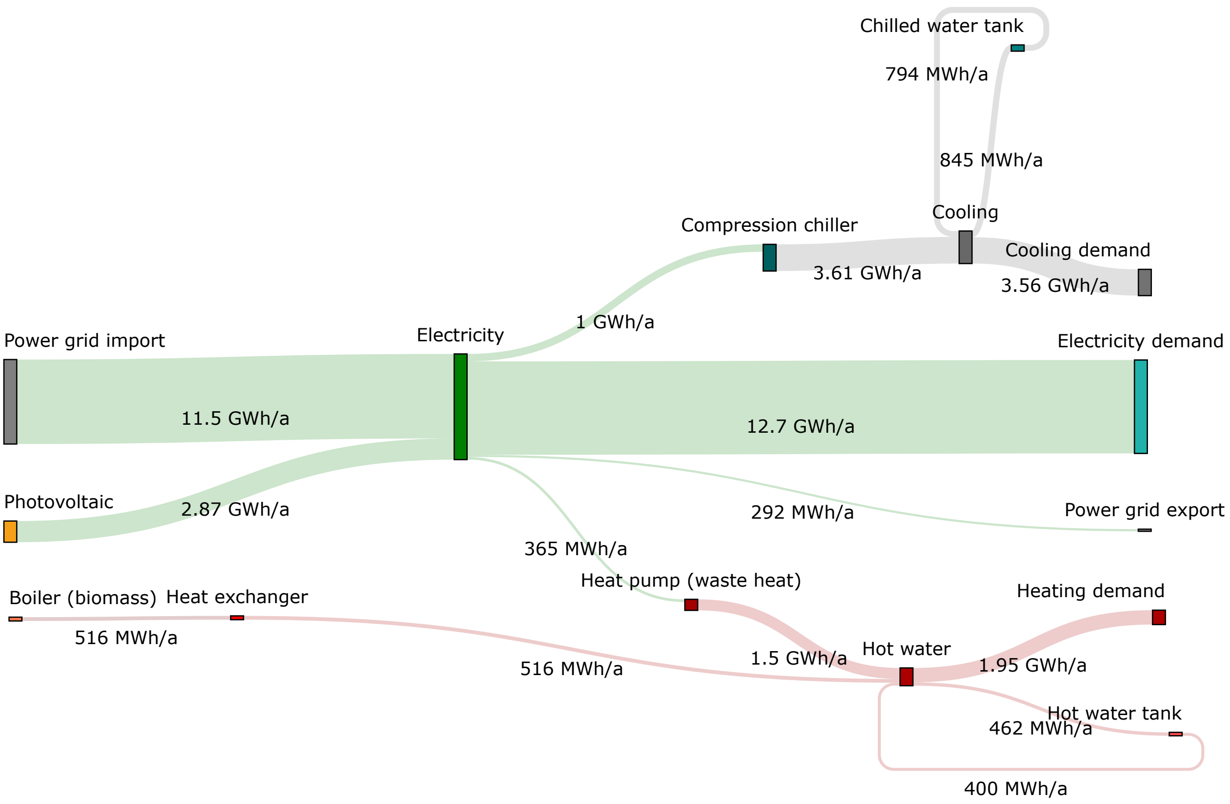

Figure A.1.: Annual energy flows in carbon optimal scenario of the automotive site